TARGETS OF TRANSCRIPTION INHIBITION BY THE ANTIBIOTICS LIPIARMYCIN, GE23077, AND SALINAMIDE

By

DAVID D. DEGEN

A Dissertation submitted to the

Graduate School-New Brunswick

Rutgers, The State University of New Jersey

and

The Graduate School of Biomedical Sciences

University of Medicine and Dentistry of New Jersey

in partial fulfillment of the requirements

for the degree of

Doctor of Philosophy

Graduate Program in Biomedical Engineering

written under the direction of

Dr. Richard H. Ebright

and approved by

_____

_____

_____

_____

New Brunswick, New Jersey

January, 2014

ABSTRACT OF THE DISSERTATION

Targets of transcription inhibition by the antibiotics

lipiarmycin, GE23077, and salinamide

by DAVID D. DEGEN

Dissertation Director:

Dr. Richard H. Ebright

The antibiotics lipiarmycin (Lpm), GE23077 (GE), and salinamide (Sal) function by inhibiting bacterial RNA polymerase (RNAP). In this work, the targets (and mechanisms) of transcription inhibition by Lpm, GE, and Sal are identified and characterized through a combination of genetic, biochemical, and structural approaches. Each of these compounds functions through a different target on the enzyme that does not significantly overlap the targets of other bacterial RNAP inhibitors. Elucidation of these targets may prove useful for antibacterial drug discovery and design.

To define the functional target of Lpm, we isolated and sequenced 160 Lpm-resistant mutants. In the structure of RNAP, sites of substitutions conferring Lpm-resistance cluster to define the "Lpm target," which includes residues in the RNAP switch-region, as well as one wall of the RNA exit channel. Biochemical experiments show that Lpm inhibits the RNAP-DNA interaction, and appears to function by trapping the RNAP clamp in a fully-to-partially closed state.

To define the functional target of GE, we isolated and sequenced 35 GE-resistant mutants. In the structure of RNAP, sites of substitutions conferring GE-resistance cluster to define the "GE target," which includes residues in the RNAP active-center subregions, the "β D2-loop" and the "link region." Biochemical experiments reveal that GE inhibits nucleotide addition during transcription initiation, after open complex formation, but prior to phosphodiester bond formation. The crystal structure of RNAP in complex with GE confirms that GE binds to the GE target, and indicates that GE functions by precluding the binding of NTP substrates to the RNAP active-center "i site" and "i+1 site."

To define the functional target of Sal, we isolated and sequenced 47 Sal-resistant mutants. In the structure of RNAP, sites of substitutions conferring Sal-resistance cluster to define the "Sal target," which includes residues in the RNAP active-center subregions: the "bridge-helix N-terminal hinge" (BH-H_N), the "F-loop," and the "link region." Biochemical experiments reveal that Sal inhibits nucleotide addition during both transcription initiation and elongation. The crystal structure of RNAP in complex with Sal confirms that Sal binds to the Sal target, and suggests that Sal functions by trapping the BH-H_N in a straight (unbent) conformation.

Acknowledgements

I would like to thank my thesis advisor, Dr. Richard Ebright, for his guidance and support in doing the research presented here. I would also like to thank my committee members, Dr. Li Cai, Dr. Bryce Nickels, and Dr. Patrick Sinko, for their time and review of this work.

In addition, I would like to thank the Ebright lab members both past and present who were involved either directly or indirectly in the various projects presented in this work. I have tried my best to acknowledge specific contributions wherever possible. There are too many to list, but, in particular, I have to thank Richard Y. Ebright and Katherine Y. Ebright for their help during several summers in isolating lipiarmycin-resistant, GE23077-resistant, and salinamide-resistant mutants in *E. coli*; Aashish Srivastava for his work in isolating lipiarmycin-resistant mutants in *S. aureus* and developing the fitness cost assays; Mary Ho and Yu Zhang for their work in crystallizing RNAP in complex with GE23077; Yu Feng for his work in crystallizing RNAP in complex with salinamide; and both Yu Zhang and Yu Feng for their work in studying the mechanism of salinamide.

Finally, I would like to thank my mom, dad, family, and friends for all of their help and support over the years. I could not have done this without them.

Preface

Most of the work presented in this thesis is expected to appear in future scientific journal publications. Work involving the target of lipiarmycin in *E. coli* will hopefully be submitted to a journal such as *PNAS* or *PLOS ONE*. Some of the earliest results involving the lipiarmyin target have been previously published in a patent (Ebright, 2005). Some of the more recent lipiarmycin target results from this work have been presented, and referenced as being unpublished, in Srivastava et al., 2011. The work involving lipiarmycin-resistant mutants in *S. aureus* and their fitness costs will hopefully be submitted to a journal such as *Antimicrobial Agents and Chemotherapy*.

The work involving GE23077 is being prepared for submission to a journal such as *Cell*. The design of RifaGE and SoraGE compounds as well as some preliminary results will appear in a patent filing (Ebright et al., 2011).

The work involving salinamide will soon be submitted to the journal *eLIFE* or *Molecular Cell* for review. The design of and preliminary results for salinamide derivatives will appear in two patent filings (Ebright et al., 2012a, 2012b). The salinamide target has also been published in a patent filing (Ebright et al., 2012c).

I would also like to note that the ideas, methods, and strategies used in this work rely heavily on previously publications from the Ebright lab including, but not limited to, Mukhopadhyay et al., 2004; Tuske et al., 2005; and Mukhopadhyay et al., 2008; and Srivastava et al., 2012.

Table of Contents

List of Tables

Appendix SA: Methods (Chapter 2) Supplements

Appendix SB: Lipiarmycin (Chapter 3) Supplements

Appendix SC: GE23077 (Chapter 4) Supplements

Appendix SD: Salinamide (Chapter 5) Supplements

List of Illustrations

Appendix SB: Lipiarmycin (Chapter 3) Supplements

Appendix SC: GE23077 (Chapter 4) Supplements

Appendix SD: Salinamide (Chapter 5) Supplements

Chapter 1:
Introduction

The emergence of antibacterial drug resistance is an important public health issue of increasing concern. Nearly all major bacterial pathogens have developed resistance to at least one clinically used antibiotic, and many have developed resistance to multiple classes of antibiotics. There are even reports of clinical resistance developing against the current "last line of defense" antibiotics, including daptomycin and vancomycin (reviewed in Livermore, 2009; Rice, 2009; Bayer et al., 2013; Cattoir and Leclercq, 2013). There is an urgent need for new antibacterial agents to be developed into drugs for the clinical treatment of these antibacterial-drug resistant pathogens.

One of the most serious global pathogens is *Mycobacterium tuberculosis*, the causative agent of tuberculosis (TB). In 2011, there were over eight million new cases of TB, and over one million deaths resulting from the disease (World Health Organization [WHO], 2012). TB infections are notoriously difficult to cure due to the persistence of slow-growing, non-replicating bacterial cells in infected individuals (reviewed in Barry et al., 2009). Treatment must last for at least six months with a cocktail of several different antibiotics in order to avoid and overcome the development of antibiotic resistance. A cocktail of four front-line drugs is currently recommended for the initial treatment of active TB infections: isoniazid, ethambutol, pyrazinamide, and rifampin (Rif) (WHO, 2012). Of these four drugs, only Rif is able to kill the slow-growing, non-replicating form of *M. tuberculosis* (Mitchison, 2000).

Rif functions by inhibiting bacterial RNA polymerase (RNAP) (Hartmann et al., 1967; Lancini and Sartori, 1968; McClure and Cech, 1978). There are several factors that

make bacterial RNAP an excellent target for antibacterial therapy (presented in Chopra, 2007; Villian-Guillot et al., 2007; Mukhopadhyay et al., 2008; Ho et al., 2009; Srivastava et al., 2011). Being an essential enzyme, RNAP is required for survival even in non-replicating cells. Inhibition of RNAP results in cell death. The sequences of bacterial RNAP subunits are highly conserved across bacterial species, giving inhibitors of bacterial RNAP the potential for broad spectrum antibacterial activity (Mukhopadhyay et al., 2008; Ho et al., 2009; Srivastava et al., 2011). Rif, in fact, is used in combination drug therapy for the treatment of both Gram-positive and Gram-negative bacterial infections, including methicillin-resistant *Staphylococcus aureus* (MRSA), bacterial meningitis, leprosy, and brucellosis, in addition to TB (reviewed in Bullock, 1983; Vesely, et al. 1998). On the other hand, the sequences of bacterial RNAP subunits are less well conserved with those of the human RNAP enzymes. This provides a bacterial RNAP inhibitor with the potential for therapeutic selectivity, i.e. an antibacterial agent, like Rif, can inhibit the bacterial RNAP enzyme, while having no effect on eukaryotic/human RNAP (Villian-Guillot et al., 2007; Mukhopadhyay et al., 2008; Sousa, 2008; Ho et al., 2009; Srivastava et al., 2011).

As with most antibiotics, there is a large and increasing number of bacterial infections that are resistant to Rif. In 2011, an estimated 300,000 cases of TB were multidrug-resistant (MDR-TB), meaning the *M. tuberculosis* bacteria had developed resistance to Rif (as well as isoniazid) (WHO, 2012). As one would expect, these infections are even more difficult to treat than non-resistant TB, requiring an even longer (up to 2 years) and more costly treatment period. Resistance to Rif primarily results from amino acid substitutions within its binding site on bacterial RNAP, (the Rif target)

(Ovchinnikov et al., 1983; Jin and Gross, 1988; Williams, et al., 1994; Ramaswamy and Musser, 1998; Campbell et al., 2001; reviewed in Tupin et al., 2010a). These substitutions prevent Rif from binding to and inhibiting RNAP (Campbell et al., 2001).

Given the many advantages and unique properties of bacterial RNAP as a target for antibacterial therapy, there is an urgent need for new antibacterial agents that inhibit bacterial RNAP; but function through sites different from the Rif target, and, therefore, would be expected to have no cross-resistance with Rif. The work presented here identifies and characterizes three new sites for the inhibition of bacterial RNAP. These sites are the respective targets of the antibiotics, lipiarmycin, GE23077, and salinamide. Each of these sites is different from the Rif target and demonstrates minimal to no cross resistance with Rif. Each of these inhibitors also functions by a different mechanism than Rif. Elucidation of these targets and inhibition mechanisms could aid in the development of new antibacterial drugs that target bacterial RNAP, and are effective against bacterial pathogens.

Bacterial RNAP

Bacterial RNA polymerase (RNAP) is the enzyme responsible for transcription inside the bacterial cell. It is a large (~450 kD), multi-subunit protein that has a shape reminiscent of a crab claw, with two "pincers" on either side of an active-center cleft (Zhang et al., 1999; Ebright, 2000). The enzyme has dimensions of ~150 Å x ~100 Å x ~100 Å (Zhang et al., 1999; Ebright, 2000). The active-center cleft is ~25 Å in diameter, large enough to accommodate double-stranded DNA, which must enter the cleft and partially unwind for transcription to occur (Ebright, 2000).

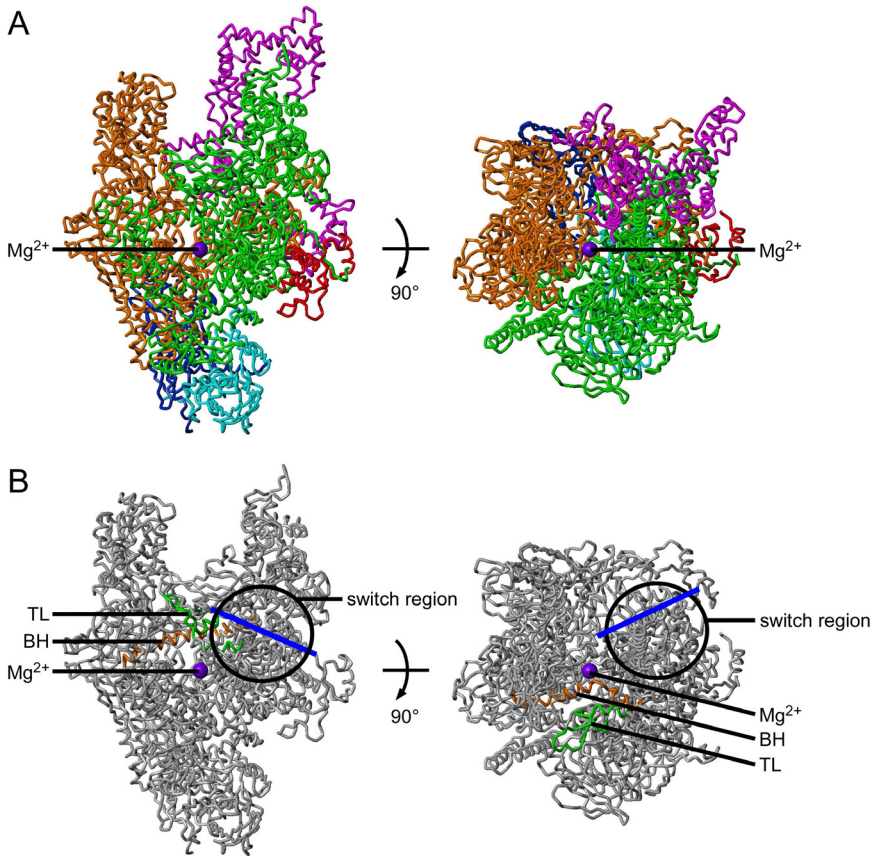

Figure 1. Structure of bacterial RNAP

(A) Two orthogonal views highlighting the different RNAP subunits in the crystal structure of *Thermus thermophilus* RNAP holoenzyme, (PDB 2CW0). The β′ non-conserved region is omitted for clarity. The left panel view is looking through the RNAP secondary channel. Green, β′ subunit; orange, β subunit; blue, α^{I} subunit; aqua, α^{II} subunit; red, omega subunit; magenta, σ^{70} subunit; violet sphere, active-center Mg^{2+}.

(B) Simplified view of bacterial RNAP highlighting several important structural components, including the bridge helix, trigger loop (TL), switch region, and RNA exit channel. The view orientation here is identical to that in panel (A), but with the σ^{70} subunit omitted for clarity. This view will be used as a starting point for figures throughout this thesis. Orange, bridge helix (BH); green, trigger loop (TL); black circle, switch region; blue line, RNA exit channel; violet sphere, active-center Mg^{2+}.

The "core" bacterial RNAP enzyme, (which is capable of non-specific, promoter-independent transcription), is composed of five subunits (α^{I}, α^{II}, β, β′, and ω) (Figure 1A; these view orientations will be used throughout the rest of this dissertation, unless noted otherwise) (Zhang et al., 1999; Minakhin et al., 2001; Vassylyev et al., 2002). The largest subunit, the β′ subunit, forms one of the pincers and part of the base of the active-center cleft. The second largest subunit, the β subunit, forms the other pincer and part of the base of the active-center cleft. Both the β′ subunit and the β subunit interact with DNA

and the RNA product during transcription (Korzheva et al., 2000; Naryshkin et al., 2000; Mekler et al., 2002; Vassylyev et al., 2007a; Zhang et al., 2012). Parts of these two subunits perform the catalytic activity of RNAP, i.e. phosphodiester bond formation (Zhang et al., 1999; Korzheva et al., 2000; Sosunov et al., 2003).

The two α subunits of RNAP are located distal to the active-center cleft with the α^{I} subunit primarily contacting the β subunit and the α^{II} subunit primarily contacting the β′ subunit. The α subunits help to initiate assembly of the RNAP subunits, and sometimes also interact with transcriptional regulators, (like catabolite gene activator protein [CAP]) (Wang et al., 1997, Naryshkin et al., 2000; Hudson et al., 2009). The smallest subunit, the ω subunit, is located near the base of the β′ pincer, distal to the active-center cleft. The ω subunit is not essential to RNAP function, but helps to stabilize the enzyme (Minakhin et al., 2001).

The β′ pincer is also known as "the clamp." The clamp is able to rotate, causing the active-center cleft to be open, (and accessible to duplex DNA), or closed, (inaccessible to duplex DNA) (Cramer et al., 2001; Gnatt et al., 2001; Murakami and Darst, 2003; Mukhopadhyay et al., 2008; Chakraborty et al., 2012). Opening and closing of the clamp is controlled through a "hinge" located at its base, known as "the switch region" (Figure 1B; Cramer et al., 2001; Gnatt et al., 2001; Mukhopadhyay et al., 2008). Three bacterial RNAP inhibitors that target the switch region, (myxopyronin, corallopyronin, and ripostatin), lock the β′ clamp in a partly-to-fully closed state, preventing duplex DNA from entering the active-center cleft and, thereby, inhibiting transcription (Mukhopadhyay et al., 2008; Srivastava et al., 2011; Chakraborty et al., 2012).

At the base of the active-center cleft sits the active-center Mg^{2+} ion (Figure 1). This Mg^{2+} ion is coordinated by three universally conserved aspartic acid residues (Zhang et al., 1999; Sosunov et al., 2003). Near the active-center Mg^{2+} ion, there are two critical structural features of the RNAP active center: the bridge helix and the trigger loop (Figure 1B; Cramer et al., 2001; Gnatt et al., 2001; Vassylyev et al., 2002). These structures are believed to undergo conformational changes, (bending, opening/closing), that are essential for transcription (Cramer et al., 2001; Gnatt et al., 2001; Bar-Nahum et al., 2005; Vassylyev et al., 2007b; Nudler, 2009). The bacterial RNAP inhibitor streptolydigin targets the bridge helix and trigger loop (Tuske et al., 2005; Temiakov et al., 2005; Vassylyev et al., 2007b; Ho et al., 2009). It traps the bridge helix in a straight (unbent, helical) conformation, and traps the trigger loop in an open (unfolded) conformation. It thereby prevents structural changes necessary for transcription.

In addition to the active-center cleft, the RNAP enzyme contains two other primary channels. The "secondary channel" is formed by parts of both the β′ and β subunits (Figure 1; Zhang et al., 1999; Ebright, 2000; Korzheva et al., 2000). This channel connects the active-center Mg^{2+} ion of the enzyme to the external environment, even when the active-center cleft is occupied by DNA. Nucleotide triphosphates, (NTPs), enter the active center through this channel during transcription. The bacterial RNAP inhibitor microcin J25 functions by blocking this channel; thereby preventing NTPs from accessing the active center and being incorporated into RNA (Mukhopadhyay et al., 2004).

The other major channel within the RNAP enzyme is the "RNA exit channel" (traced with a blue line in Figure 1B; Ebright, 2000; Korzheva et al., 2000; Vassylyev et

al., 2002). The RNA exit channel is formed by parts of both the β′ and β subunits. Some of the switch region residues actually line part of this channel which connects the exterior of the enzyme to the active-center cleft (Srivastava et al., 2011). As is suggested by its name, this is the channel through which the RNA product is threaded during transcription.

As mentioned earlier, the core enzyme of bacterial RNAP is fully capable of performing non-specific, promoter-independent transcription. However, in order to perform specific, promoter-dependent transcription, bacterial RNAP requires an additional subunit, the σ subunit, forming the bacterial RNAP "holoenzyme" (Figure 1A; Record et al., 1996). Bacterial cells can express a number of different σ subunits depending on environmental and physiological conditions. The primary σ subunit used by healthy, exponentially growing *E. coli* cells is the σ^{70} subunit, (the 70 refers to the approximate molecular weight of the subunit in kDa.)

The σ subunit can be further divided into four conserved regions: σR1, σR2, σR3, and σR4 (Campbell et al., 2002; Mekler et al., 2002; Vassylyev et al., 2002). Of particular note here are σR1.1 and the σR3-σR4 linker. σR1.1 is highly flexible and highly negatively charged. It is believed to lie in the active-center cleft and act as a DNA mimic, helping to stabilize the interaction of the σ subunit with the core enzyme until it is displaced by DNA (Mekler et al., 2002). The σR3-σR4 linker is also negatively charged and lies in the RNA exit channel (Murakami et al., 2002a; Vassylyev et al., 2002). The σR3-σR4 linker is thought to act as an RNA mimic, helping to stabilize interactions between the σ subunit with the core enzyme (Mekler et al., 2002). The σR3-σR4 linker must eventually be displaced from the RNA exit channel during transcription by the

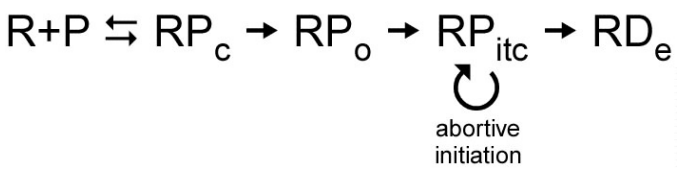

Figure 2. Simplified schematic of transcription

extending RNA product (Mekler et al., 2002; Murakami et al., 2002a). This is believed to weaken the interaction between the σ subunit and the core enzyme, potentially leading to its release from the complex.

Transcription

Transcription is the process by which RNAP synthesizes RNA from a DNA template. This is an essential function in all cells, such that inhibition of transcription can lead to cell death. Transcription can occur through both promoter-independent and promoter-dependent mechanisms. We will focus on promoter-dependent transcription here. Promoter-dependent transcription can be divided into three primary stages: initiation, elongation, and termination (Record et al., 1996; deHaseth et al., 1998; Murakami and Darst, 2003; Saecker et al., 2011).

During transcription initiation, the RNAP holoenzyme first binds to a promoter region on DNA, forming the RNAP-promoter closed complex (RP_c) (Figure 2). Bacterial DNA promoters contain a -10 element and a -35 element (Record et al., 1996; deHaseth et al., 1998). These elements are located ~10 and ~35 nucleotides upstream of the transcription start site, respectively. σR1.2 and σR2 make specific interactions with the -10 element, while σR4 makes specific interactions with the -35 element (Mekler et al., 2002; Murakami et al., 2002b; Vassylyev et al., 2002). These interaction between the σ

subunit and the promoter DNA, hold RNAP in position on the promoter during initiation, preventing it from translocating.

After binding, the double-stranded promoter DNA is inserted into the active-center cleft of RNAP, displacing σR1.1, and forming the RNAP-promoter intermediate complex (RP_i) (Murakami and Darst, 2003). This complex isomerizes whereby the β′ clamp, (which must be open to allow double-stranded DNA into the cleft), closes to stabilize the complex (Chakraborty et al., 2012); and the promoter DNA is unwound to form a ~12 nucleotide bubble of single-stranded DNA (Saecker et al., 2011; Zhang et al., 2012). This results in the RNAP-promoter open complex (RP_o) (Figure 2).

Once RP_o has formed, RNA synthesis can begin with the enzyme transitioning into the initial transcribing complex (RP_{itc}) (Figure 2). This step of transcription initiation is referred to as abortive initiation. During this stage RNAP undergoes iterative cycles of RNA synthesis, producing short, abortive RNA transcripts, 2-10 nucleotides in length (Kapanidis et al., 2006; Revyakin et al., 2006). This occurs by a process known as scrunching, whereby RNAP remains fixed on the –10 and –35 promoter elements of the DNA, while downstream DNA is pulled, ("scrunched"), into the active center (Kapanidis et al., 2006; Revyakin et al., 2006).

Once a sufficiently long RNA transcript is produced, (~9-11 nucleotides in length), the σ subunit can be released, or its interactions with the core RNAP enzyme are at least weakened (Record et al., 1996; Murakami and Darst, 2003; Mooney et al., 2005; Saecker et al., 2011). (As mentioned earlier, RNA passing through the RNA exit channel is thought to displace the σR3-σR4 linker, and destabilize the binding of the σ subunit to the core enzyme [Mekler et al., 2002; Murakami et al., 2002a; Murakami and Darst,

2003].) This begins the transcription stage of elongation. RNAP, now as an elongation complex (RD_e), is free from the upstream promoter DNA elements, and can translocate down the DNA synthesizing an RNA transcript (Figure 2; Record et al., 1996; Richardson and Greenblatt, 1996).

RNA synthesis can be terminated by one of two mechanisms (Richardson and Greenblatt, 1996; von Hippel, 1998). In the first mechanism, intrinsic termination sequences in DNA result in the formation of an RNA hairpin when transcribed. This hairpin secondary structure stalls the RD_e complex, such that a subsequent (weak-bonding) poly-uracil sequence will destabilize the complex, resulting in the release of the RNA transcript (Richardson and Greenblatt, 1996; von Hippel, 1998; Nudler, 1999). In the second mechanism, an additional termination factor protein is involved. The best understood termination factor, Rho, binds to a specific sequence of the RNA transcript and forces the RD_e complex to dissociate, releasing the RNA transcript (Richardson and Greenblatt, 1996; von Hippel, 1998).

Bacterial RNAP inhibitors and their targets

There are several bacterial RNAP inhibitors whose functional targets are known, including, streptolydigin, microcin J25, CBR703, myxopyronin, corallopyronin, and ripostatin. There are, however, only two classes of bacterial RNAP inhibitors that are currently approved for clinical use as antibiotic drugs: the rifamycins (which includes Rif) and, more recently, lipiarmycin. (Lipiarmycin will be discussed later in its own chapter.)

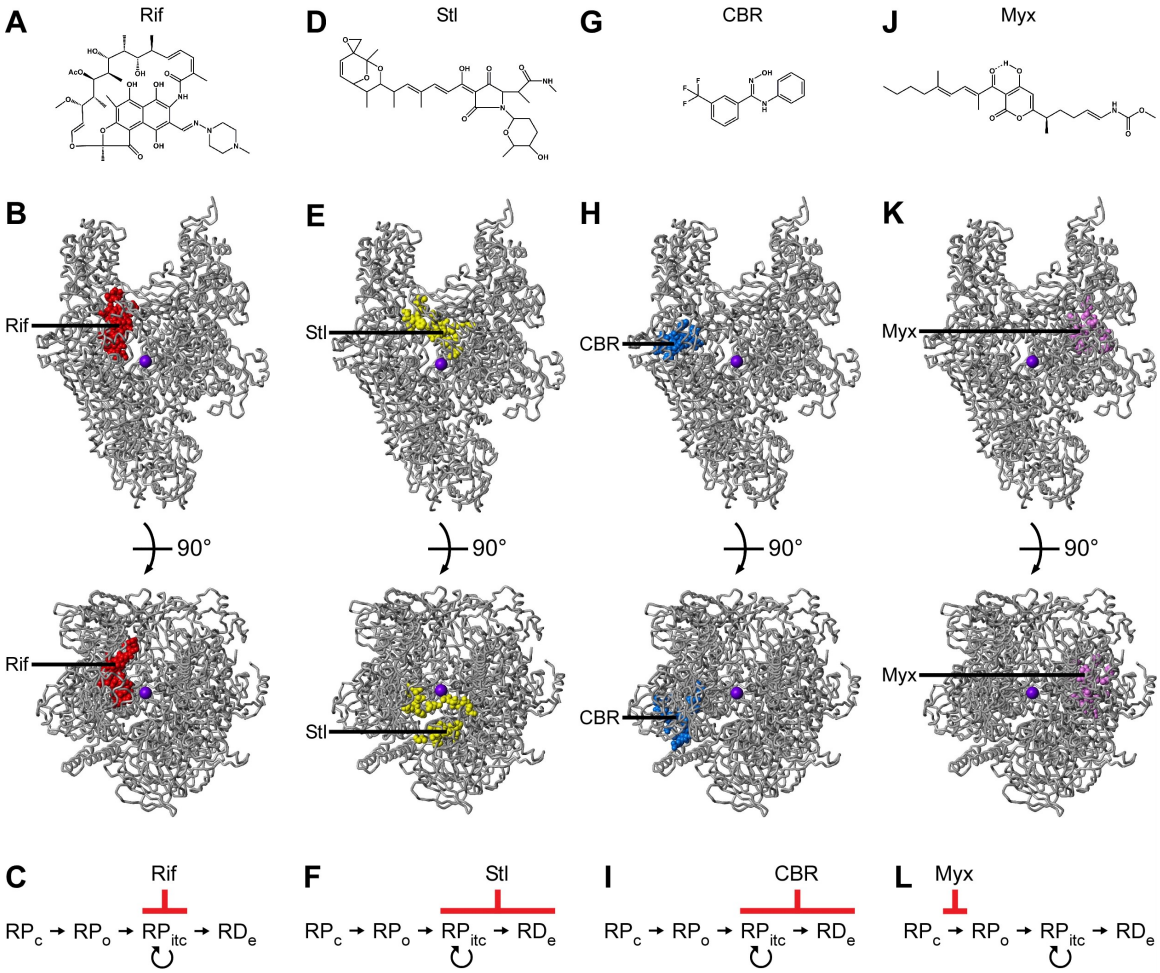

Figure 3. Structures, targets, and mechanisms of select bacterial RNAP inhibitors

(A-C) Rifamycins. (A) Structure of rifampin (Rif). (B) Target of Rif. Red spheres, sites of substitutions conferring resistance to Rif in *E. coli*. Sorangicin also binds to this site. (C) Rif inhibits the RNAP initial transcribing complex (RP_{itc}).

(D-F) Streptolydigin. (D) Structure of streptolydigin (Stl). (E) Target of Stl. Yellow spheres, sites of substitutions conferring resistance to Stl in *E. coli*. (F) Stl inhibits transcription initiation and elongation.

(G-I) CBR703. (G) Structure of CBR703 (CBR). (H) Target of CBR. Blue spheres, sites of substitutions conferring resistance to CBR in *E. coli*. (I) CBR inhibits transcription initiation and elongation.

(J-L) Myxopyronin. (J) Structure of myxopyronin B (Myx). (K) Target of Myx. Pink spheres, sites of substitutions conferring resistance to Myx in *E. coli*. (L) Myx inhibits the formation of RNAP-promoter open complex (RP_o).

The rifamycins are macrocyclic antibiotics first isolated from *Amycolatopsis mediterranei* (originally *Streptomyces mediterranei*) soil bacterium in 1957 by the Lepetit Pharmaceutical Group in Milan, Italy (Sensi et al., 1959; reviewed in Sensi, 1983). Over the following decades, a number of semisynthetic rifamycin derivatives were made

having improved potency over the naturally-occurring compounds (Sensi, et al., 1964; Maggi, et al., 1965; Lester, 1972). These semisynthetic derivatives include several that are currently in clinical use: rifampin (Rif; Figure 3A), rifapentine, rifabutin, and rifaximin (reviewed in Aristoff et al., 2010). All of the rifamycins function by binding to and inhibiting bacterial RNAP through the Rif target located near the RNAP active center (Figure 3B; Hartmann, 1967; Wehrli and Staehelin, 1971; Ovchinnikov et al., 1983; Lisitsyn et al., 1984, 1985; Severinov et al., 1993, 1994; Jin and Gross, 1988; Campbell, et al., 2001; Garibyan et al., 2003; Ho et al., 2009). (The macrolide antibiotic sorangicin also functions through this target [Campbell et al., 2005].) These compounds sterically block the formation of RNA chains longer than 2-3 nucleotides in length, thereby inhibiting transcription during the abortive initiation stage (Figure 3C; McClure and Cech, 1978; Campbell et al., 2001; Feklistov et al., 2008).

Of the bacterial RNAP inhibitors not in clinical use, streptolydigin was one of the first identified. Streptolydigin (Stl) is a tetramic-acid antibiotic originally isolated from *Streptomyces lydicus* in 1955 by the Upjohn Company in Kalamazoo, Michigan (Figure 3D; Crum et al., 1956). Stl binds to a site adjacent to the RNAP active center, locking the bridge helix in a straight (unbent, helical) conformation and trapping the trigger loop in an open (unfolded) conformation (Figure 3E; Heisler et al., 1993; Severinov et al., 1995; Tuske et al., 2005; Temiakov et al., 2005; Vassylyev et al., 2007b; Ho et al., 2009). This prevents the conformational cycling needed for phosphodiester bond formation. Stl can inhibit bacterial RNAP during both initiation and elongation (Figure 3F; Siddhikol et al., 1969; Cassani et al., 1971).

Microcin J25 is a 21-residue lariat peptide antibiotic isolated in 1992 by researchers in Argentina from the fermentation culture of a fecal *Escherichia coli* strain (Salomón and Farías, 1992; Bayro et al., 2003). Microcin J25 binds within the secondary channel of bacterial RNAP, obstructing the uptake of NTPs, and, thereby, inhibiting both transcription initiation and elongation (Delgado et al., 2001; Yuzenkova et al., 2002; Mukhopadhyay et al., 2004).

CBR703 (and its derivatives) is a small molecule identified in a 2003 large-scale chemical library screen for inhibitors of *E. coli* RNAP by the Landick lab in collaboration with Cumbre Pharmaceuticals (Figure 3G; Artsimovitch et al., 2003). CBR703 functions through a target adjacent to the RNAP active center (Figure 3H; Artsimovitch et al., 2003; Xinyue Wang and R.H.E., unpublished). It is believed to allosterically inhibit the catalytic activity of the enzyme during both initiation and elongation (Figure 3I; Artsimovitch et al., 2003).

Finally, myxopyronin (Myx; Figure 3J), corallopyronin (Cor), and ripostatin (Rip), as mentioned earlier, inhibit bacterial RNAP by binding to a site in the switch region (Figure 3K; Belogurov, et al., 2008; Mukhopadhyay et al., 2008; Ho et al., 2009; Srivastava et al., 2011). Myx is an alpha-pyrone antibiotic originally isolated in 1983 from the soil myxobacterium *Myxococcus fulvus* Mxf50 (Irschik et al., 1983). Cor is also an alpha-pyrone antibiotic that was originally isolated in 1985 from the soil myxobacterium Corallococcus coralloides Cc c127 (Irschik et al., 1985). Rip is a macrocyclic-lactone antibiotic isolated in 1995 from the soil myxobacterium Sorangium cellulosum So ce377 (Irschik et al., 1995). Each of these inhibitors functions by locking

the β′ clamp of bacterial RNAP in a partly-to-fully closed state, thereby preventing RP_o formation (Figure 3L; Mukhopadhyay et al., 2008; Chakraborty et al., 2012).

The study of these various bacterial RNAP inhibitors has led not only to the identification of several different inhibitory targets within the enzyme, but also to a better understanding of how bacterial RNAP functions. As with the bacterial RNAP inhibitors being studied in this work, (lipiarmycin, GE23077, and salinamide), this information could be utilized in the development new antibacterial drugs that function by inhibiting bacterial RNAP.

Chapter 2:
Methods

The functional determinants of the three bacterial RNAP inhibitors being studied here, (lipiarmycin, GE23077, and salinamide), were identified through the isolation and characterization of inhibitor-resistant mutants. Resistant mutants were isolated by spontaneous resistance, saturation mutagenesis, or induced mutagenesis. Once isolated, the *rpoB* and/or *rpoC* genes of the resistant mutants were sequenced in order to identify any substitutions in the β and/or β′ subunits of RNAP respectively. Resistant mutants were then characterized through extensive measurements of their resistance levels as well as their cross-resistance with other known bacterial RNAP inhibitors, (always including rifampin). In the case of lipiarmycin and GE23077, select chromosomal resistance mutations were also characterized by determining their biological fitness costs. In conjunction with *in vitro* studies into the mechanisms of these inhibitors, and, when available, the crystal structures of these inhibitors in complex with bacterial RNAP, this work provides extensive insights into three new targets for the inhibition of bacterial RNAP.

Antibiotics

Lipiarmycin and GE23077 were provided by Stefano Donadio at NAICONS, (New Anti-Infectives Consortium), in Milan, Italy. More recently, lipiarmycin has also been purchased, (as fidaxomicin), from BioAustralis. Salinamide was provided by William Fenical from the Scripps Institution of Oceanography, having been prepared from cultures of *Streptomyces* sp. CNB-091 as in Moore et al., 1999. Rifampin was

purchased from Sigma-Aldrich. Streptolydigin was previously provided to the lab by E. Steinbrecher of Pharmacia & Upjohn in Kalamazoo, MI, and was also purchased from Sourcon-Padena. CBR703 was purchased from Ryan Scientific. Myxopyronin A was provided by Rolf Jansen and Herbert Irschik, having been prepared as in Irschik et al., 1983. Myxopyronin B was provided by Yon Ebright, having been synthesized as in Hu et al., 1998. (Myxopyronin A was used when studying lipiarmycin in *Escherichia coli*. All other studies involving myxopyronin in this work used myxopyronin B.)

Most of these compounds were dissolved in methanol for experiments. GE23077 was dissolved in water for most experiments, but was dissolved in methanol for electrophoretic mobility shift assays and abortive initiation assays.

Strains

Much of the work presented here was performed in the hyper-sensitive *Escherichia coli* strain, D21f2*tolC::*Tn*10* (*tolC210*::Tn*10 rfa proA23 lac28 trp30 his51 rpsL173 tsx81 ampC*) (Fralick and Burns-Keliher, 1994). This strain contains two primary outer membrane defects that result in increased susceptibility to hydrophobic agents, including antibacterial compounds.

The first defect is known as a "deep rough" (*rfa*) mutation that results in the loss of heptose from the cell's outer-membrane lipopolysaccharides (Fralick and Burns-Keliher, 1994). This mutation increases the permeability of the bacterial cells to hydrophobic compounds (Fralick and Burns-Keliher, 1994; Tuske et al., 2005; Mukhopadhyay et al., 2008; Ebright lab, unpublished). The second defect is a Tn10 insertion mutation of the *tolC* gene which disrupts the TolC protein. The TolC protein is

an outer membrane channel used by efflux pumps in order to remove toxic materials, including antibacterial compounds, from the bacterial cell (reviewed in Blair and Piddock, 2009). Disruption of this channel results in a build-up of these compounds within the cell.

The combination of the *rfa* influx defect with the *tolC* efflux defect makes this strain an excellent tool for the study of antibacterial agents. In cases where compounds have particularly poor permeability, *E. coli* D21f2tolC is one of the few strains that can be used to study the compound. (This is the case with GE23077.) In addition, D21f2tolC often allows for the use of much lower RNAP inhibitor concentrations than would be required when using other bacterial strains. This is particularly helpful when an inhibitor is in limited supply, as is often the case.

Staphylococcus aureus ATCC 12600 was also used in the study of lipiarmycin. This strain provided a pathogenic organism in which to confirm lipiarmycin's target as well as to assess the biological fitness of lipiarmycin-resistant mutants.

Streptococcus pyogenes ATCC 12344 was used in the study of GE23077. This strain provided a pathogenic organism in which to further confirm GE23077's target.

All bacterial species used in this work, (other than *E. coli* D21f2tolC) were obtained from the American Type Culture Collection.

All experiments involving *E. coli* D21f2tolC were performed in standard Luria broth (LB) and LB agar (Sambrook and Russell, 2001) under aerobic conditions. All experiments involving *S. aureus* were performed in Mueller-Hinton II cation-adjusted (MH) broth and MH agar (BD Biosciences). All GE23077-related experiments involving *S. pyogenes* were performed with Todd-Hewitt broth (THB; BD Biosciences) and THB

agar [THB supplemented with 1.5% Bacto Agar (BD Biosciences)] under a 7% CO_2/6% O_2/4% H_2/83% N_2 atmosphere.

Plasmids

Plasmid pRL706 carries the *E. coli rpoB* gene, encoding a C-terminal hexahistidine-tagged β subunit under control of the *trc* promoter (Severinov et al., 1997). Plasmid pRL663 carries the *E. coli rpoC* gene, encoding a C-terminal hexahistidine-tagged β′ subunit under control of the *tac* promoter (Wang et al., 1995). These two plasmids were used in the construction of saturation mutagenesis libraries as well as in the purification of RNAP enzymes.

Plasmid pKD46 was used for lambda red-mediated recombineering (Datsenko and Wanner, 2000). This plasmid carries the Red genes of lambda bacteriophage, (*gam*, *bet*, and *exo*), under the control of the arabinose-inducible promoter, *araB*. Importantly, this plasmid also has a temperature-sensitive origin of replication, *repA101ts*, which prevents replication of the plasmid at temperatures at or above 37°C.

RNAP

Both wild-type and mutant *E. coli* RNAP enzymes were prepared essentially as in Niu et al., 1996. Enzymes harboring substitutions in the β subunit were purified from *E. coli* strain XE54 (*lac*$^+$ *thi*; Tang et al., 1994) transformed with pRL706 derivatives. Enzymes harboring substitutions in the β′ subunit were purified from *E. coli* strain 397c (*rpoC*^{ts}397 *argG thi lac* [λcI$_{857}$h$_{80}$S$_{t68}$d*lac*$^+$]; Christie et al., 1996) transformed with pRL663 derivatives. (Strain 397c has a temperature sensitive mutation in the rpoC

subunit.) Wild-type *E. coli* RNAP enzyme was purified from either of these *E. coli* strains in the same manner.

Briefly, a 3 L culture of 4x LB containing 170 mM NaCl and 200 μg/ml ampicillin was grown to mid-log phase and induced with 1 mM IPTG. Following an additional 3 h of growth, cells were harvested and pelleted. The pellet was then resuspended in a lysis buffer, and lysed by emulsification (Emusiflex-C5, Avestin). Protein was then precipitated out of the lysate with polyethyleneimine (Polymin P), washed several times in buffer, and precipitated with ammonium sulfate. Following resuspension, the pellet was applied to a Ni-NTA column and the his-tagged RNAP enzyme was eluted with increasing imidazole concentrations. The RNAP enzyme is then further purified by separation on a MonoQ (GE Healthcare) column. The purified enzyme is stored at –80°C in a solution of 55% glycerol, 5 mM Tris-HCl (pH 7.9), 150 mM NaCl, 0.05 mM EDTA, and 2.5 mM DTT.

Wild-type *E. coli* RNAP holoenzyme was also sometimes purchased from Epicentre.

Macromolecular synthesis

Macromolecular synthesis assays were performed with salinamide in order to determine its mechanism of action within bacterial cells (methods developed from King and Wu, 2009). Using radiolabeled precursors for DNA, RNA, and proteins, the synthesis of these molecules in cells could be tracked over time in the presence and absence of salinamide. This assay can provide direct evidence for the functional cellular target of an antibacterial compound.

E. coli D21f2tolC cells were grown to mid-log phase, adjusted to a cell density of ~$4x10^7$ cfu/ml, and mixed with either ^{14}C-thymidine (>50 mCi/mmol), ^{14}C-uridine (60 mCi/mmol), or ^{14}C-L-amino acid mix (>50 mCi/mmol) (all from Perkin Elmer; final concentrations of 0.25 μCi/ml, 1 μCi/ml, and 2 μCi/ml, respectively) in a volume of 97 μL. The cells were then incubated for 10 min at 37°C with shaking to equilibrate. Following this incubation, 3 μL of salinamide (or methanol alone) was added to a final concentration of 2x the minimum inhibitory concentration (MIC). (As will be discussed later, the MIC value is defined here as the concentration of inhibitor required to inhibit ≥90% of cell growth in a 16 h culture.) These cultures were then grown at 37°C with shaking, and terminated at various time points (0, 10, 20, or 30 min) by adding the entire 100 μL culture volume to an equal volume of cold 10% trichloroacetic acid (TCA). This mixture was incubated on ice at 4°C with occasional swirling for 1 h in order to precipitate the macromolecules.

All of the reaction conditions described above were tested in parallel on a 96-well plate in quadruplicate. Following the 1 h incubation on ice, the 96-well plate was placed in a Packard Filtermate 196 cell harvester and the solution drawn through a pre-wet glass fiber filter (printed filtermat A, Perkin Elmer). (The large, precipitated macromolecules adhere to the filter, while the soluble, unincorporated, radiolabeled precursors do not.) The filter was then washed twice with 5% TCA, followed by three times with water, and then twice more with 10% ethanol. After drying under a heat lamp for at least 15 min, the filter is exposed to a phophorimaging screen for 16-18 h, and quantified using a Typhoon phosphorimager (GE Healthcare). Results were compared to reactions performed with Rif under identical conditions. In addition, t-tests were performed for each data point to

compare reactions in the presence of inhibitor with those in the absence of inhibitor, (using SigmaPlot software; SPSS). A p-value of less than 0.01 was considered to be a statistically significant difference.

Spontaneous resistance: rates

Spontaneous resistant mutants were identified in fluctuation assays where a defined number of cells, (~$1x10^9$ cfu/plate), were plated onto media containing an RNAP inhibitor at a concentration 2x or 4x the MIC (methods essentially as in Srivastava et al., 2012) (Luria and Delbrük, 1943; Lea and Coulson, 1949; Foster, 2006; Young, 2006). Plates were then incubated for at least 24 hours at 37°C. The resulting inhibitor-resistant colonies were counted for each concentration and time point being tested. Resistance rates were calculated using the Ma-Sandri-Sarkar maximum-likelihood estimator (MSS-MLE; Ma et al., 1992; Sarkar et al., 1992) as implemented on the Fluctuation Analysis Calculator website (FALCOR [http://www.keshavsingh.org/protocols/FALCOR.html]; Hall et al., 2009).

This MSS-MLE method provides a more accurate assessment of resistance than a typical spontaneous resistance "frequency" calculation, (i.e., the number of resistant colonies divided by the number of cfu plated) (Stewart et al., 1994; Foster, 2006). Spontaneous resistance frequencies are easily biased by the occurrence of "jackpot" mutations, i.e. when a resistance mutation occurs during an early cell division cycle in a bacterial culture, leading to many duplicate colonies of this resistant mutant being counted on the screening plate. This results in an unusually high spontaneous resistance frequency for certain cultures, ultimately over-estimating the true resistance rate. The

MSS-MLE algorithm utilizes a probability algorithm to overcome this outlier effect, and produce a more accurate resistance rate.

Spontaneous resistance: isolation and sequencing

Any potential resistant mutants identified during the fluctuation assays were restreaked on inhibitor-containing media in order to confirm resistance. Glycerol stocks were prepared for all resistant mutants, and genomic DNA was purified using a Wizard Genomic DNA purification kit, (Promega). The *rpoB* and *rpoC* genes were then amplified by Taq PCR from this genomic DNA using the appropriate primers (Table SA1 in Appendix SA) (methods essentially as in Srivastava et al., 2012). (In some cases, the purification of genomic DNA could be skipped with PCR proceeding directly from a small, overnight culture aliquot of a resistant mutant.) All PCR products were resolved on an agarose gel, and extracted from gel slices using a Gel/PCR DNA Fragments Extraction Kit (IBI Scientific). Purified PCR products were then submitted for standard Sanger sequencing (seven or eight primers per gene; using sequencing facilities at the University of Washington, Genewiz, or Genscript). Mutations were then identified by comparison to the wild-type *rpoB* and *rpoC* gene sequences.

**Note: All mutations identified in this text will be numbered as in *E. coli* RNAP for consistency. This applies even when mutations are identified in a bacterial species other than *E. coli*.

Saturation mutagenesis

Saturation mutagenesis was performed by transforming *E. coli* D21f2tolC cells with a library of either pRL706 or pRL663 plasmids containing mutagenized versions of the *rpoB* or *rpoC* genes (methods essentially as in Mukhopadhyay et al., 2004; Tuske et al., 2005; Mukhopadhyay et al., 2008). The *rpoB* and *rpoC* genes were mutagenized using "doped" PCR primers designed to provide all possible amino acid substitutions within a desired region of the genes, typically covering all residues within 30Å of the suspected target of an inhibitor, (sets and sequences in Tables SA2-SA4).

Doped, (nucleotide mis-incorporated), primers were synthesized using solid-phase β-cyanoethylphosphoramidite chemistry on an AB392 automated synthesizer (Applied Biosystems). Doped primers generally contained a central doped region of 15-30 nucleotides flanked by non-doped, (100% correct), regions, 10-15 nucleotides in length, on either end of the primer. Doped regions less than ~18 nucleotides in length were synthesized using a mixture of 92% of the correct phophoramidite and 8% of a 1:1:1:1 mixture of dA, dC, dG, and dT phosphoramidites at each position. Doped regions greater than 18 nucleotides in length were synthesized using a mixture of 98% of the correct phosphoramidite and 2% of a 1:1:1:1 dA, dC, dG, and dT phosphoramidites at each position. These amounts of doping were selected so as to ultimately generate ~0.4-1 amino acid substitutions per molecule of PCR primer (Hermes et al., 1989, 1990).

Once synthesized, a doped primer was paired with its non-doped complement and used with a QuikChange Site-Directed Mutagenesis kit (Stratagene/Agilent) in order to mutagenize pRL706 (*rpoB*) or pRL663 (*rpoC*). *E. coli* XL1-Blue cells (Stratagene/ Agilent) were then transformed with the mutagenezied plasmid DNA, grown in LB at

37°C for ~1.5 h with shaking, plated on LB-agar containing 200 μg/ml ampicillin, and the plates were grown overnight at 37°C. The resulting colonies were counted (aiming for more than 6000 colonies per primer pair), pooled together, and purified using a plasmid DNA purification kit (Qiagen or Sigma). This forms one passaged mutagenesis library and was done for each doped primer that was synthesized.

Passaged mutagenesis libraries were mixed into sets appropriate for the inhibitor being studied (Tables SA2-SA4), and introduced into *E. coli* D21f2tolC by transformation. These cells were grown in LB containing 200 μg/ml ampicillin for 1 h with shaking at 37°C. Expression of the mutagenized *rpoB* or *rpoC* genes was then induced by the addition of 1 mM IPTG, and the cells grown for an additional 1.5 h at 37°C. The transformants (~10^3 cfu/plate) were plated on LB containing 200 μg/ml ampicillin, 1 mM IPTG, and the RNAP inhibitor being studied at a concentration just above its MIC, (≤ 2x the MIC). These plates were incubated for 16-48 h at 37°C. Potential resistant mutants were further restreaked two more times on the same media from which they were isolated in order to confirm their resistance. Isolates were then grown for 16 h at 37°C in LB containing 200 μg/ml ampicillin, and their plasmid DNA purified using a plasmid DNA purification kit. Purified plasmids were submitted for standard Sanger sequencing (eight primers per gene; using sequencing facilities at the University of Washington or Genewiz).

Induced mutagenesis

In studying Sal, it was desirable to obtain plasmid-based Sal-resistant mutants in order to further confirm that mutations within the *rpoB* and *rpoC* genes were solely

responsible for resistance to Sal. Since I am only sequencing the *rpoB* and *rpoC* genes from the chromosomes of spontaneous Sal-resistant mutants, I cannot guarantee that there are not mutations elsewhere on their chromosomes that contribute to their Sal resistance. The isolation of induced Sal-resistant mutants on plasmids allows for a Sal-resistant mutation in either *rpoB* or *rpoC* to be observed and analyzed in a wild-type *E. coli* D21f2tolC background.

These experiments were performed analogously to the saturation mutagenesis experiments described above except that a master mutagenesis pool, rather than a set of passaged mutagenesis libraries, for *rpoB* or for *rpoC* was introduced into D21f2tolC by transformation. This master mutagenesis pool consisted of the passaged saturation mutagenesis libraries from Mukhopadhyay et al., 2004, Tuske et al., 2005, and Mukhopadhyay et al., 2008, pooled together, and mixed in a 1/1 (w/w) ratio with a random mutagenesis library, (generated essentially as described in Mukhopadhyay et al., 2008; see supplemental method in Appendix SA).

Saturation (and induced) mutagenesis: mutant confirmation

All plasmids isolated by saturation mutagenesis were further analyzed in order to confirm that the mutated *rpoB* or *rpoC* genes that they expressed were responsible for their RNAP inhibitor resistance. In many cases, the plasmids were digested with restriction enzymes to cut out the *rpoB* or *rpoC* gene. These PCR gene fragments were then purified by gel extraction, and reintroduced into the wild-type vector backbone of pRL706 or pRL663 accordingly by ligation. These subclones were then re-tested for inhibitor resistance. This process helped to ensure that any potential mutations on these

plasmids that were outside of the *rpoB* or *rpoC* genes, were not responsible for their inhibitor resistance. In all cases, the mutations in *rpoB* or *rpoC* were responsible for the inhibitor resistance of the plasmids.

Complementation assays were also performed in order to determine if the mutated *rpoB* and *rpoC* genes carried on the plasmids were sufficient to support cell viability (methods modified from Tuske et al., 2005). In order to do this, *E. coli* strains with temperature-sensitive, RNAP-subunit-linked phenotypes were used. Mutant pRL706 plasmids were transformed into RL585, a strain whose *rpoB* gene expression is temperature-sensitive, (*rpoB*^{am}*cI supD*^{ts}*43,74* Δ*[recA-srl]306 lacZ*^{am}*2110 galEK*^{am} *leu*^{am} *trp*^{am} *sueA rpsL tsx srl-301*::Tn*10-84*; Landick et al., 1990). The transformants were then grown overnight at 30°C, and plated on LB-agar containing 200 µg/ml ampicillin and 10 µg/ml tetracycline. These plates were incubated at 43°C for 24-48h, and compared to plates containing RL585 transformed with the wild-type pRL706 plasmid. Under these conditions, growth similar to that of the wild-type-transformed cells indicated that a mutant *rpoB* gene was sufficient to support viable cell growth.

For mutations in *rpoC*, mutant pRL663 plasmids were transformed into strain 397c, whose *rpoC* gene is temperature sensitive (genotype provided earlier in the "RNAP" methods section; Christie et al., 1996). The transformants were then grown overnight at 30°C, and plated on LB-agar containing 200 µg/ml ampicillin. These plates were incubated at 37°C for 24 h, and compared to plates containing 397c transformed with the wild-type pRL663 plasmid.

Mutant characterization: minimum inhibitory concentration (MIC)

The levels of resistance and cross-resistance for wild-type and mutant bacterial strains were determined by minimum inhibitory concentration (MIC) assays (methods essentially as in Srivastava et al., 2012). These assays were performed by either a standard broth microdilution assay or by a spiral exponential gradient assay (Wallace et al., 1989; Paton et al., 1990; Schalkowsky, 1994; CLSI, 2009a, 2009b). In both cases, cultures were inoculated with a single, well-isolated colony of the strain to be tested and grown to log phase (OD = 0.4-0.8). The cell density was then adjusted to either ~$5x10^5$ cfu/ml, in the case of broth microdilution assays, or ~$1x10^8$ cfu/ml, in the case of spiral gradient endpoint assays. In broth microdilution assays, 100 μL aliquots of the cells were treated with 2-fold serial dilutions of the RNAP inhibitor being tested and grown at 37°C with shaking for 16 h. The plates were then visually inspected and the MIC defined as the concentration at which 90% of cell growth was inhibited.

In spiral gradient endpoint assays, cells were swabbed radially onto plates containing an exponential gradient of the RNAP inhibitor being tested. These plates were prepared using an Autoplate 4000 spiral plater (Spiral Biotech) using a stock inhibitor concentration determined by the SGE software program (Spiral Biotech). Once swabbed, plates were incubated for 16 h at 37°C. The length of each streak was then measured using a plastic template (Spiral Biotech), and the MIC value was calculated by entering these length measurements into the SGE software. This software calculates the concentration of inhibitor present at the endpoint of a streak based on its location on the testing plate.

Broth microdilution assays were used in all testing of GE23077-resistant mutants and cross-resistance testing of GE23077. This is also true for all testing involving salinamide. Lipiarmycin resistance was measured using both broth microdilution assays spiral gradient endpoint assays. Lipiarmycin cross-resistance was measured using spiral gradient endpoint assays.

Mutant characterization: fitness costs

Lipiarmycin-resistant chromosomal mutants in *S. aureus* as well as GE23077-resistant chromosomal mutants in *E. coli* D21f2tolC were assessed for their fitness costs (Lenski, 1988; Wichelhaus et al., 2002). Mutations that confer resistance in bacteria often come at the cost of the cell's biological fitness. In the case of Rif, there is a strong correlation between the fitness cost of a resistance mutation and its clinical prevalence (Billington et al., 1999; Wichelhaus et al., 2002; Gagneux, et al., 2006; O'Neill et al., 2006; Comas et al., 2011; Srivastava et al., 2012). Rif-resistant mutations that have little to no fitness cost are the mutations most frequently identified in clinical specimens.

Pairwise-competition fitness assays were performed as in Wichelhaus et al., 2002 and Srivastava et al., 2012. Equal numbers (~10^3 cfu) of log-phase cells of a Lpm-resistant (or GE23077-resistant) mutant and its isogenic wild-type parent were mixed and grown for 20 h at 37°C with shaking. At time point zero and at 20 h, the number of Lpm-resistant (or GE20377-resistant) colonies and the number of isogenic wild-type parent colonies were determined by plating dilutions of the mixed culture, in parallel, on media containing Lpm (or GE23077; at a concentration greater than the MIC), and on media not containing Lpm (nor GE23077). These plates were incubated at 37°C for 24-40 h, and the

number of colonies counted. The number of isogenic wild-type parent colonies was determined by counting the total number of colonies on plates without inhibitor and subtracting the number of Lpm-resistant (or GE23077-resistant) colonies, (counted from the plates containing Lpm or GE23077). The number of generations of the resistant mutant (G_{mut}) and the isogenic wild-type parent (G_{wt}) could then be calculated as follows (Wichelhaus et al. 2002):

$G_{mut} = (\log B_{mut} - \log A_{mut})/\log 2$

$G_{wt} = (\log B_{wt} - \log A_{wt})/\log 2$

where A_{mut} and A_{wt}, are the number of cfu/ml for the mutant and wild-type parent, respectively, at time zero. B_{mut} and B_{wt} are the number of cfu/ml for the mutant and wild-type parent, respectively, at 20 h. The fitness cost (FC) for each mutant tested was then calculated as (Sander et al., 2002):

$FC = (1 - G_{mut}/G_{wt}) \times 100\%$

As indicated by the equation, the resulting fitness cost provides a direct evaluation of a mutant's ability to grow in the presence of the isogenic wild-type parent. Mutants that are able to grow as well as the wild-type parent have a fitness cost of zero, and a distinct advantage over mutants that have fitness costs.

Mutant characterization: lambda red-mediated recombination

Lambda red-mediated recombination was employed in order to transfer inhibitor-resistance mutations from plasmids onto the chromosome (reviewed in Sawitzke et al.,

2007). This system utilizes three proteins from the lambda bacteriophage, (Exo, Beta, and Gam), that are able to perform recombination between linear fragments of double-stranded DNA (dsDNA) and the *E. coli* chromosome. This process requires the linear dsDNA fragment to have at least 35 bp of homology on both of its ends to a region of the chromosome (Sawitzke et al., 2007). The Gam protein protects the linear dsDNA fragment from nuclease degradation. The Exo protein is an exonuclease that degrades one strand of the linear dsDNA fragment, leaving a single-stranded fragment; (or creates single-stranded 3' overhangs on either end of the linear dsDNA fragment) (Mosberg et al., 2010). The Beta protein helps to anneal this ssDNA fragment, (or the single-stranded ends of the partially-digested dsDNA fragment), to a complementary region on the chromosome (in place of an Okazaki fragment during DNA replication) (Mosberg et al., 2010).

A subset of plasmids isolated during saturation mutagenesis against lipiarmycin or GE23077 and carrying single-substitution, inhibitor-resistance mutations in *rpoB* or *rpoC* were selected for transfer onto the chromosome. (This was also done for select Rif-resistant and Myx-resistant plasmids [from Sajida Ismail, D.D., and R.H.E., unpublished; Mukhopadhyay et al., 2008].) PCR reactions were performed using these plasmids such that ~300 bp regions containing the mutated portion of either the *rpoB* or *rpoC* gene were amplified. These amplifications were performed such that at least 50 bp of wild-type homologous sequence existed on either side of any mutated bases. The resulting PCR fragments were resolved on an agarose gel, and extracted from gel slices using a Gel/PCR DNA Fragments Extraction Kit (IBI Scientific). The PCR fragments were often sequenced in order to confirm that they carried the expected mutation.

The three proteins of the lambda red system used here were expressed from the pKD46 plasmid (methods developed from Datsenko and Wanner, 2000). Chemically-competent *E. coli* D21f2tolC cells were prepared carrying this plasmid. These cells were then transformed by the addition of ~200 ng of purified PCR product. The transformants were grown for ~1.5 h at 37°C with shaking and plated on selective LB media containing 1x MIC of either lipiarmycin or GE23077, (depending on the mutation being recombineered). Plates were grown at 37°C for 24-48 h. Potential recombinants were restreaked on selective LB-agar containing 1x MIC of either lipiarmycin or GE23077 in order to confirm their resistance. In parallel, the colonies were also streaked on LB-agar containing 1 mM ampicillin in order to determine if they still harbored the pKD46 plasmid. Confirmed recombinants that still harbored the pKD46 plasmid were repeatedly restreaked on LB media and grown at 37°C for 24 h until the plasmid was lost. (This helps to avoid any potential future problems with continued non-specific, lambda-red-mediated recombination in these strains.)

Glycerol stocks were prepared of confirmed recombinants that no longer harbored the pKD46 plasmid. The chromosomal identities of these recombinants were confirmed by sequencing their genomic *rpoB* or *rpoC* genes as described earlier. Once on the chromosome, inhibitor resistance-mutations were again assessed for resistance levels, cross-resistance levels, and, when applicable, for fitness costs.

Transcription assays: human RNAP

Transcription experiments were performed with human RNAP in order to determine the selectivity of the RNAP inhibitors being studied here. For an RNAP

inhibitor to have potential as an antibiotic drug, it must be selective for bacterial RNAP without affecting human RNAP. Compounds that inhibit human RNAP, like alpha-amanitin from the death-cap mushroom, are highly toxic to humans (reviewed in Wieland and Faulstich, 1991; Bensaude, 2011).

The assay used here is a non-enzyme-specific measure of human RNAP activity. Human placental DNA is used as the template DNA. HeLa cell nuclear extract (Promega) is used as the source of human RNAP. This extract contains a mixture of all three human RNAPs, (hRNAP I, hRNAP II, and hRNAP III). In these assays most of the transcriptional activity (~60-70%) is generated by hRNAP II, (as indicated when testing against alpha-amanitin, which primarily inhibits RNAP II [Weinmann et al., 1974; Wieland and Faulstich, 1991; Bensaude, 2011]).

The assays were performed essentially as in Dignam et al., 1983 as well as Sawadogo and Roeder, 1985. Reaction mixtures contained (20 µl): 0-100 µM test compound, 8 U HeLaScribe Nuclear Extract (Promega), 1 µg human placental DNA (Sigma-Aldrich), 400 µM ATP, 400 µM [α^{32}P]UTP (0.11 Bq/fmol), 400 µM CTP, 400 µM GTP, 50 mM Tris-HCl (pH 8.0), 7 mM HEPES-NaOH, 70 mM $(NH_4)_2SO_4$, 50 mM KCl, 12 mM $MgCl_2$, 5 mM DTT, 0.1 mM EDTA, 0.08 mM phenylmethylsulfonyl fluoride, and 16% glycerol. Reaction components other than DNA and NTPs were pre-incubated for 10 min at 30°C. DNA was then added and reaction mixtures were incubated for 15 min at 30°C. RNA synthesis was initiated by the addition of NTPs and reaction mixtures were incubated for 60 min at 30°C. Reaction mixtures were spotted on DE81 filter discs (Whatman; pre-wet with water) and incubated for 1 min at room temperature. The filter discs were then washed (with 1 min incubations), three times with

3 ml 0.5M Na_2HPO_4, two times with 3 ml water, and one time with 3 ml 95% ethanol, using a filter manifold (Hoefer). Filter discs were then placed in liquid scintillation vials containing 10 ml ScintiVerse BD Cocktail (Thermo Fisher), and radioactivity was quantified by scintillation counting (LS6500; Beckman-Coulter). Half-maximal inhibitory concentrations (IC50s) were calculated by non-linear regression in SigmaPlot (SPSS).

RNAP-DNA interaction assays (RP_o formation)

Electrophoretic mobility shift assays were performed in order to determine if an inhibitor specifically affects the RNAP-DNA interaction, (i.e. interferes with the formation of RP_o) (method essentially as that used by Yu Feng in the Ebright lab; based on Mukhopadhyay et al., 2004 and Mukhopadhyay et al., 2008). These assays observe the shift in the electrophoretic mobility of a DNA fragment when it is bound by bacterial RNAP, (i.e. it migrates more slowly through a polyacrylamide gel). When the assay is performed using a saturating concentration of an inhibitor that disrupts the RNAP-DNA interaction, such as Myx, no such mobility shift is seen.

Reaction mixtures contained (20 µl): test compound (0 or 0.5 µM GE23077, 0.2 µM Rif, 20 µM MyxB, or 100 µM Lpm), 40 nM *E. coli* RNAP holoenzyme, 10 nM DNA fragment containing positions -42 to +426 of the *lacUV5(ICAP)* promoter (Naryshkin et al., 2001), and 100 µg/ml heparin, in TB [50 mM Tris-HCl (pH = 8.0), 100 mM KCl, 10 mM $MgCl_2$, 5.5% glycerol, 1 mM dithiothreitol (DTT), and 10 µg/ml bovine serum albumin (BSA)]. Reaction components other than DNA and heparin were pre-incubated for 10 min at 37°C. DNA was then added and reaction mixtures were incubated for 15

min at 37°C. Heparin was added and reactions were incubated for 2 min at 37°C. (Heparin disrupts non-specific RNAP-DNA complexes [Walter et al., 1967; Cech and McClure, 1980].) The reactions were then applied to 5% TBE precast polyacrylamide gels (Bio-Rad), gels were electrophoresed in TBE, [90 mM Tris-borate (pH = 8.3) and 2 mM EDTA], (15 V/cm; 1 h at 37°C), gels were stained with SYBR Gold Nucleic Acid Gel Stain (Life Technologies), and gels were analyzed using a Bio-Rad Gel Doc system.

Transcription assays: primer-dependent initiation

Transcription assays were preformed with GE23077 to test its ability to inhibit RNA transcripts 3 or 4 nucleotides in length. The *lacCONS* promoter DNA fragment that is used in these experiments has an A-A-U-U-G start (promoter fragment prepared by annealing two synthetic oligodeoxyribonucleotides; Mukhopadhyay et al., 2001). As such reactions initiated with the ribodinucleotide primer ApA and containing UTP, will only produce RNA products 3 to 4 nucleotides in length. Under the conditions used here, Rif is able to inhibit the formation of 4-nucleotide RNA products, but not 3 nucleotide RNA products (McClure and Cech, 1978).

The method used was derived from transcription assays performed in Mukhopadhyay et al., 2004 and Mukhopadhyay et al., 2008. Reaction mixtures contained (20 µl): test compound (0 or 0.5 µM GE23077 or 0.2 µM Rif), 5 nM *E. coli* RNAP holoenzyme, 2.5 nM DNA fragment containing positions -49 to +30 of the *lacCONS* promoter (Mukhopadhyay et al., 2001), 25 µg/ml heparin, 500 µM ApA, and 25 µM [α^{32}P]UTP (0.09 Bq/fmol) in TB. Reaction components other than DNA, heparin, ApA, and [α-^{32}P]UTP were pre-incubated for 10 min at 37°C. DNA was then added and

reaction mixtures were incubated for 15 min at 37°C. Heparin was added and reaction mixtures were incubated for 2 min at 37°C. RNA synthesis was initiated by the addition of ApA and [α^{32}P]UTP and reaction mixtures were incubated for 10 min at 37°C. Reactions were terminated by adding 10 µl formamide loading buffer (80% formamide, 10 mM EDTA, 0.04% bromophenol blue, 0.04% xylene cyanol, and 0.08% amaranth red). Products were heated for 5 min at 90°C, cooled for 5 min on ice, applied to 16% TBE-urea polyacrylamide gels (19:1 acrylamide:bisacrylamide, 7 M urea), electrophoresed in TBE, and analyzed by storage-phosphor scanning (Typhoon; GE Healthcare).

Transcription assays: *de novo* ribodinucleotide synthesis

Transcription assays were preformed with GE23077 in order to determine if it could inhibit the formation of the smallest RNA product, a ribodinulceotide. These experiments are performed using a T7A1 promoter DNA fragment, which has an A-U-C-G start (prepared by PCR amplification of a synthetic, nontemplate-strand oligodeoxyribonucleotide; Stackhouse et al., 1989). As such, reactions containing only ATP and UTP, will produce RNA transcripts 2 nucleotides in length.

Again, the method used was derived from transcription assays performed in Mukhopadhyay et al., 2004 and Mukhopadhyay et al., 2008. Reaction mixtures contained (20 µl): test compound (0 or 0.5 µM GE23077), 100 nM *E. coli* RNAP holoenzyme, 20 nM DNA fragment containing positions -65 to +35 of the T7A1 promoter (Stackhouse et al., 1989), 25 µg/ml heparin, 25 µM ATP, and 25 µM [α^{32}P]UTP (0.07 Bq/fmol) in TB. Reaction components other than DNA, heparin, ATP, and [α-^{32}P]UTP were pre-

incubated for 10 min at 23°C. DNA was then added and reaction mixtures were incubated for 15 min at 37°C. Heparin was added and reaction mixtures were incubated for 2 min at 37°C. RNA synthesis was initiated by the addition of ATP and [α^{32}P]UTP and reaction mixtures were incubated for 10 min at 37°C. Reactions were terminated by adding 10 µl formamide loading buffer. Products were heated for 5 min at 90°C, cooled for 5 min on ice, applied to 16% TBE-urea polyacrylamide gels (19:1 acrylamide:bisacrylamide, 7 M urea), electrophoresed in TBE, and analyzed by storage-phosphor scanning (Typhoon; GE Healthcare).

Transcription assays: nucleotide addition in elongation

Transcription assays were performed with GE23077 in order to determine if it could inhibit nucleotide addition by a halted transcription elongation complex. These experiments were performed using the N25-100-tR2 DNA fragment from Revyakin et al. (2006), which contains its first non-template strand "C" at position +30. Performing transcription reactions with this DNA template using only ATP, UTP, and GTP (i.e. no CTP), results in the formation of a halted transcription elongation complex containing RNAP halted on the DNA template with a 29-nucleotide RNA product. Further extension of the RNA product can be initiated by the addition of CTP to the reaction mixture. This re-initiation is done in the presence and absence of GE23077 in order to assess its effects on transcription elongation.

This procedure was based on the method used by Yu Zhang in the Ebright lab, and was derived from Revyakin et al., 2006. Initial reaction mixtures contained (18 µL): 40 nM *E. coli* RNAP holoenzyme, 10 nM DNA fragment N25-100-tR2 (Revyakin et al.,

2006), 100 μg/ml heparin, 5 μM ATP, 5 μM GTP, and 5 μM [α^{32}P]UTP (4.4 Bq/fmol) in TB. Reaction components other than heparin and NTPs were pre-incubated for 15 min at 37°C. Heparin was then added and reaction mixtures were incubated for 2 min at 37°C. RNA synthesis was initiated by the addition of ATP, GTP and [α^{32}P]UTP and reaction mixtures were incubated for 5 min at 37°C. The resulting halted transcription elongation complexes were then treated with 1 μL methanol or 1 μL of 10 μM GE23077 to the resulting halted transcription elongation complexes, and the reaction mixtures were incubated for 5 min at 37°C. Transcription was restarted adding 1 μL of 1 mM CTP, and the reactions were allowed to proceed for 5 min at 37°C. Reactions were terminated by adding 10 μl formamide loading buffer. Products were heated for 5 min at 90°C, cooled for 5 min on ice, applied to 16% TBE-urea polyacrylamide gels (19:1 acrylamide:bisacrylamide, 7 M urea), electrophoresed in TBE, and analyzed by storage-phosphor scanning (Typhoon; GE Healthcare). Formation of the full length run-off transcription product is observed for analysis.

Transcription assays: nucleotide addition kinetics

Kinetics experiments were performed in order to determine if salinamide competes with NTPs for binding to bacterial RNAP. A T7A1 promoter DNA fragment was again used (A-U-C-G start), such that reactions containing ATP, UTP, and CTP would only produce RNA transcripts up to 3 nucleotides in length (Stackhouse et al., 1989). The formation of the trinucleotide product was observed under varying inhibitor concentrations and varying concentrations of either ATP or UTP. This allowed me to

determine the effects of each inhibitor on NTPs binding to the "i site" (by varying ATP) or the "i+1 site" (by varying UTP).

This method was derived from transcription kinetics experiments performed in Mukhopadhyay et al., 2004. Reaction mixtures contained (20 µl): test compound (0, 200, or 400 nM SalA), 10 nM *E. coli* RNAP holoenzyme (Epicentre), 5 nM DNA fragment containing positions -65 to +35 of the T7A1 promoter (Stackhouse et al., 1989), 25 µg/ml heparin, 0-6.4 mM ATP, 0-1.6 mM UTP, and 25 µM [α^{32}P]CTP (0.44 Bq/fmol), in TB. Reaction components other than DNA, heparin, and NTPs were pre-incubated for 30 min at 37°C. DNA was then added and reaction mixtures were incubated for 15 min at 37°C. Heparin was added and reaction mixtures were incubated for 2 min at 37°C. RNA synthesis was initiated by the addition of NTPs and reactions mixtures were incubated for 10 min at 37°C. Reactions were terminated by addition of 10 µl formamide loading buffer. Products were heated for 5 min at 90°C, cooled for 5 min on ice, applied to 23% (or 30%) TBE-urea polyacrylamide (19:1 acrylamide:bisacrylamide, 7 M urea) gels, electrophoresed in TBE, and analyzed by storage-phosphor scanning (Typhoon; GE Healthcare).

Data for synthesis of the trinucleotide product pppApUp[α^{32}P]C were fitted to full-competitive, partial-competitive, full-noncompetitive, partial-noncompetitive, full-uncompetitive, partial-uncompetitive, full-mixed, and partial-mixed models of inhibition using the Fit-to-Model feature of the SigmaPlot Enzyme Kinetics Module v1.1 (SPSS). Fits were ranked based on the AICc statistic (Akaike Information Criterion corrected), the Sy.x statistic (standard error of the estimate), the R^2 statistic (coefficient of multiple determination), and the number of model parameters.

The above procedure does not work for GE23077. Due to its tight-binding nature, equilibrium cannot be achieved under these conditions, i.e. the enzyme concentration is too close to the K_i for GE23077. As such, GE23077 will always appear to be a noncompetitive inhibitor with respect to NTP substrates in these experiments (data not shown; reviewed in Copeland, 2000; Strelow et al., 2012). I am currently attempting to overcome these limitations by effectively reducing the K_i for GE23077, thereby enabling a detectable and, hopefully, reliable analysis of its transcription kinetics. This can be done in a number of ways, including using *T. thermophilus* RNAP (which is inhibited much less well by GE23077 than *E. coli* RNAP), by using derivatives of GE23077 (which inhibit *E. coli* RNAP less well than GE23077), or by using GE23077-resistant *E. coli* RNAP enzymes (which are inhibited less well by GE23077 than wild-type *E. coli* RNAP). In each of these cases, I will use fluorescence-detected abortive initiation in order to monitor the transcription reactions, (a faster process than radiochemical experiments). The method used will be similar to that described in Mukhopadhyay et al., 2004 and Mukhopadhyay et al., 2008. Briefly, RNAP will be pre-incubated with promoter DNA for 15 min at 37°C in a sub-micro fluorometer cuvette (Starna). Heparin will then be added and reaction mixtures incubated for 2 min at 37°C. RNA synthesis will be initiated by the addition of GE23077, ATP, and [γ-AmNS]UTP (or [γ-AmNS]CTP) simultaneously. The fluorescence emission intensity of the reactions will be monitored for 5 min at 37°C using a QuantaMaster QM1 spectrofluorometer (PTI; excitation = 360 nm, emission = 500 nm; slit width = 5 nm). Data for synthesis of the pppApU (or pppApC) product will then be fitted using the SigmaPlot Enzyme Kinetics Module as described above.

Chapter 3:

Target of transcription inhibition by the macrocyclic-lactone antibiotic lipiarmycin: the RNAP switch region

David Degen, Aashish Srivastava, Elena Sineva, Sajida Ismail, Richard Y. Ebright, Sujoy Chatterjee, Jayanta Mukhopadhyay, Vladimir Mekler, Anirban Chakraborty, Sergei Druzhinin, Yon W. Ebright, Shimon Weiss, Stefano Donadio, and Richard H. Ebright

BACKGROUND

Lipiarmycin (Lpm), (also known as clostomicin, tiacumicin, PAR-101, OPT-80, difimicin, fidaxomicin, and Dificid), is a macrocyclic-lactone antibiotic that was originally purified by the Lepetit Pharmaceutical Group from fermentation cultures of the actinomycete soil bacterium *Actinoplanes deccanensis* (Figure 4; Parenti et al., 1975; Coronelli et al., 1975; Martinelli et al., 1983; Arnone et al., 1987; Cavalleri et al., 1988; reviewed in Srivastava et al., 2012; Erb and Zhu, 2013). (The strain was isolated in Italy during a leap year on Feb 29, 1972, giving Lpm its name [Parenti et al., 1975].) Lpm was also subsequently isolated from three other species of soil bacterium *Micromonospora echinospora* subsp. Armeniaca, Dactylosporangium *aurantiacum* subsp. *hamdenesis*, and, most recently, *Catellatospora* sp. Bp3323-81 (Omura et al., 1986; Theriault et al., 1987; Hochlowski et al., 1987; Kurabachew et al., 2008). Lpm has good antibacterial activity against many Gram-positive bacteria, including the clinically significant pathogens *Staphylococcus aureus, Streptococcus pyogenes*, *Clostridium difficile*, and *Mycobacterium tuberculosis* (Coronelli et al., 1975;

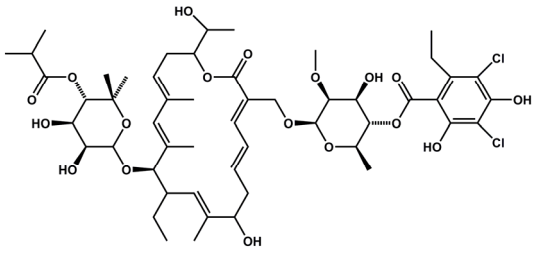

Figure 4. Structure of Lpm.

Theriault et al., 1987; Swanson et al., 1991; Hochlowski et al., 1987; Credito and Appelbaum, 2004; Goldstein et al., 2012). Lpm also has some activity against certain Gram-negative pathogens including *Neisseria gonorrhoeae* and *Francisella tularnesis* (Cavalleri, 1988; Srivastava, 2011; Goldstein et al., 2012).

Mechanism of action studies revealed that Lpm rapidly suppresses RNA synthesis in cultures of exponentially growing *Bacillus subtilis*, followed by the inhibition of protein synthesis (Coronelli et al., 1975; Sergio et al., 1975). This is the classical pattern seen with inhibitors of bacterial RNA polymerase including Rif and Stl (Lancini and Sartori, 1968; Siddhikol et al., 1969). Subsequent experiments using purified RNA polymerase enzymes from *E. coli* and *B. subtilis* showed that Lpm directly inhibits these enzymes *in vitro*, (but only when added before the addition of DNA template to the reactions) (Sergio et al., 1975; Talpaert et al., 1975; Sonenshein and Alexander, 1979).

In the early 1990s, research at Abbott Labs indicated that Lpm could be a promising treatment for *C. difficile* infections (Swanson et al., 1991). *C. difficile* infections have risen rapidly in the last several decades as a result of increased antibiotic use (reviewed in Miller, 2010; Poxton, 2010). When a patient is treated with antibiotics, the natural bacterial flora that inhabit the gut are killed off, allowing room for an opportunistic pathogen like *C. difficile* to move in. This can result in severe cases of pseudomembranous colitis. The current standard treatment for these infections is vancomycin. The Abbott researchers showed that Lpm was at least as effective as vancomycin, in treating these infections (Swanson et al., 1991). When administered orally, Lpm (like vancomycin) does not significantly enter blood stream, such that very high concentrations accumulate in the intestines, making it very effective in treating *C.*

difficile infections of the gut (Swanson et al., 1991; Louie et al., 2009a). Further research revealed that Lpm has an advantage over vancomycin, such that patients treated with Lpm have a lower rate of *C. difficile* infection recurrence (Louie et al., 2009a, 2011; reviewed in Miller, 2010; Poxton, 2010). This is believed to be related to Lpm's more narrow spectrum of antibacterial activity, resulting in less of an impact on natural gut flora (Credito and Appelbaum, 2004; Louie et al., 2009a, 2009b, 2011). After years of development, Optimer Pharmaceuticals received FDA approval in May 2011 to market Lpm (under the trade name Dificid) for the treatment of *C. difficile*-associated diarrhea (Traynor, 2011).

RESULTS

Lpm target: *E. coli* saturation mutagenesis

In the early 2000s, the Ebright lab obtained three Lpm-resistant *B. subtilis* mutants from Abraham Sonenshein's lab at Tufts University Medical School (Sonenshein et al., 1977). Sequencing of the *rpoB* and *rpoC* genes of these mutants by Elena Sineva revealed that each of them contained a single amino acid substitution in the switch region of RNAP, specifically at β subunit residue 1256, β′ subunit residue 249, and β′ subunit residue 337 (residue numbering is as in *E. coli*) (Ebright, 2005).

In order to thoroughly define the target of Lpm on bacterial RNAP, Elena and Sajida Ismail proceeded with, and I subsequently continued, saturation mutagenesis experiments in *E. coli* D21f2tolC covering all residues within 30 Å of the resistance residues previously identified in *B. subtilis*. In total, we isolated and sequenced over 230

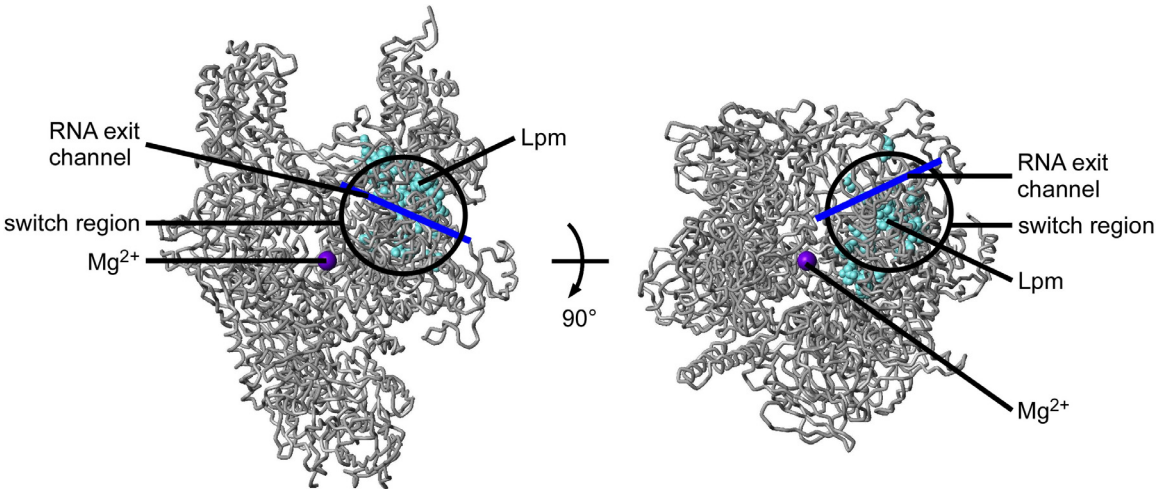

Figure 5. Target of transcription inhibition by Lpm

Lpm targets the switch region and one wall of the RNA exit channel of bacterial RNAP. Two orthogonal views of RNAP. Cyan spheres, sites of substitutions conferring resistance to Lpm in *E. coli*; black circle, switch region; blue line, approximate path of the RNA exit channel; violet sphere, active-center Mg^{2+}.

Lpm-resistant mutants. Of these mutants, 83 independent isolates have single amino acid substitutions in the β subunit, and 77 independent isolates have single substitutions in the β′ subunit (see Supplemental Tables SB1 and SB2 in Appendix SB). (There are an additional 26 isolates in the β subunit and 24 isolates in the β′ subunit that contain multiple amino acid substitutions. Most multiple-substitution isolates contain a mutation of at least one residue that was also identified in a single-substitution isolate.) There are 22 distinct single substitutions in the β subunit occurring at 15 different residues: 892, 1251, 1252, 1256, 1263, 1288, 1297, 1302, 1308, 1318, 1319, 1321, 1323, 1324, and 1325. There are also 22 distinct single substitutions in the β′ subunit occurring at 16 different residues: 96, 248, 249, 263, 330, 334, 337, 341, 348, 349, 428, 1323, 1325, 1326, 1327, and 1354. (Residue numbering is always as in *E. coli* RNAP.)

In the three-dimensional structure of RNAP, these residues define the functional determinant of Lpm, ("the Lpm target"), with dimensions of ~35 Å x ~25 Å x ~20 Å (Figure 5; Srivastava et al., 2011). The Lpm target includes parts of the RNAP switch

region subregions, switch 2 and switch 3, as well as one wall of the RNA exit channel (Tupin et al., 2010b; Srivastava et al., 2011). The Lpm target is distant from the Rif target, and only minimally overlaps the target of other RNAP switch region inhibitors, Myx, Cor, and Rip, (which involves residues in switch region subregions, switch 1 and switch 2) (Figure 6; Mukhopadhyay et al., 2008; Belogurov et al., 2009; Srivastava et al., 2011). As such, Lpm is expected to have minimal cross-resistance with Rif, Myx, Cor, and Rip.

Lpm target: conservation

Most of the residues in the Lpm target, (28 out of 31), are highly conserved among bacterial RNAPs (see supplemental Figure SB1 in Appendix SB). This is consistent with the relatively broad-spectrum antibacterial activity of Lpm. Residues in the Lpm target are much less well conserved between bacterial RNAP and human RNAPs I, II, and III. (Only 4 out of the 31 Lpm target residues identified in the saturation mutagenesis experiments here are conserved between bacterial RNAPs and all three human RNAPs: β′ 334, β′ 348, β′ 1325, and β′ 1354.) This allows for target specificity, such that Lpm is able to inhibit bacterial RNAP, while not inhibiting human RNAP. This is further supported by my *in vitro* experiments demonstrating that Lpm does not inhibit human RNAP at concentrations up to 100 μM. Studies have shown that Lpm is well tolerated, (i.e. not cytotoxic), in animals and humans (Louie et al., 2009a, 2011; reviewed in Miller, 2010). (Lpm has a very high LD50 of >500 mg/kg in mice [Coronelli et al., 1975; Omura et al., 1986; Swanson et al., 1991].)

Lpm target: characterization in *E. coli*

In order to further characterize the Lpm target, I first performed complementation studies to determine if the Lpm-resistant mutants isolated on plasmids were sufficiently capable in transcription to support viable cell growth. All Lpm-resistant mutants with substitutions in the β subunit were able to complement an *E. coli* strain harboring an *rpoB*^{ts} mutation for growth at the non-permissive temperature (Table SB2). Nineteen out of the 22 Lpm-resistant mutants with substitutions in the β′ subunit were able to complement an *E. coli* strain harboring an *rpoC*^{ts} mutation at the non-permissive temperature (Table SB1). Of the three mutants that failed the complementation assay, one (β′ D348Y), occurs at the same residue where a different substitution, (β′ D348H), passed the complementation assay. The other two mutants that failed, (β′ A1323P and β′ F1325V), are adjacent to mutants that passed the complementation assay, (i.e. β′ Q1326E, β′ E1327A, and β′ E1327G).

I next determined the level of Lpm resistance for all Lpm-resistant mutants. Similar results were obtained when MIC measurements were made by either broth microdilution assays or SGE assays (Tables SB1 and SB2). For simplicity, subsequent MIC results will only include the 27 Lpm-resistant mutants that demonstrated Lpm resistance of at least 2x the wild-type MIC (MIC_{wt}) when measured by both broth microdilution assays and SGE assays (Table 1). Fourteen out of the 27 Lpm-resistant mutants have high-level, (≥4x the wild-type MIC by SGE measurement), resistance to Lpm (Tables 1, B1, and B2). The strongest resistance substitutions, (8x MIC_{wt} by SGE assay), occur at β subunit residues 1251, 1297, 1319, and 1325.

I also determined the levels of cross-resistance for Lpm-resistant mutants against Rif in SGE assays. Correspondingly, I measured the cross-resistance level for the four most frequently isolated Rif-resistant mutants in clinical isolates against Lpm in SGE assays. As mentioned earlier, the Lpm target does not overlap the Rif target, and, in fact, is distant from the Rif target (Figure 6A). As such, the Lpm target should have minimal to no cross resistance with the Rif target, and this is verified by my measurements. None of the Lpm-resistant mutants showed significant, (>2x MIC_{wt}), cross-resistance with Rif (Table 1); and, correspondingly, none of the Rif-resistant mutants showed significant, (>2x MIC_{wt}), cross-resistance against Lpm (Table SB3). (Lpm is also not cross-resistant when tested against several Stl-resistant mutants and CBR-resistant mutants [Tables SB4 and SB5].)

Table 1. Lpm-resistant mutants from saturation mutagenesis: absence of cross-resistance to Myx, Cor, Rip, and Rif

amino acid substitution	MIC ratio ($MIC/MIC_{wild\text{-}type}$)[a]				
	Lpm	Myx	Cor	Rip	Rif
***rpoC* (RNAP β' subunit)**					
96 Lys→Ile	2	1	0.5	1	0.5
249 Leu→Arg	4	1	0.5	1	2
263 Ser→Thr	2	1	1	1	1
337 Arg→Cys	2	1	0.5	1	1
337 Arg→His	4	2	1	2	2
337 Arg→Ser	4	2	1	2	2
341 Asn→Ser	2	2	1	1	2
***rpoB* (RNAP β subunit)**					
892 Glu→Ala	2	1	1	1	1
1251 Tyr→Phe	8	1	0.5	1	1
1252 Ser→Gly	2	1	1	1	1
1256 Gln→Glu	4	1	0.5	1	2
1256 Gln→Leu	2	1	0.5	0.5	2
1288 Gln→Leu	2	1	1	1	1
1297 Asp→Ala	8	1	1	1	1
1297 Asp→Tyr	4	1	1	1	1
1302 Thr→Pro	2	1	0.5	0.5	2
1318 Gly→Ser	2	1	1	1	1
1319 Met→Arg	8	1	0.5	1	1
1319 Met→Ile	2	1	1	1	1
1319 Met→Lys	8	1	0.5	1	1
1321 Glu→Val	4	1	0.5	1	1
1323 Phe→Leu	2	2	1	1	1
1324 Asn→Lys	2	1	1	1	2
1325 Val→Ala	8	1	1	1	2
1325 Val→Glu	8	1	1	1	2
1325 Val→Gly	8	1	1	1	2
1325 Val→Leu	4	1	1	1	2

[a] The SGE MIC values with wild-type *rpoB* are as follows: Lpm = 3.13 μg/ml, Myx = 0.098 μg/ml, Cor = 0.78 μg/ml, Rip = 3.13 μg/ml, and Rif = 0.39 μg/ml. The SGE MIC values with wild-type *rpoC* are as follows: Lpm = 6.25 μg/ml, Myx = 0.098 μg/ml, Cor = 0.78 μg/ml, Rip = 3.13 μg/ml, and Rif = 0.39 μg/ml.

Three other bacterial RNAP inhibitors have been shown to function through the switch region: myxopyronin (Myx), corallopyronin (Cor), and ripostatin (Rip). These

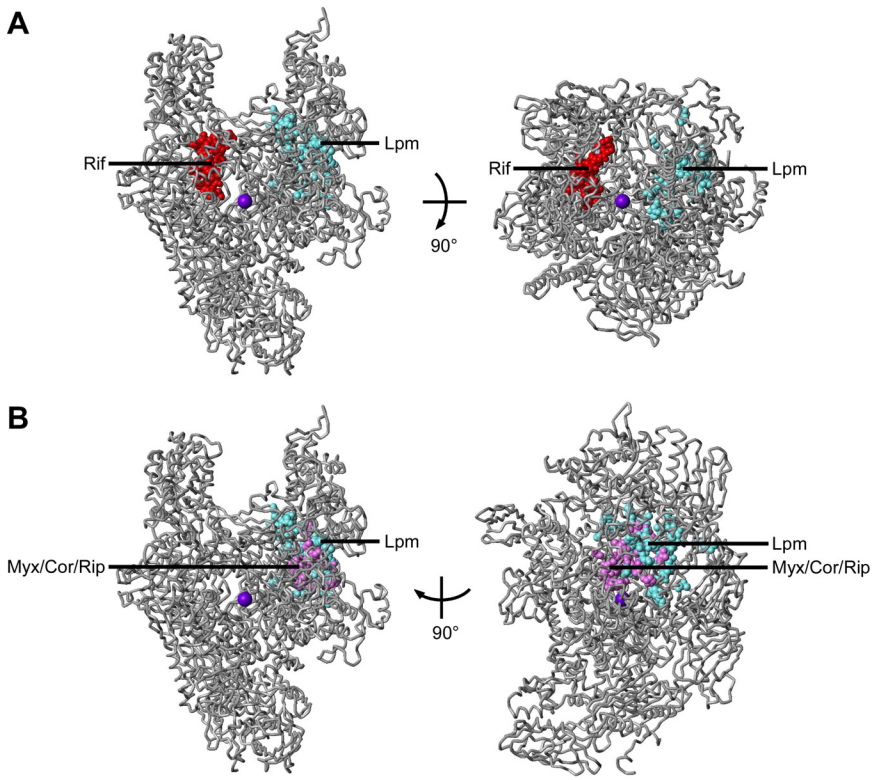

Figure 6. Relationship of the Lpm target to the Rif target and the Myx/Cor/Rip target

(A) The Lpm target does not overlap, and is distant from, the Rif target.

(B) The Lpm target is adjacent to, but only minimally overlaps, the Myx/Cor/Rip target.

Each panel shows two orthogonal views of RNAP. Red spheres, sites of substitutions conferring resistance to Rif in *E. coli*; cyan spheres, sites of substitutions conferring resistance to Lpm in *E. coli*; magenta spheres, sites of substitutions conferring resistance to Myx/Cor/Rip in *E. coli*; violet sphere, active-center Mg^{2+}.

inhibitors target the switch region subregions, switch 1 and switch 2, and adjacent residues in the β and β′ subunits (Mukhopadhyay et al., 2008; Belogurov et al., 2009; Srivastava et al., 2011). The Lpm target is adjacent to, but only minimally overlaps, the target defined by Myx, Cor, and Rip (Figure 6B). In fact, only two residues, (β 1325 and β′ 1354) are shared by the two targets. This suggests that Lpm should have minimal cross-resistance with Myx, Cor, and Rip. This is supported by my results. Cross-resistance testing against Myx, Cor, and Rip, reveals that only one Lpm-resistant substitution had significant, (4x MIC_{wt}), cross-resistance with these inhibitors when

measured in SGE assays (Table 1). This substitution, (β V1325L), occurs at one of the residues shared by the Lpm and Myx/Cor/Rip targets.

I also tested the 30 resistant mutants previously isolated against Myx, Cor, or Rip for cross-resistance with Lpm (Table SB6). Excluding the previously discussed β V1325L substitution, only one other resistance substitution, (β′ G1354C), was significantly cross-resistant to Lpm, (4x MIC_{wt}). As mentioned previously, β′ subunit residue 1354 is the one other residue that is shared by the functional determinants of Lpm and Myx/Cor/Rip.

Lpm target: *E. coli* chromosomal mutants

Using lambda red-mediated recombination a subset of the Lpm-resistant mutations isolated on plasmids by saturation mutagenesis was transferred onto the chromosome of *E. coli* D21f2tolC. These mutants were all 8x resistant to Lpm, typically demonstrating higher levels of resistance than their plasmid-based counterparts (Table 2). In particular, mutants β′ D348H and β′ Y349S both went from borderline resistant in the plasmid-based system, (i.e. less than 2x resistant when measured by broth microdilution), to strongly resistant when on the chromosome. (This increased resistance is true of most RNAP inhibitor resistance mutations that I have moved from plasmids onto the

Table 2. Chromosomal Lpm-resistant mutants in *E. coli* D21f2tolC: sequences, resistance levels, and absence of cross-resistance to Myx, Rif, Stl, and CBR703

amino acid substitution	MIC ratio (MIC/$MIC_{wild\text{-}type}$)[a]				
	Lpm	Myx	Rif	Stl	CBR703
***rpoC* (RNAP β' subunit)**					
337 Arg→His	8	1	1	1	1
337 Arg→Ser	8	1	1	2	1
348 Asp→His	8	0.5	1	1	0.5
348 Asp→Tyr	8	2	1	1	1
349 Tyr→Ser	8	2	1	1	1
***rpoB* (RNAP β' subunit)**					
1256 Gln→Glu	8	2	1	1	1
1256 Gln→Leu	8	1	1	1	1

[a] The wild-type broth microdilution MIC values are as follows: Lpm = 1.56 μg/ml, Myx = 0.20 μg/ml, Rif = 0.20 μg/ml, Stl = 3.13 μg/ml, and CBR703 = 6.25 μg/ml.

chromosome of *E. coli* D21f2tolC. This likely reflects the heterozygous nature of the plasmid-based system.)

The chromosomal Lpm-resistant mutants also displayed minimal to no cross-resistance when tested against other bacterial RNAP inhibitors, (Myx, Rif, Stl, and CBR703) (Table 2). Similarly, *E. coli* D21f2tolC chromosomal mutants resistant to Myx or *E. coli* D21f2tolC chromosomal mutants resistant to Rif display minimal cross-resistance when tested against Lpm (mutants also constructed by lambda red-mediated recombineering; Tables SB7 and SB8). Only one of the Myx-resistant mutants tested, (β 1291F), had significant cross-resistance to Lpm, (8x cross-resistant to Lpm, but 128x resistant to Myx). On the other hand, two of the Myx-resistant mutants that were tested, (β′ K345N and β V1275M), actually demonstrated significant hyper-sensitivity, (≤4x MIC_{wt}), to Lpm. These results provide further support for the Lpm target identified in the saturation mutagenesis studies, such that the Lpm target is distinct from, and only minimally overlaps, the Myx target.

Lpm target: *S. aureus*

Additional experiments were performed to identify the target of Lpm in *S. aureus*. These experiments were done in conjunction with a research associate in the lab, Aashish Srivastava. Lpm-resistant mutants were isolated in *S. aureus* by spontaneous resistance. We found the spontaneous resistance rate of Lpm in *S. aureus* to be $5x10^{-8}$ cfu per generation. This is essentially the same as the rates for Rif and Myx in *S. aureus*, (~$6x10^{-8}$ cfu per generation) (Srivastava et al., 2012).

The *rpoB* and *rpoC* genes of ten Lpm-resistant mutants were sequenced, identifying nine independent, single-substitution mutants (Table 3). One distinct substitution was identified in the β subunit, (V1325E) (numbering as in *E. coli*). Seven distinct substitutions were identified on four residues of the β′ subunit: G63E, G63R, R99C, R99P, P246R, R337C, and R337L. Two of these residues are identical to those previously identified in my *E. coli* saturation mutagenesis studies, (β 1325 and β′ 337). In the three-dimensional structure of RNAP these residues cluster to the same target previously identified in *E. coli* RNAP (Figure 7A and 7B). (An additional 20 spontaneous resistant mutants were also isolated against two derivatives of Lpm, which lack either one or both of its chlorine atoms, [deschloro-Lpm and dideschloro-Lpm]. All of these mutants carried substitutions at residues in the β subunit or β′ subunits of RNAP that were, again, identical to or near to those that I previously identified in *S. aureus* and *E. coli* [Table SB9].)

Table 3. Spontaneous Lpm-resistant mutants in *S. aureus*: sequences, resistance levels, and fitness costs

amino acid substitution[a]	number of independent isolates	resistance level ($MIC/MIC_{wild\text{-}type}$)[b]	fitness cost[c] (% per generation) (± SEM)
***rpoC* (RNAP β' subunit)**			
63 [53] Gly→Glu	1	2	16 (±2)
63 [53] Gly→Arg	1	2	27 (±3)
99 [89] Arg→Cys	1	4	2 (±1)
99 [89] Arg→Pro	1	8	0 (-2 ±1)
246 [235] Pro→Arg	1	2	20 (±1)
337 [326] Arg→Cys	2	4	6 (±3)
337 [326] Arg→Leu	1	4	4 (±4)
***rpoB* (RNAP β' subunit)**			
1325 [1130] Val→Glu	1	4	22 (±5)

[a] Residues are numbered as in *E. coli* RNAP and, in brackets, as in *S. aureus* RNAP.

[b] The SGE MIC for wild-type *S. aureus* is 6.25 μg/ml. MIC values were determined solely by Aashish Srivastava.

[c] An observed fitness cost that is less than zero is shown as zero, with the actual value displayed in parenthesis along with the SEM.

As an additional means of characterizing the Lpm target, the pairwise fitness cost of these Lpm-resistant mutants in *S. aureus* was determined (Table 3). We found that half of the Lpm-resistant mutants tested (four out of eight) have large, fitness costs of ≥15% per generation. In contrast, when tested under identical conditions, zero out of nine Rif-resistant mutants in *S. aureus* had fitness costs ≥15% per generation (Srivastava et al.,

2012). Given the strong correlation between fitness cost and the clinical prevalence of antibiotic-resistant mutants, particularly for Rif (Billington et al., 1999; Wichelhaus et al., 2002; Gagneux, et al., 2006; O'Neill et al., 2006; Comas et al., 2011; Srivastava et al., 2012), these results suggest that resistance to Lpm may occur less frequently in a clinical setting than resistance to Rif.

DISCUSSION

Comparison of the Lpm-target to Lpm-resistant mutants identified in other bacterial species

Several Lpm-resistant isolates have been identified in *B. subtilis*, *M. tuberculosis*, *Mycobacterium bovis* BCG, *Enterococcus faecalis*, and *C. difficile* (Gualtieri et al., 2006, 2009; Kurabachew et al., 2008; Babakhani et al., 2011; Leeds et al., 2013). In *B. subtilis* two out of ten Lpm-resistant isolates were identified as having a substitution at β′ residue 337, (numbering as in *E. coli*) (Gualtieri et al., 2006). As noted earlier, this same residue had been previously identified by the Ebright lab in the sequencing of Lpm-resistant *B. subtilis* mutants from the Sonenshein lab (Sonenshein et al., 1977). I also identified many Lpm-resistant isolates with substitutions at this residue during saturation mutagenesis screening in *E. coli* and spontaneous resistance screening in *S. aureus*.

It is worth noting that no resistance substitutions were identified in the β or β′ subunits of the remaining eight Lpm-resistant isolates in Gualtieri et al., 2006. Permeabilization of these mutants revealed that they were not resistant to the inhibition of RNA synthesis by Lpm (Gualtieri et al., 2006). This suggests that the Lpm-resistance of these mutants was not due to changes in the bacterial RNAP enzyme, but likely due to

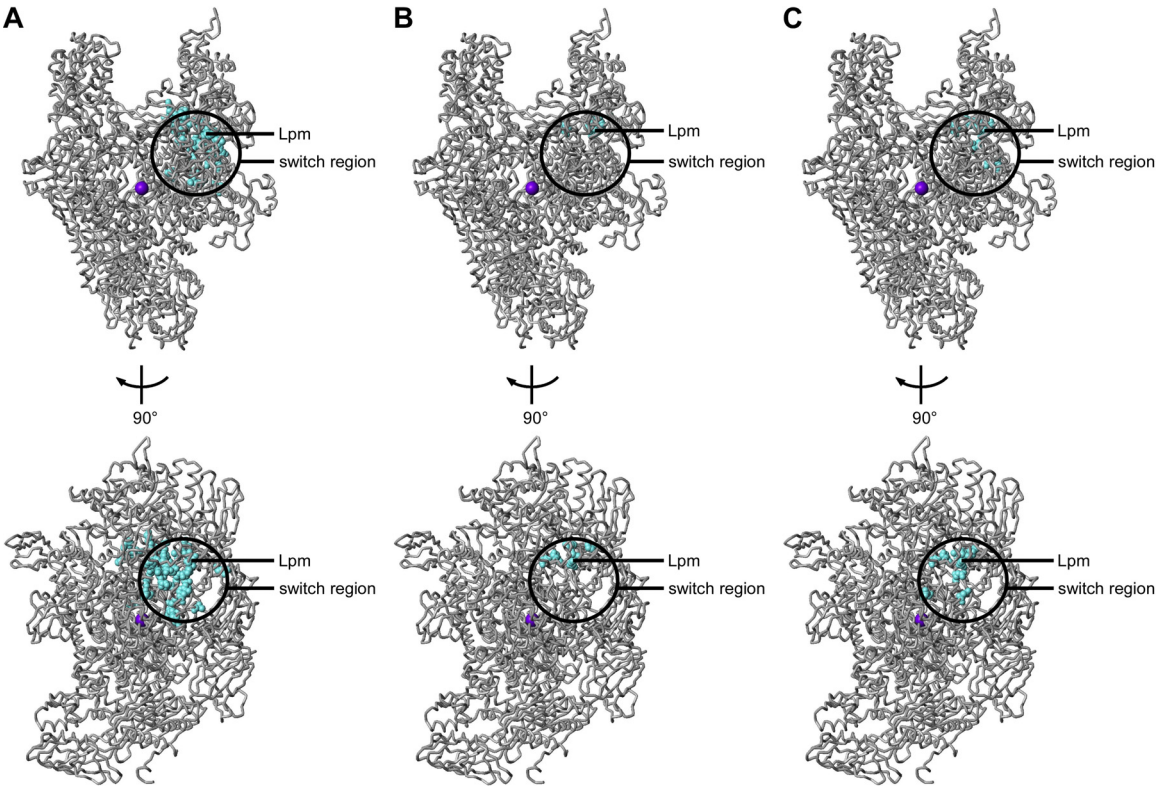

Figure 7. The Lpm target is the same across different bacterial species

(A) Lpm-resistant residues in *E. coli* that were identified in this work.

(B) Lpm-resistant residues in *S. aureus* that were identified in this work.

(C) Lpm-resistant residues in *B. subtilis*, *M. tuberculosis, M. bovis*, *E. faecalis*, and *C. difficile* that have been identified in published studies.

Each panel shows two orthogonal views of RNAP rotated about the vertical axis here. Cyan spheres, sites of substitutions conferring resistance to Lpm; black circle, switch region; violet sphere, active-center Mg^{2+}.

cell membrane changes that prevented the entry of Lpm into these mutants. This is a common mechanism by which bacteria can become resistant to antibiotics [Nikaido, 1994].

Researchers from Novartis fully sequenced the *rpoB* and *rpoC* genes of 18 Lpm-resistant isolates in *M. tuberculosis*, and six isolates in *M. bovis* BCG (Kurabachew et al., 2008). All of these isolates were found to contain single amino acid substitutions in either *rpoB* or *rpoC*, and all but one of these substitutions occur at a residue that is identical to those identified in my work, (i.e. β 1256, β 1288, β 1325, and β′ 337). The remaining

substitution, (β′ 251), was not identified in my studies, but is very close to residues β′ 248 and β′ 249, at which Lpm-resistant substitutions were identified.

In *E. faecalis*, Lpm-resistant substitutions were again identified at β 1256 and β 1325 (Gualtieri et al., 2009). Three mutants were found to have a substitution at a previously unidentified residue for Lpm-resistance, (β 1302 or β′ 99). A Lpm-resistance substitution at β 1302 was also identified in my saturation mutagenesis studies, and substitutions at β′ 99 were identified in our *S. aureus* spontaneous resistance screens.

Most recently, three lab-generated Lpm-resistant mutants have been sequenced in *C. difficile* (Babakhani et al., 2011; Leeds et al., 2013). Two of these mutants, as has been found in all of the bacterial species discussed here, had a substitution at β 1256. The third mutant contained two substitutions, (β′ Q805; β′ D1342), neither of which were identified as conferring Lpm-resistance in my work; however, β′ 1342 is located in the vicinity of other residues at which Lpm-resistant substitutions occur.

The sum of these results indicates that Lpm targets the same site on bacterial RNAP across many different bacterial species (Figure 7), and suggests that Lpm likely inhibits different bacterial RNAPs by the same mechanism.

Mechanism of transcription inhibition by Lpm

As mentioned previously, the target of Lpm involves residues in the switch region subregions, switch 2 and switch 3 (Tupin et al., 2010b; Srivastava et al., 2011). This target suggests that Lpm may function in a way similar to that of the other known switch region inhibitors of bacterial RNAP, (Myx/Cor/Rip); that is Lpm may inhibit movement of the β′ clamp, thereby preventing the formation of a stable promoter open complex.

Early studies of Lpm noticed a distinct order of addition effect, whereby Lpm would only inhibit transcription *in vitro* when added to reactions prior to the addition of DNA (Sergio et al., 1975; Sonenshein and Alexander, 1979). Experiments by Jayanta Mukhopadhyay, Sujoy Chatterjee, and Sergei Druzhinin in the Ebright lab, as well as a recently published study, have clearly shown that Lpm interferes with the RNAP-DNA interaction, preventing the formation of a stable, heparin-resistant RNAP-promoter open complex (RP_o) (Figure 8; Tupin et al., 2010b; Artsimovitch et al., 2012; J.M., S.C., S.D., and R.H.E., unpublished). (More specifically Lpm interferes with the interaction of RNAP and promoter DNA only when positions –11 to +15 of the promoter are double-stranded [S.C., J.M., and R.H.E., unpublished].) Tupin et al. (2010b) further suggested that σR3.2 plays a critical role in the inhibition of bacterial RNAP by Lpm, and fluorescence-energy transfer (FRET) experiments by Vladimir Mekler in the Ebright Lab indicated that Lpm interferes with/displaces σR3.2 (Tupin et al., 2010b; Brodolin, 2011; V.M. and RHE, unpublished). However, experiments by Sujoy Chatterjee have shown that Lpm can still inhibit RNAP even when σR3.2 is deleted (S.C. and R.H.E., unpublished; Artsimovitch et al. 2012). Finally, single-molecule FRET studies performed in the Ebright lab by Anirban Chakraborty demonstrate that Lpm locks the RNAP β′

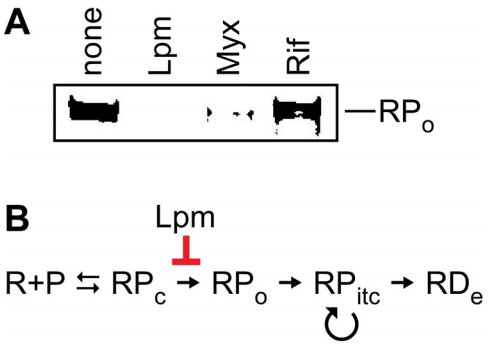

Figure 8. Mechanistic basis of transcription inhibition by Lpm: Lpm inhibits the RNAP-DNA interaction

(A) My results from an electrophoretic mobility shift assay are shown. Like Myx, Lpm inhibits the formation of a stable RNAP-promoter open complex (RP_o) (no band). This is unlike Rif, which does not inhibit RP_o formation.

(B) Simplified schematic showing the step of transcription inhibited by Lpm.

clamp in a partly-to-fully closed state, an effect similar to that of the other switch region inhibitors Myx, Cor, and Rip (Chakraborty et al., 2012; A.C. and R.H.E., unpublished).

Conclusions

My results clearly define the functional determinant of Lpm in bacterial RNAP as involving a cluster of nearby residues in the switch region and one wall of the RNA exit channel. This target is distant from the target of Rif, the only other bacterial RNAP inhibitor currently approved for clinical use. There is minimal to no cross-resistance between the Lpm target and the Rif target. Furthermore, the Lpm target is distinct from, and only minimally overlaps, the target of other switch region RNAP inhibitors, Myx, Cor, and Rip. There is minimal cross-resistance between the Lpm target and the Myx/Cor/Rip target.

The Lpm-resistance mutations presented here in *E. coli* and *S. aureus*, as well as the published Lpm-resistant mutants in *B. subtilis*, *M. tuberculosis*, *M. bovis* BCG, *E. faecalis*, and *C. difficile* show that the Lpm target is essentially the same across different bacterial strains (Gualtieri et al., 2006, 2009; Kurabachew et al., 2008; Babakhani et al., 2011; Leeds et al., 2013). This is consistent with the high degree of sequence conservation within the Lpm target among bacteria. Residues within the Lpm target are less well conserved between bacterial RNAP and the human RNAPs. This allows for Lpm to specifically target bacterial RNAP while having no apparent effect on human RNAP. In particular, β subunit residue 1256, at which Lpm-resistance substitutions have been identified in each of the bacterial species described above, is conserved as glutamine

among bacterial RNAPs; but is asparagine in human RNAP I, and is arginine in human RNAPs II and III.

As described earlier, the ability of Lpm to accumulate in the digestive system, rather than being absorbed into the bloodstream, has made Lpm an excellent new treatment for *C. difficile*-associated diarrhea (Swanson et al., 1991; Louie et al., 2009a; reviewed in Miller, 2010; Poxton, 2010). Lpm also appears to be more sparing of native gut flora than vancomycin, (the current standard of care for these infections), resulting in a reduced rate of recurrence (Credito and Appelbaum, 2004; Louie et al., 2009a, 2009b, 2011; reviewed in Miller, 2010; Poxton, 2010). Our fitness results in *S. aureus* suggest that Lpm may have an additional advantage over other antibiotics in that the fitness cost of becoming resistant to Lpm may be higher than that of other antibiotics, like Rif. This could contribute to the apparent low rate of Lpm-resistance in *C. difficile* that has been clinically observed so far, (only one resistant isolate has been identified) (Goldstein et al. 2012).

Chapter 4:
Target, mechanism, and structural basis of transcription inhibition by the cyclic-peptide antibiotic GE23077: occlusion of the RNAP active-center "i site" and "i+1 site"

David Degen*, Yu Zhang*, Mary Ho*, Steve Tuske, Vladimir Mekler, Elena Sineva, Katherine Y. Ebright, Sajida Ismail, Hanif Vahedian-Mohaved, Mathivanan Chinnaraj, Yon W. Ebright, Stefano Donadio, Eddy Arnold, and Richard H. Ebright

BACKGROUND

GE23077 (GE) is a cyclic heptapeptide antibiotic isolated from an actinomycete soil bacterium, *Actinomadura* sp. DSMZ 13491, by BioResearch Italia/Vicuron Pharmaceuticals in 2001 (Ciciliato et al., 2003, 2004; Marazzi et al., 2005). GE has good antibacterial activity against *Moraxella catarrhalis* (Ciciliato et al., 2004), a common Gram-negative pathogen of the human upper respiratory system (reviewed in Enright and McKenzie, 1997). Macromolecular synthesis assays revealed that GE inhibits RNA synthesis in permeabilized *E. coli* cells, while having no effect on DNA or protein synthesis (Sarubbi et al., 2004).

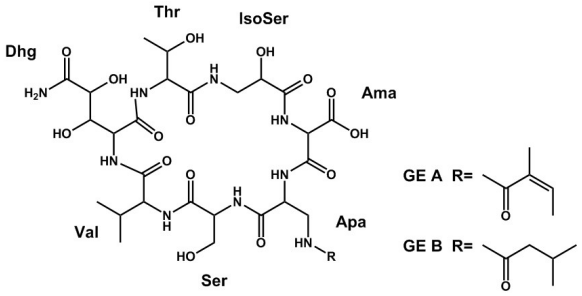

Figure 9. Structure of GE

Dhg = β,γ-dihydroxyglutamine; Thr = threonine; IsoSer = isoserine; Ama = α-amino-malonic acid; ApA = α,β-diaminopropanoic acid; Ser = serine; Val = valine.

GE potently inhibits *in vitro* transcription by both Gram-negative (*E. coli*) and Gram-positive (*B. subtilis*) bacterial RNAPs (Ciciliato et al., 2004; Sarubbi et al., 2004). Conversely, GE does not inhibit eukaryotic wheatgerm RNAP II or *E. coli* DNA

polymerase, (IC50s > 100 μM), demonstrating that it is a specific inhibitor of bacterial RNAP (Ciciliato et al., 2004; Sarubbi et al., 2004). Experiments by Sarubbi et al. (2004) suggested that GE functions in a similar way to Rif, such that it inhibits transcription initiation; but GE does not inhibit transcription elongation, nor does it inhibit the RNAP-DNA interaction. GE was also able to inhibit Rif-resistant *E. coli* RNAPs *in vitro*, suggesting that GE may function through a site that is different from the Rif target (Sarubbi et al., 2004).

RESULTS

GE target: *E. coli* saturation mutagenesis

As a first step in studying GE, Vladimir Mekler in the Ebright lab assessed whether GE competes with Rif for binding to bacterial RNAP. In fluorescence resonance energy transfer (FRET) experiments, he monitored the fluorescence of a site-specific fluorescein label, (the FRET donor), on the *E. coli* RNAP holoenzyme. When Rif binds to the fluorescently-labeled RNAP enzyme, its naphthyl group serves as a FRET acceptor, and quenches the enzyme's fluorescence (Knight et al., 2005; Feklistov et al., 2008). Performing these experiments in the presence of a saturating concentration of Rif, and varying concentrations of GE, Vladimir determined that GE partially competes with Rif for binding to RNAP (supplemental Table SC1 and Figure SC1 in Appendix SC; method as in Feklistov et al., 2008). A saturating concentration of GE increases the dissociation constant (K_d) for Rif 120-fold (from 0.5 nM to 60 nM), indicating partial competition for binding. (A fully competitive compound would increase the K_d towards infinity.)

These results suggested that GE binds to a target on bacterial RNAP that is near to and may partially overlap the Rif binding site. In order to identify the GE target, Elena Sineva and Sajida Ismail in the Ebright lab began, and I subsequently continued, saturation mutagenesis experiments in *E. coli* D21f2tolC covering all residues within 30 Å of the Rif binding site. In total, we isolated and sequenced over 70 GE-resistant mutants. Of these mutants, 35 were independent isolates containing single amino acid substitutions in the β subunit (Table SC2). Only 8 different single-substitution mutants were isolated, occurring at 5 different residues: T563P, P564R, E565D, G566C, G566R, G566S, N684K, and N684T. (One additional single-substitution mutant was identified as β D516V. However, this mutant often appears non-specifically in saturation mutagenesis screens and should not be considered a real GE-resistance mutation, as will be demonstrated later.) No GE-resistant, single-substitution mutants were identified in the β′ subunit.

The five residues at which GE-resistant substitutions were identified, cluster together in the three-dimensional structure of bacterial RNAP to form a functional determinant, ("the GE target"), with dimensions of ~16 Å x ~10 Å x ~9 Å (Figure 10A). The GE target is located adjacent to the RNAP active center and involves residues in the active-center subregions, the "β D2-loop" and the "β link region" (Weinzierl, 2010). The GE target is located adjacent to, but only minimally overlaps, the Rif target (Figure 10B). It is located at roughly the midpoint of a line connecting the Rif target to the RNAP active center. Only residues β 563 and β 564 are shared between the Rif target and the GE target. This is consistent with the observed partial competitive binding between GE

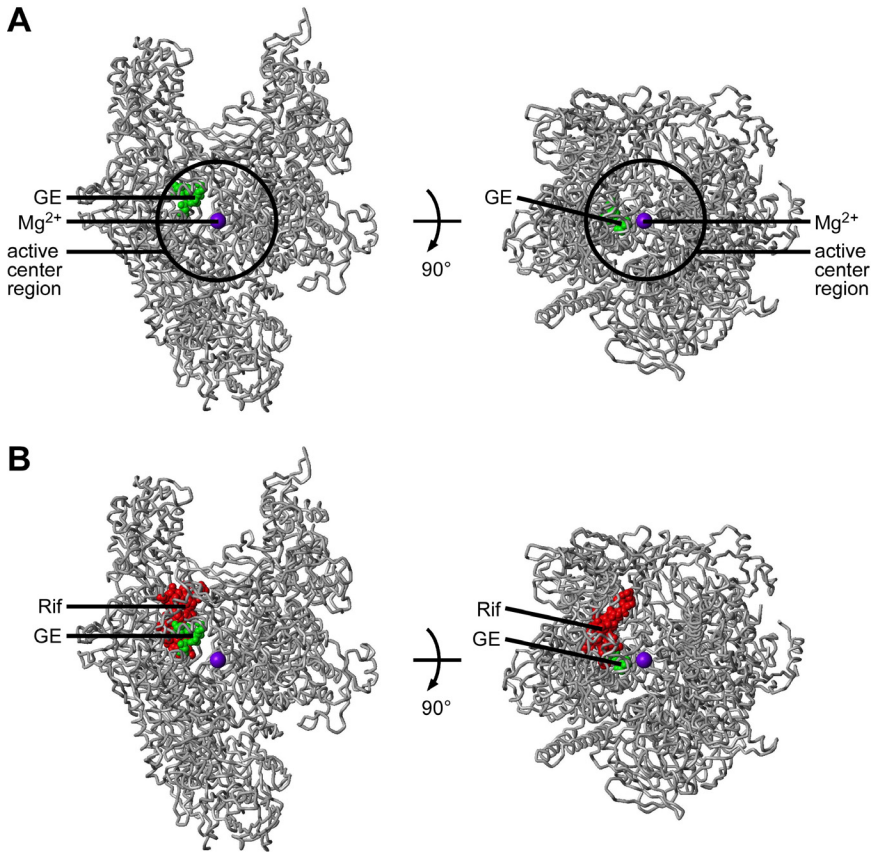

Figure 10. Target of transcription inhibition by GE

(A) GE targets a site adjacent to the RNAP active center.

(B) The GE target is adjacent to, but only minimally overlaps, the Rif target.

Each panel shows two orthogonal views of RNAP. Green spheres, sites of substitutions conferring resistance to GE in *E. coli*; red spheres, sites of substitutions conferring resistance to Rif in *E. coli*; black circle, active center region; violet sphere, active-center Mg^{2+}.

and Rif. The GE target would be expected to have some, but minimal cross-resistance with Rif.

The GE target is unusually small (5 residues, 8 substitutions). It is much smaller than the Rif target, (>28 residues, >70 substitutions) (Figure 10), and is much smaller than the Lpm target identified earlier in this work, (>31 residues, >44 substitutions) (refer back to Figure 5). The size of the GE target is small relative to the size of GE and the size expected for the GE binding site. This small size may indicate that at least part of the GE

Table 4. GE-resistant mutants from saturation mutagenesis: absence of cross-resistance to Rif, Sor, Stl, CBR703, Myx, and Lpm

amino acid substitution	MIC ratio (MIC/MIC$_{wild-type}$)[a]						
	GE	Rif	Sor	Stl	CBR703	Myx	Lpm
***rpoB* (RNAP β subunit)**							
563 Thr→Pro	2	1	0.5	1	1	0.5	2
564 Pro→Arg	2	1	1	1	2	1	1
565 Glu→Asp	>16	1	1	1	1	1	1
566 Gly→Arg	8	1	1	1	1	1	1
566 Gly→Cys	16	1	1	1	1	1	1
566 Gly→Ser	4	1	1	1	1	1	1
684 Asn→Lys	>16	1	1	1	1	1	1
684 Asn→Thr	4	1	1	1	2	1	1

[a] The MIC values with wild-type *rpoB* are as follows: GE = 500 μg/ml, Rif = 0.20 μg/ml, Sor = 1.56 μg/ml, Stl = 0.78 μg/ml, CBR703 = 6.25 μg/ml, Myx = 0.098 μg/ml, and Lpm = 0.78 μg/ml.

binding site consists of invariant residues of the RNAP active center that cannot be mutated in *E. coli* RNAP without a loss of function.

GE target: characterization in *E. coli*

Complementation studies revealed that all eight of the GE-resistant substitutions isolated are able to support viable cell growth when tested in an *E. coli* strain harboring an *rpoB*^{ts} mutation and grown at the non-permissive temperature (Table SC2). MIC assays were then used to determine the levels of resistance for these substitutions (Table 4). The two substitutions with the highest level of GE-resistance, (>16x MIC$_{wt}$), are β E565D and β N684K. These two substitutions were also the most frequently isolated in GE-resistant mutants, accounting for 80% of the independent, single-substitution isolates, (28 out of 35; see Table SC2).

As mentioned earlier, the GE-resistant substitutions β T563P and β P564R, occur at residues that are shared with the Rif target. Both of these substitutions have low level resistance to GE, (2x MIC$_{wt}$), but, under the conditions used here, neither showed cross-resistance to Rif (Table 4). Further cross-resistance testing demonstrated that none of the

eight GE-resistant substitutions have significant cross-resistance against Rif or Sor, (which, as mentioned earlier, also functions through the Rif target). The GE target does not show significant cross-resistance with several other bacterial RNAP inhibitors, including Stl, CBR703, Myx, and Lpm (Table 4). Conversely, I tested the four most frequently isolated Rif-resistant substitutions in clinical settings against GE, and found none of them to be GE-resistant (Table SC3). These results further support that, under these testing conditions, the GE target is distinct from the Rif target (and the Sor target); and does not overlap the targets of other bacterial RNAP inhibitors, including Stl, CBR703, Myx, and Lpm.

I next purified an *E. coli* RNAP enzyme having one of the high-level GE-resistance substitutions, (β E565D). I confirmed that this enzyme is highly resistant to GE *in vitro*, (>3000-fold resistant; IC50 > 100 μM for [Asp565]β-RNAP versus IC50 = 0.03 μM for wild-type RNAP; Table SC4). Additionally, when Vladimir Mekler repeated his earlier FRET experiments observing the binding of GE to RNAP, he found that this GE-resistant RNAP derivative is highly resistant to the binding of GE, (the inhibition constant (K_i) is >1 μM for [Asp565]β-RNAP versus K_i = 0.01 μM for wild-type RNAP; Figure SC2). This result confirms that the GE target contains the binding site for GE on RNAP.

GE target: conservation

All of the residues at which GE-resistant substitutions were isolated, with the exception of β subunit residue 684, are universally conserved among bacterial and eukaryotic RNAPs (Figure SC3). Residue β 684 is an asparagine in bacterial RNAP, a

glutamine in human RNAP I, and is an alanine in human RNAP II and RNAP III. This residue, and possibly other nearby residues that are also not conserved between bacterial and eukaryotic RNAPs, may provide the basis for GE's target specificity in inhibiting bacterial RNAP while not inhibiting eukaryotic RNAP. As mentioned previously, GE has been shown to not inhibit wheatgerm RNAP II (Sarubbi et al., 2004). Similarly, I have found that GE does not significantly inhibit human RNAP (IC50 > 50 μM).

In order to provide further support for this target specificity, I generated the two substitutions found in human RNAP, β N684A and N684Q, and tested them for GE-resistance in *E. coli*. (This was done by QuikChange mutagenesis on the pRL706 plasmid, [Agilent/Stratagene; methods as specified by the manufacturer].) Both of these substitutions provided some low-level, (~2x MIC_{wt}), resistance to GE. While not definitive, this result supports the hypothesis that β 684, and possibly other less-well-conserved residues nearby, are responsible for GE's target specificity.

GE target: *E. coli* chromosomal mutants

GE has a relatively high spontaneous resistance frequency in *E. coli* D21f2tolC, $>6x10^{-6}$ cfu per generation. This high frequency likely reflects mutations that prevent GE from entering the cell, and effectively precludes the isolation of GE-resistant mutations within RNAP by spontaneous resistance. Instead, I utilized lambda red-mediated recombination in order move some of the GE-resistant RNAP substitutions, which were isolated by saturation mutagenesis, from plasmids onto the chromosome. After numerous attempts, I was successful in moving three GE-resistant substitutions onto the chromosome of *E. coli* D21f2tolC: β P564R, β E565D, and β N684T. (One of these

mutants, β E565D, was actually isolated on the chromosome during the spontaneous resistance screening of a novel RNAP inhibitor, PUM. PUM has a lower spontaneous resistance frequency than GE and its target partially overlaps that of GE's, thereby enabling isolation of this mutant.) All three of these mutants are significantly resistant to GE, (≥4x MIC_{wt}), and none are cross-resistant to Rif or Stl (Table 5). Similarly, *E. coli* D21f2tolC chromosomal mutants resistant to Rif displayed no significant cross-resistance when tested against GE (mutants also constructed by lambda red-mediated recombineering; Table SC5). Fitness experiments involving two of the GE-resistant mutants, (β E565D and β N684T), indicate that these mutants have low fitness costs, (<5% per generation) (Table SC6).

Table 5. Chromosomal GE-resistant mutants in *E. coli* D21f2tolC: sequences, resistance levels, and absence of cross-resistance to Rif and Stl

amino acid substitution	MIC ratio (MIC/$MIC_{wild\text{-}type}$)[a]		
	GE	Rif	Stl
***rpoB* (RNAP β subunit)**			
564 Pro→Arg	4	1	0.25
565 Glu→Asp	>16	1	1
684 Asn→Thr	16	1	0.5

[a] The wild-type MIC values are as follows: GE = 500 µg/ml, Rif = 0.20 µg/ml, Stl = 0.78 µg/ml.

The lack of Rif-cross-resistance is particularly noteworthy for the *E. coli* D21f2tolC chromosomal mutant carrying the β P564R GE-resistant substitution. Several publications have identified Rif-resistant substitutions at this residue in *E. coli* Ovchinnikov et al., 1983; Jin and Gross, 1988; Reynolds, 2000; Garibyan et al., 2003). Garibyan et al. (2003) even claim to have isolated this exact substitution in a screen for Rif-resistant mutants in *E. coli* CC107. My results, however, clearly show that this mutant is not Rif-resistant in *E. coli* D21f2tolC (Tables 4 and 5). This discrepancy could be the result of differences in the *E. coli* strains, or the testing conditions being used, between my work and that of Garibyan et al. (2003). It is also quite possible that, given their use of chemical mutagens, the mutant obtained by Garibyan et al. (2003) may have

actually contained other, unidentified mutations that were actually responsible for the mutant's Rif-resistance.

The three chromosomal GE-resistant mutants tested here provide further confirmation of the GE target in *E. coli*, and further confirm that the GE target does not significantly overlap the Rif target.

GE-target: *S. pyogenes*

I have also been able to identify GE-resistant mutations in the pathogenic bacterium *S. pyogenes* (Table 6). This was done indirectly, through the isolation of spontaneous resistance mutants against the novel bacterial RNAP inhibitor PUM, whose target overlaps that of GE's. Four GE-resistant substitutions were identified. Three of the substitutions, (β E565G, β E565V, and β N684I) occur at residues identical to those previously identified in *E. coli*. The fourth substitution, β M681K, occurs at a nearby residue in the link region. All four of these substitutions display very high resistance to GE in *S. pyogenes*, (≥16x MIC_{wt}).

Table 6. GE-resistant mutants in *S. pyogenes*: sequences and properties

amino acid substitution[a,b]	resistance level ($MIC/MIC_{wild\text{-}type}$)[c,d]
***rpoB* (RNAP β subunit)**	
565 [525] Glu→Gly	32
565 [525] Glu→Val	32
681 [643] Met→Lys	16
684 [646] Asn→Ile	>32

[a] These mutants were isolated as spontaneous PUM-resistant mutants (D.D. and R.H.E., unpublished).

[b] Residues are numbered as in *E. coli* RNAP and, in brackets, as in *S. pyogenes* RNAP.

[c] MIC values were determined with a reduced starting cell density of ~$2x10^4$ cfu/ml.

[d] The wild-type MIC value for GE is 250 µg/ml.

These results illustrate that the GE target is the same in both Gram-negative (*E. coli*) and Gram-positive (*S. pyogenes*) bacteria. This, again, is consistent with the high conservation of residues within the GE target among bacteria.

Mechanism of transcription inhibition by GE

In order to determine the mechanism by which GE inhibits transcription, I performed a series of *in vitro* transcription experiments. Like Rif, I found that GE does

not inhibit the RNAP-DNA interaction (Figure 11A). This is consistent with previously reported results indicating that the inhibition of transcription by GE was not dependent upon its order of addition relative to DNA, (i.e. GE will still inhibit transcription regardless of whether it is added before or after the addition of DNA to RNAP *in vitro*) (Sarubbi et al., 2004).

Also like Rif, GE inhibits primer-dependent transcription initiation (Figure 11B). Unlike Rif, however, GE is able to inhibit the formation of RNA products both 3 nucleotides and 4 nucleotides in length; whereas, under these conditions, Rif is only able to inhibit the formation of RNA products ≥4 nucleotides in length (Figure 11B; McClure and Cech, 1978). (As discussed previously, Rif bound to RNAP is directly in the path of the RNA product; and it sterically occludes its elongation beyond 2-3 nucleotides in length [McClure and Cech, 1978; Campbell et al., 2001].) Furthermore, unlike Rif, GE is able to inhibit the *de novo* formation of even the smallest RNA product, a ribodinucleotide

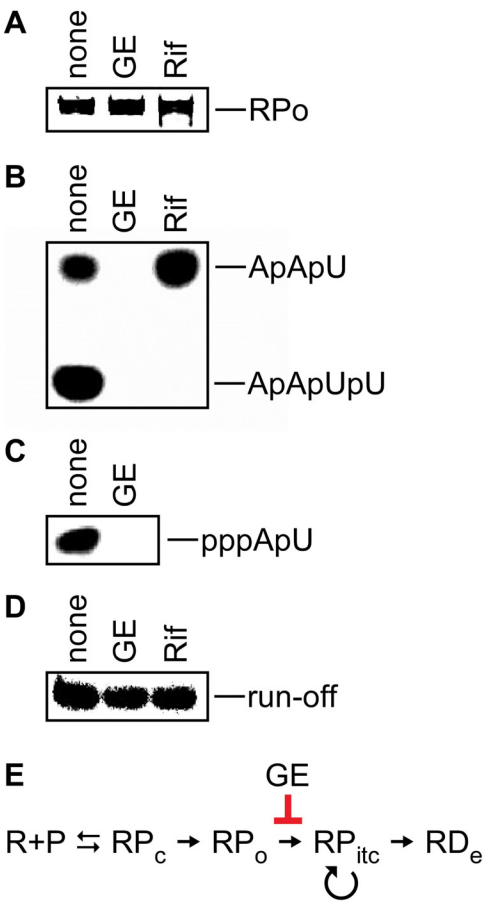

Figure 11. Mechanistic basis of transcription inhibition by GE

(A) Results from an electrophoretic mobility shift assay. Like Rif, GE does not inhibit the RNAP-DNA interaction, (all have RPo bands). RPo, heparin-resistant RNAP-promoter open complex.

(B) Results from a primer-dependent transcription initiation assay. GE inhibits transcription initiation (no bands). Like Rif, GE inhibits the formation of 4 nucleotide (ApApUpU) RNA products. Unlike Rif, GE also inhibits the formation of 3 nucleotide (ApApU) RNA products.

(C) Results from a *de novo* transcription initiation assay. GE inhibits the formation of 2 nucleotide (pppApU) RNA products.

(D) Results from a transcription elongation complex assay. GE does not inhibit nucleotide addition by a halted transcription elongation complex.

(E) Simplified schematic showing the step of transcription inhibited by GE.

(Figure 11C). Finally, GE does not inhibit nucleotide addition from a transcription elongation complex (Figure 11D).

Taken together, these biochemical results show that GE inhibits transcription at a step after the formation of a stable, heparin-resistant RP_o complex, but prior to or at the formation of the first phosphodiester bond (Figure 11E). The GE mechanism is different from the mechanism of Rif, i.e. GE can inhibit formation of the first phosphodiester bond in both primer-dependent and *de novo* transcription initiation (Figures 11B and 11C; McClure and Cech, 1978). The GE mechanism is also different from the mechanisms of the bacterial RNAP inhibitors Stl, CBR703, Myx, Cor, Rip, and Lpm, i.e., as discussed earlier, Stl and CBR703 can inhibit nucleotide addition during elongation (Artsimovitch et al., 2003; Tuske et al., 2005, Temiakov et al., 2005; Vassylyev et al., 2007b; Ho et al., 2009); and Myx, Cor, Rip, and Lpm inhibit the RNAP-DNA interaction (Belogurov et al., 2008; Mukhopadhyay et al., 2008; Ho et al., 2009; Tupin et al., 2010b; Srivastava et al., 2011; Artsimovitch et al., 2012; Figure 8).

GE target: crystal structure of the RNAP-GE complex

In order to better understand the GE target and its mechanism of inhibition, Mary Ho in the Eddy Arnold's lab at Rutgers, as well as Yu Zhang in the Ebright lab, were able to determine a crystal structure of GE in complex with *Thermus thermophilus* RNAP at 3.3 Å resolution (Figure 12). This structure confirms that GE binds to the GE target; a site overlapping the active-center subregions, the β D2-loop and the β link region (Figure 12A), and adjacent to the Rif binding site (Figure 12D). GE is located within 2.2 Å of the active-center Mg^{2+} ion. The residues at which GE-resistant substitutions were identified

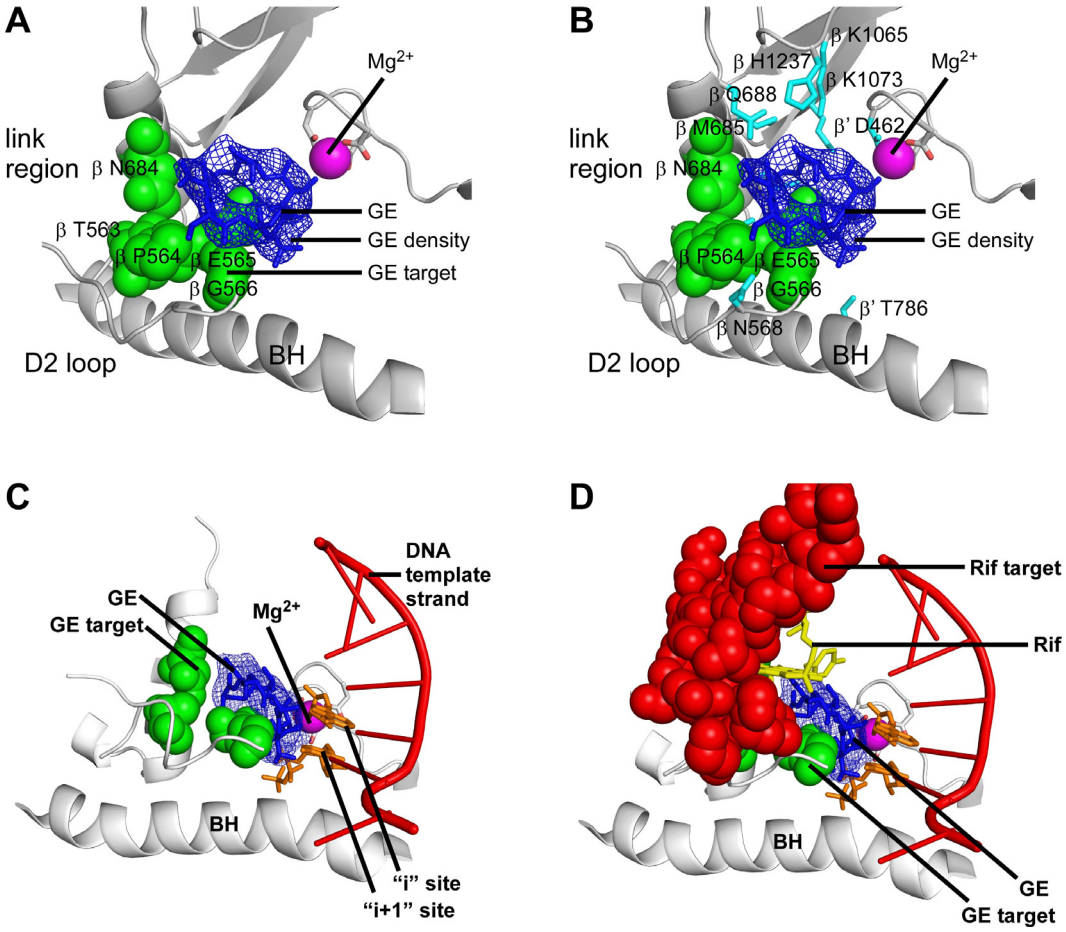

Figure 12. Crystal structure of the RNAP-GE complex

(A) View of the RNAP active center region where an electron density for GE is found adjacent to the active-center Mg^{2+}, and makes direct contact with several of the residues at which GE-resistant substitutions have been identified. The structure of GE can be fit into this density. The RNAP active-center subregions, the β D2-loop, the β link region, and the bridge helix (BH) are labeled.

(B) Residues that appear to make direct contact with, (are within 4.5 Å of), GE. There are ten additional residues, not previously identified in the GE target from *E. coli*. Cyan sticks, sidechains of the additional residues that make contact with GE, labeled with their residue identities, β residues L680 and M681 are obscured behind GE in this view orientation; β residue T563 is not labeled since it does not make direct contact with GE.

(C) Structural basis of inhibition by GE: GE is positioned to clash with NTPs bound to the RNAP active-center "i site" and "i+1 site." GE, therefore, occludes the active-center "i site" and "i+1 site." (GE is also positioned to interfere with the coordination of the active-center Mg^{2+} ion.) Red tubes, modeled template strand of DNA; orange sticks, modeled nucleotides.

(D) Relationship between Rif and GE: GE is located immediately adjacent to the Rif target. Only the sidechain of Rif overlaps a sidechain of GE. Red spheres, sites of substitutions conferring resistance to Rif in *E. coli*; yellow sticks, Rif.

Green spheres, sites of substitutions conferring resistance to GE in *E. coli*, labeled with their identities in panels A and B; blue mesh, electron density for GE; blue sticks, GE with R group omitted; violet sphere, active-center Mg^{2+}. Panels C and D were generated by Yu Zhang.

either make direct contact with GE, or contact other residues that make direct contact with GE (Figure 12A). In particular, one of the residues at which the highest-resistance-level and most-frequently-isolated GE-resistant substitutions occur, β E565, makes direct hydrogen bond contacts with GE. The cyclic structure of GE makes it appear like a doughnut in three dimensions, and this doughnut sits directly on top of the glutamic acid sidechain of residue β E565.

The cyclic nature of GE presented a challenge in order to properly orient GE within the doughnut-shaped electron density seen in the crystal structure. My cross-resistance measurements proved helpful in this regard. In testing all available plasmid-based mutants in the lab having substitutions in the β D2-loop and the β link region, I discovered that one, β Q688K, showed significant hypersensitivity, (~0.25x MIC_{wt}), to GE. (It is very unusual to observe hypersensitivity in the plasmid-based system given its merodiploid nature.) The fact that the hypersensitivity resulted from the substitution of an uncharged glutamine residue with a charged lysine residue suggested that residue β Q688 makes contact with a charged residue of GE. GE only contains one charged residue, α-amino-malonic acid. Using this information to restrict the possible orientations of GE within the doughnut-shaped electron density enabled the proper fitting of GE within the density.

The crystal structure of the RNAP-GE complex shows that GE makes direct contact with, (is within 4.5 Å of), ten additional residues that were not previously identified in the GE target in *E. coli*: β residues N568, L680, M681, M685, Q688, K1065, K1073, and H1237, as well as β′ residues D462 and T786 (Figure 12B). All of these residues are conserved among bacterial RNAPs, and only two of these residues are not

conserved between bacterial and eukaryotic RNAPs. This suggests that most of these residues may be critical for the function of RNAP, and cannot be easily mutated without a loss of function. In fact, substitutions at residues K1065, K1073, and H1237 have actually been shown to be lethal in *E. coli*, i.e. unable to support viable cell growth in complementation assays (Kashlev et al., 1990; Mustaev et al., 1991; Sagitov et al., 1993). This high degree of conservation helps to explain why I was unable to obtain GE-resistance mutations at all but one these residues, (β residue M681 in *S. pyogenes*), and, thereby why the GE-resistance determinant is unusually small.

The two residues that are not conserved between bacterial and eukaryotic RNAPs, (β L680 and β M681), may be less critical for RNAP function. As was just mentioned, I was able to obtain a chromosomal GE-resistant mutant in *S. pyogenes* with a substitution at residue β M681 (Table 6). These two residues, in addition to residue β N684, (which was discussed earlier), may provide for the target specificity of GE towards bacterial RNAP over eukaryotic RNAP.

The crystal structure of the RNAP-GE complex shows that GE is positioned to interact with β′ residue D462. Residue β′ D462 is one of the three aspartic acid residues that coordinates the active-center Mg^{2+} ion of bacterial RNAP (Figures 11B and 11C; Zhang et al., 1999; Sosunov et al., 2003). GE appears to interact with the carboxylate sidechain of this residue which is directly involved in the coordination of the active-center Mg^{2+} ion. Any disruption or interference with this coordination would be expected to inhibit the catalytic activity of the Mg^{2+} ion, thereby preventing phosphodiester bond formation (Sosunov et al., 2005).

Most significantly, the crystal structure of the RNAP-GE complex reveals that GE is positioned to clash with NTPs bound to the RNAP active-center "i site" and the "i+1 site" (Figure 12C). The "i site" is the catalytic binding site of the first initiating nucleotide in RNA synthesis, and is occupied by the 3′-end of an RNA product strand (Zhang et al., 1999; Murakami et al., 2002a, 2002b; Sosunov et al., 2003). The "i+1 site" is the catalytic binding site of the extending nucleotide in RNA synthesis (Zhang et al., 1999; Murakami et al., 2002b; Sosunov et al., 2003). GE would be expected to clash with the α-, β-, and γ-phosphates of an NTP bound to the active-center "i site," as well as part of the NTP base. This clash occludes the active-center "i site." GE would also be expected to clash with the α-phosphate and part of the base of an NTP bound to the "i+1 site." This clash occludes the active-center "i+1 site." These clashes indicate that GE inhibits transcription by preventing the binding of NTPs to the active-center "i site" and "i+1 site."

This hypothesis is consistent with the fact that GE does not inhibit the RNAP-DNA interaction (i.e. RP_o formation), but does inhibit the formation of the first phosphodiester bond during transcription initiation. This hypothesis is further consistent with the fact that GE does not inhibit nucleotide addition from a transcription elongation complex. In a transcription elongation complex, the 3′-end of the RNA product strand is already occupying the active-center "i site," and likely prevents GE from being able to bind to this site in RNAP.

To further support this hypothesis, Yu Zhang soaked NTPs (or NTP analogs) into crystals of *T. thermophilus* RNAP-promoter open complex (RP_o) in the presence or absence of GE, under identical conditions. In the absence of GE, electron density for

NTPs can be observed in the RNAP active-center "i site" and in the "i+1 site." In the presence of GE, however, electron density for NTPs cannot be observed in the RNAP active-center "i site" nor in the "i+1" site, and instead, electron density for NTP is seen in the nucleotide entry "E site" in the RNAP secondary channel (Sosunov et al., 2003). These results structurally illustrate that GE functions by precluding the binding of NTPs to the active-center "i site" and "i+1 site."

I am currently attempting to further confirm this hypothesis through biochemical kinetics experiments assessing the effects of GE on RNA synthesis in the presence of varying amounts of NTP substrate. These experiments are complicated by the fact that GE is a "tight-binding" inhibitor of *E. coli* RNAP, (K_i = 10 nM), and, as such, the equilibrium binding conditions required for a Michaelis-Menten analysis are difficult to achieve and easily misinterpreted [see "transcription assays: nucleotide addition kinetics" in Chapter 2; reviewed in Copeland, 2000; Strelow et al., 2012]. Through the use of several methods intended to effectively increase the K_i of RNAP for GE, I hope to be able to accurately assess the competition between GE and NTP substrate for binding to the RNAP active-center "i site" and "i+1 site."

A final insight from the crystal structure of the RNAP-GE complex is the positioning of GE relative to Rif (Figure 12D). As has been noted several times, the GE target is located immediately adjacent to the Rif target. The crystal structure reveals that GE bound to RNAP would only minimally overlap Rif bound to RNAP, with only the sidechain of Rif overlapping one sidechain of GE (Figure 12D). This structural evidence further supports and helps to explain Vladimir Mekler's earlier FRET observations that GE is partially competitive with Rif with respect to binding to RNAP.

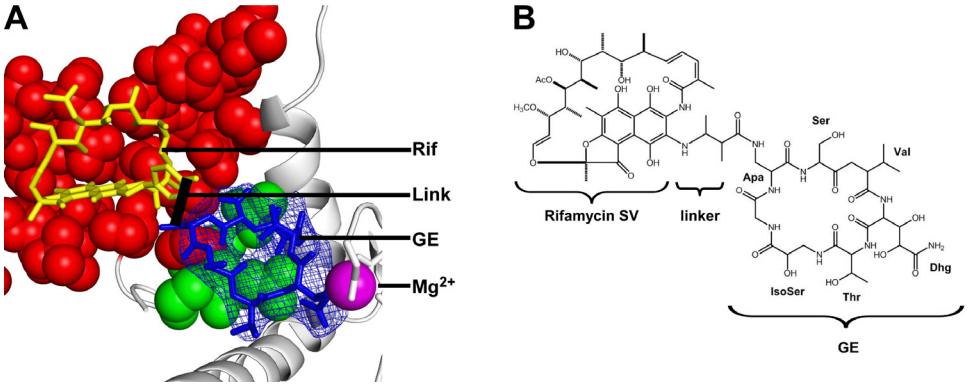

Figure 13. RifaGEs: connecting Rif to GE

(A) Rif could potentially be connected to GE through a linker on its naphthyl moiety, creating a RifaGE compound. Heavy black line, example of a link. Image created by Yu Zhang.

(B) Structure of an example RifaGE compound where rifamycin SV (left) is connected to GE (right) through a very short linker. The linker connects the Apa sidechain of GE to the naphthyl moiety of rifamycin SV. Several of the amino acids within GE are labeled for reference. Dhg = β,γ-dihydroxyglutamine; Thr = threonine; IsoSer = isoserine; ApA = α,β-diaminopropanoic acid; Ser = serine; Val = valine. Image modified from Ebright et al., 2011.

DISCUSSION

RifaGE

The crystal structure of the RNAP-GE complex suggests that Rif and GE, (or derivatives of either compound), could be joined together through a short linker to form a bipartite RNAP inhibitor, (rifaGE). This would involve connecting one of the most easily modifiable parts of a rifamycin, the sidechain to the naphthyl moiety, with one of the most easily modifiable parts of GE, the α,β-diaminopropanoic acid sidechain or the α-amino-malonic acid sidechain (Figure 13; Ebright et al., 2011). Such an inhibitor would be expected to have a very high potency, effectively combining the already high individual *in vitro* potencies of Rif and GE. RifaGE would also be expected to have a very low susceptibility to resistance. In order for an RNAP enzyme to be resistant to rifaGE, it would need to have resistance substitutions in both the Rif target and in the GE target. RifaGE would be expected to be active against mutants having Rif-resistant

substitutions, since it would still be able to bind to and inhibit RNAP through the GE target if the Rif target is inaccessible.

Another possibility would be to link together sorangicin and GE, (or derivatives of either compound), creating soraGE (Figure SC4) (Ebright et al., 2011). As mentioned in the introduction, sorangicin binds to the same target as Rif, but sorangicin is a more flexible molecule than the rifamycins, allowing it to more easily tolerate changes to its binding pocket (Campbell et al., 2005). As such, soraGE compounds would have the potential to be even more active than rifaGE compounds against Rif-resistant mutants.

The Ebright lab, in collaboration with Zoltan Szekely of the Sinko lab at Rutgers, is currently pursuing a total chemical synthesis of GE in order to aid in the development of rifaGE and soraGE derivatives. My studies of some preliminary rifaGE derivatives have demonstrated good potency against *E. coli* D21f2tolC (Table SC7). Results so far, however, have only hinted that a rifaGE derivative may actually be binding to both the Rif and GE targets. Currently, these compounds appear to be primarily functioning through the Rif target alone, (effectively acting like Rif with a very large sidechain attached to it) (Table SC8; note that a Rif-resistant *E. coli* D21f2tolC strain is resistant to the RifaGEs, but a GE-resistant strain is not resistant). Additional development will be needed in order to optimize rifaGE derivatives that function through both the Rif and GE targets simultaneously.

Conclusions

Genetic, experimental, and structural information all support the conclusion that GE binds to and functions through a target overlapping the bacterial RNAP active-center subregions, the β D2-loop and the β link region. This target is adjacent to, but only

minimally overlaps, the Rif target. As such, GE only has minimal, if any, cross-resistance with Rif. The GE target is also distinct from those of other previously identified bacterial RNAP inhibitors, including Stl, CBR703, Myx, and Lpm; and GE does not exhibit cross-resistance with these other inhibitors. GE appears to function through a different mechanism than these other bacterial RNAP inhibitors. GE inhibits RNA synthesis by directly precluding the binding of NTPs to the active-center "i site" and "i+1 site."

The GE target is much smaller than the identified targets of other bacterial RNAP inhibitors (compare Figure 19 with Figure 3). Most of the residues with which GE makes direct contact are invariant among bacterial RNAP, and likely cannot be altered without a loss of function. In fact, even substitutions at residues within the GE target, but different from those that I isolated, (i.e. substitutions T563I and G566D), have been shown to be incapable of supporting viable cell growth in *E. coli* (Tavormina et al., 1996). This suggests that the GE-resistance spectrum may be small even among the residues at which GE-resistant substitutions have been isolated, i.e. only certain substitutions can provide resistance to GE and still be viable.

The small size and minimal cross-resistance of the GE target make it an excellent target for the development of new antibacterial drugs. Compounds that function through this target would be expected to have minimal, or no, cross-resistance with other bacterial RNAP inhibitors. Given the high degree of sequence conservation within the GE target across bacterial species, a compound that functions through GE target would also be expected to have broad-spectrum antibacterial activity. Finally, these compounds would be expected to have a very low susceptibility to resistance given the conservation of and small effective size of the GE target.

Chapter 5:
Target, mechanism, and structural basis of transcription inhibition by the depsipeptide antibiotic salinamide: allosteric inhibition of nucleotide addition through the RNAP bridge-helix cap

David Degen*, Yu Feng*, Yu Zhang, Katherine Y. Ebright, Yon W. Ebright, Matthew Gigliotti, Sukhendu Mandal, Meliza Talaue, Nancy Connell, Eddy Arnold, William Fenical, and Richard H. Ebright

BACKGROUND

Salinamide (Sal) is a bicyclic depsipeptide antibiotic originally purified from a marine actinomycete bacteria, *Streptomyces sp.* CNB-091, found on the surface of a jellyfish in the Florida Keys (Trischman et al., 1994; Moore et al., 1999). Sal was also later isolated from a terrestrial actinomycete strain, *Streptomyces sp.* NRRL 21611, found in DeSoto Falls, GA (Miao, et al. 1997). There are two primary forms of Sal, SalA and SalB. SalA has an epoxide group which is changed to a chlorohydrin group in SalB (Figure 14; Trischman et al., 1994; Moore et al., 1999). (Most experiments performed here used SalA, which was available in larger quantities, unless specified otherwise.)

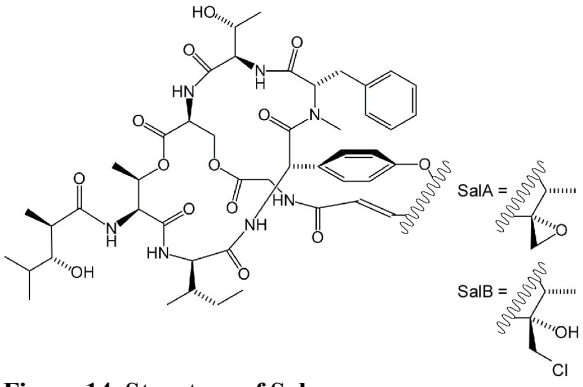

Figure 14. Structure of Sal

In addition to having some antibacterial activity, Sal was found to have good anti-inflammatory activity in mice (Trischman, et al. 1994). *In vitro* experiments indicated that Sal potently inhibits *E. coli* RNAP (Miao, et al. 1997). Experiments looking at the

biosynthesis of Sal, as well as a synthetic synthesis scheme for Sal have also been reported (Moore and Seng, 1998; Tan and Ma, 2008).

RESULTS

Sal: RNAP inhibitory activity and growth inhibitory activity

Transcription experiments performed by Sukhendu Mandal, Yu Zhang, and myself in the Ebright lab confirmed the previously reported result that Sal potently inhibits *in vitro* transcription by Gram-negative, *E. coli* RNAP (supplemental Table SD1 in Appendix SD). We further found that it also inhibits Gram-positive, *S. aureus* RNAP. I found that Sal does not inhibit human RNAP at concentrations up to 100 μM. This indicates that Sal is a specific inhibitor of bacterial RNAP.

In testing the antibacterial activity of Sal, I found that it has good activity against several pathogenic Gram-negative bacteria, in particular *Enterobacter cloacae*, *Haemophilus influenzae*, and *Neisseria gonorrhoeae* (Table SD2). Our Rutgers collaborators at the Center for Biodefense in Newark, Meliza Talaue and Nancy Connell, found that Sal is not cytotoxic to mammalian Vero cells (Table SD2). This indicates that Sal can specifically target bacterial cells while not affecting mammalian cells.

Sal: cellular target

In order to determine if Sal functions by inhibiting bacterial RNAP in cells, I performed macromolecular synthesis assays (methods developed from King and Wu, 2009). Using *E. coli* D21f2tolC cells, I monitored the incorporation of radiolabeled precursors into DNA, RNA, and protein, both in the presence and absence of Sal. These

results showed that Sal rapidly inhibits RNA synthesis in cells, while having no effect on DNA synthesis (Figure 15). Sal also inhibits protein synthesis, but this effect only occurs at time points after the inhibition of RNA synthesis has already occurred (Figure 15). (This is a logical consequence of RNA synthesis inhibition, since ribosomes cannot synthesize proteins if RNA is unavailable to direct the synthesis.) This pattern of inhibition exactly matches the pattern seen when the identical experiments are performed with the well-established bacterial RNAP inhibitor, Rif (red lines in Figure 15). As such, bacterial RNAP appears to be the functional cellular target of Sal. The antibacterial activity of Sal is likely the direct result of its inhibition of bacterial RNAP in cells.

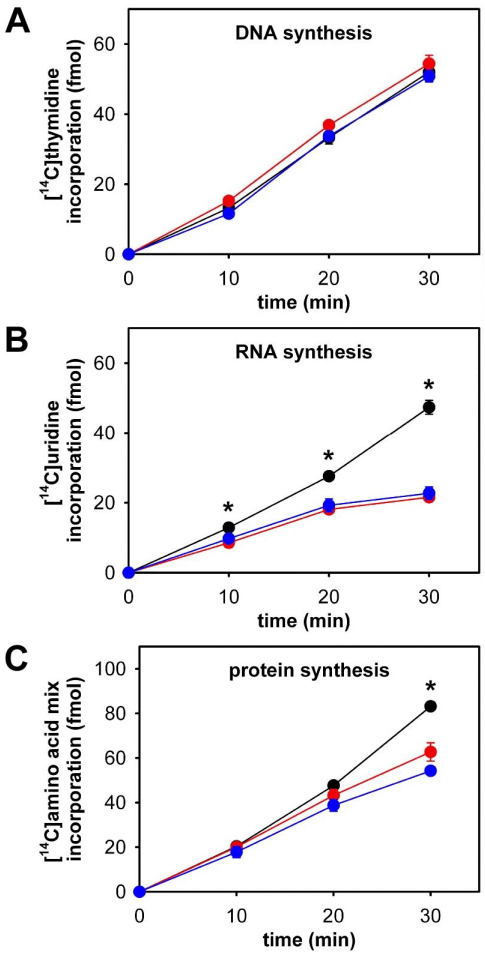

Figure 15. Sal inhibits RNAP in cells

(A) Like Rif, Sal does not inhibit DNA synthesis in *E. coli* D21f2tolC cells.

(B) Like Rif, Sal rapidly inhibits RNA synthesis in *E. coli* D21f2tolC cells.

(C) Like Rif, Sal inhibits protein synthesis only at later time points than RNA synthesis inhibition in *E. coli* D21f2tolC cells.

Asterisks indicate time points where the value with Sal is statistically different from the value with no inhibitor ($p \leq 0.01$, $n = 4$).

Black line, no inhibitor; blue line, Sal (0.39 µg/ml, 2x MIC); red line, Rif (0.098 µg/ml, 2x MIC).

Sal target: *E. coli* chromosomal mutants

I next performed spontaneous resistance experiments in *E. coli* D21f2tolC cells in order to isolate Sal-resistant mutants. In total, 68 Sal-resistant mutants were isolated and sequenced, of which 47 were independent isolates. The spontaneous resistance rate for Sal is ~$1x10^{-9}$ cfu per generation (at Sal

concentrations of 2x and 4x the MIC). This is essentially identical to the spontaneous resistance rate for Rif under identical conditions (Table SD3). All of the sequenced Sal-resistant mutants contained a mutation in either the gene encoding the RNAP β′ subunit, (*rpoC*), or the gene encoding the RNAP β subunit, (*rpoB*) (Table SD4). This further supports the hypothesis that bacterial RNAP is the functional cellular target of Sal.

Of the 47 independent Sal-resistant mutants, 35 contained single amino acid substitutions in the β′ subunit, and 11 contained single amino acid substitutions in the β subunit (Table SD5). (There was also one mutant with multiple amino acid substitutions in the β′ subunit.) The single substitutions in the β′ subunit occur at 11 different residues: 690, 697, 738, 748, 758, 763, 775, 779, 780, 782, and 783. The single substitutions in the β subunit occur at only 3 different residues: 569, 675, and 677.

In the three-dimensional structure of bacterial RNAP, these residues form a tight cluster, ("the Sal target") (Figure 16A). The Sal target does not overlap the targets of other bacterial RNAP inhibitors, including Rif, Stl, CBR703, Myx, and Lpm (Figure 16B). (The Sal target also does not overlap the GE target.) As such, the Sal target would be expected to have minimal to no cross-resistance with these other inhibitors.

The Sal target is immediately adjacent to the RNAP active center and overlaps three active-center subregions: the "bridge-helix N-terminal hinge" (BH-H_N), the "F-loop", and the "link region" (collectively "the bridge-helix cap") (Hein and Landick, 2010; Weinzierl, 2010). The BH-H_N is believed to undergo a conformational opening and closing during each nucleotide addition cycle of transcription, with these movements being coordinated by the F-loop and the link region (Hein and Landick, 2010; Weinzierl, 2010, 2012; Kireeva et al., 2012; Nedialkov et al., 2013). Disruption of this

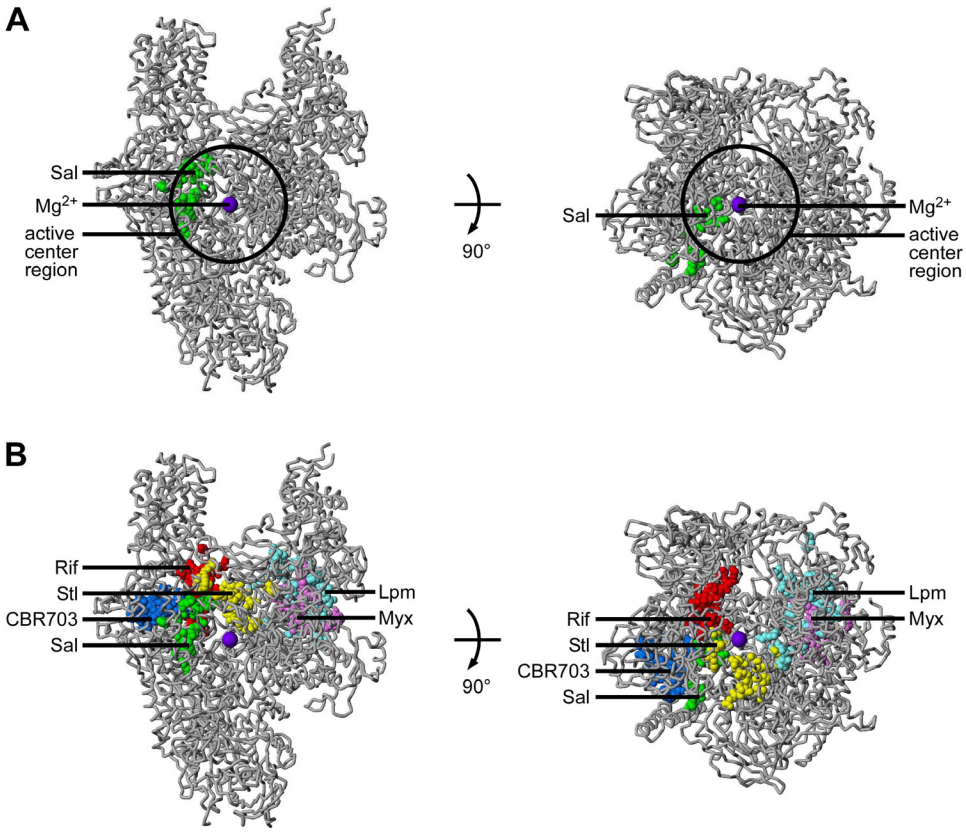

Figure 16. Target of transcription inhibition by Sal

(A) Sal targets a site adjacent to the RNAP active center.

(B) The Sal target does not overlap the targets of other bacterial RNAP inhibitors, Rif, Stl, CBR703, Lpm, and Myx.

Each panel shows two orthogonal views of RNAP. Green spheres, sites of substitutions conferring resistance to Sal in *E. coli*; red spheres, sites of substitutions conferring resistance to Rif in *E. coli*; yellow spheres, sites of substitutions conferring resistance to Stl in *E. coli*; blue spheres, sites of substitutions conferring resistance to CBR703 in *E. coli*; pink spheres, sites of substitutions conferring resistance to Myx in *E. coli*; cyan spheres, sites of substitutions conferring resistance to Lpm in *E. coli*; black circle, active center region; violet sphere, active-center Mg^{2+}.

conformational change would be expected to inhibit the catalytic activity of RNAP (Weinzierl, 2010).

Sal target: *E. coli* induced mutagenesis

In order to further confirm that the Sal target involves residues in the bridge-helix cap target, I performed induced mutagenesis experiments using plasmids carrying the gene encoding either the *E. coli* RNAP β′ subunit or the β subunit. I isolated and

identified ten single-substitution Sal-resistant mutants in this way (Table SD6). All of these substitutions were within, or near to, the Sal target. Four of the mutants had substitutions at residues that are identical to those identified in my spontaneous resistance experiments, (β′ 758, β′ 780, and β′ 782). The other mutants had substitutions at residues in the F-loop, the link region, or other nearby residues.

When the mutated plasmids isolated here were reintroduced into wild-type *E. coli* D21f2tolC cells by transformation, the resulting transformants were resistant to Sal. Complementation assays also showed that these mutants were capable of supporting viable cell growth (Table SD6). These results confirm that substitutions within the Sal target on bacterial RNAP are necessary and sufficient for resistance to Sal. This further suggests that any potential mutations on the chromosomes of the spontaneous Sal-resistant mutants, (outside of the genes encoding the RNAP β′ and β subunits), are highly unlikely to be responsible for their resistance to Sal.

Sal target: characterization in *E. coli*

Extensive MIC testing of the spontaneous Sal-resistant mutants demonstrated that all of the mutants are highly resistant to Sal, (≥16x MIC_{wt}) (Table 7). Several of the mutants have extremely high-level resistance to Sal, (>256x MIC_{wt}): β′ A779T, β′ G782A, β′ G782C, β D675A, and β N677K. These high levels of resistance are one of the advantages of working with chromosome-based resistance mutations as opposed to a merodiploid, plasmid-based system. The highest level of resistance seen among the plasmid-based Sal-resistant mutants was 16x MIC_{wt}, with most mutants being 2x resistant to Sal (Table SD6).

As expected, cross-resistance testing revealed that the Sal target is not significantly cross-resistant with Rif, Stl, CBR703, Myx, or Lpm (Table 7). Only one Sal-resistant mutant shows significant cross-resistance to only one of these inhibitors, β I569S is 8x-resistant to Stl. (Stl-resistant mutations at this residue have not been previously identified; but this residue makes contact with Stl in the published crystal structures of RNAP-Stl complexes [Tuske et al., 2005, Temiakov et al., 2005; Vassylyev et al., 2007b; Ho et al., 2009], and Stl-resistant mutations have been isolated at residues immediately adjacent to it, [β 570 and β 571; Tuske et al., 2005].)

Table 7. Spontaneous Sal-resistant mutants in *E. coli* D21f2tolC: absence of cross-resistance to Rif, Stl, CBR703, Myx, and Lpm

amino acid substitution	MIC ratio (MIC/MIC$_{wild\text{-}type}$)[a,b]					
	Sal	Rif	Stl	CBR703	Myx	Lpm
***rpoC* (RNAP β' subunit)**						
690 Asn→Asp	32	1	0.125	0.125	0.5	1
697 Met→Val	64	1	1	1	1	2
738 Arg→Cys	32	1	0.5	1	1	1
738 Arg→His	32	0.5	0.25	0.25	0.5	2
738 Arg→Pro	128	0.5	0.5	0.125	0.5	1
738 Arg→Ser	32	1	0.5	1	1	1
748 Ala→Glu	32	0.5	0.5	0.125	0.5	1
758 Pro→Ser	32	1	1	2	1	1
763 Phe→Cys	16	0.5	0.25	0.125	0.5	1
775 Ser→Ala	16	1	1	0.5	1	1
779 Ala→Thr	>256	1	0.5	1	1	1
779 Ala→Val	256	1	0.25	0.5	0.5	2
780 Arg→Cys	64	1	1	0.5	0.5	2
782 Gly→Ala	>256	1	2	0.5	1	1
782 Gly→Cys	>256	1	0.5	0.125	0.5	1
783 Leu→Arg	64	1	0.5	0.5	1	1
***rpoB* (RNAP β subunit)**						
569 Ile→Ser	32	1	8	1	1	1
675 Asp→Ala	>256	1	1	0.125	1	0.5
675 Asp→Gly	256	1	0.125	0.125	0.5	1
677 Asn→His	128	1	1	1	1	0.5
677 Asn→Lys	>256	1	1	0.125	1	1

[a] The wild-type MIC values are as follows: SalA = 0.049 μg/ml, Rif = 0.20 μg/ml, Stl = 3.13 μg/ml, CBR703 = 6.25 μg/ml, Lpm = 1.56 μg/ml, and Myx = 0.20 μg/ml.

[b] Values less than 0.5 (highlighted in blue) indicate that the substitution conferred significant hypersensitivity to the inhibitor.

I also tested select Rif-resistant, Stl-resistant, CBR703-resistant, Myx-resistant, and Lpm-resistant mutants for cross-resistance against Sal (Tables SD7-SD11). None of these mutants are significantly resistant to Sal. This further supports the fact that the Sal target does not significantly overlap the targets of Rif, Stl, CBR703, Myx, or Lpm.

Interestingly, several Sal-resistant mutants are actually hypersensitive to, (i.e. more easily inhibited by), Stl and CBR703 (Table 7). Five of the Sal-resistant mutants are significantly hypersensitive, (≤0.25x MIC$_{wt}$), to Stl; and nine of the Sal-resistant mutants are significantly hypersensitive to CBR703. Four of these mutants are hypersensitive to

both Stl and CBR703, (β′ R738H, β′ F763C, β D675G, and β′ N690D). These results indicate that some of the structural changes that allow for Sal-resistance may put bacterial RNAP in a state that is more favorable to inhibition by Stl and CBR703. This suggests that Sal inhibits RNAP in a different way from either Stl or CBR703, (possibly acting on a different conformational state of RNAP).

Sal target: conservation

Residues in the Sal target are highly conserved among bacteria, but are less highly conserved among eukaryotes (supplemental Figure SD1 in Appendix SD). Three of the four residues at which the highest level Sal-resistant substitutions occur, (β′ 779, β 675, and β 677), are not conserved in human RNAP. Further, one of the spontaneous Sal-resistant mutants that was isolated helps to directly demonstrate the specificity of Sal for bacterial RNAP over human RNAP. Mutation of β′ 738 from an arginine, (its identity in many bacterial species), to a serine, (its identity in human RNAPs II and III), results in strong resistance to Sal. These points indicate that human RNAP should be highly resistant to Sal, which is consistent with my *in vitro* transcription experiments demonstrating that Sal does not inhibit human RNAP, (IC50 > 100 μM; Table SD1).

Sal target: crystal structure of the RNAP-Sal complex

As further confirmation of the Sal target, Yu Feng in the Ebright lab was able to obtain a crystal structure of Sal in complex with *E. coli* RNAP at a resolution of 3.9 Å. (Sal does not inhibit *T. thermophilus* RNAP precluding the use of this RNAP for

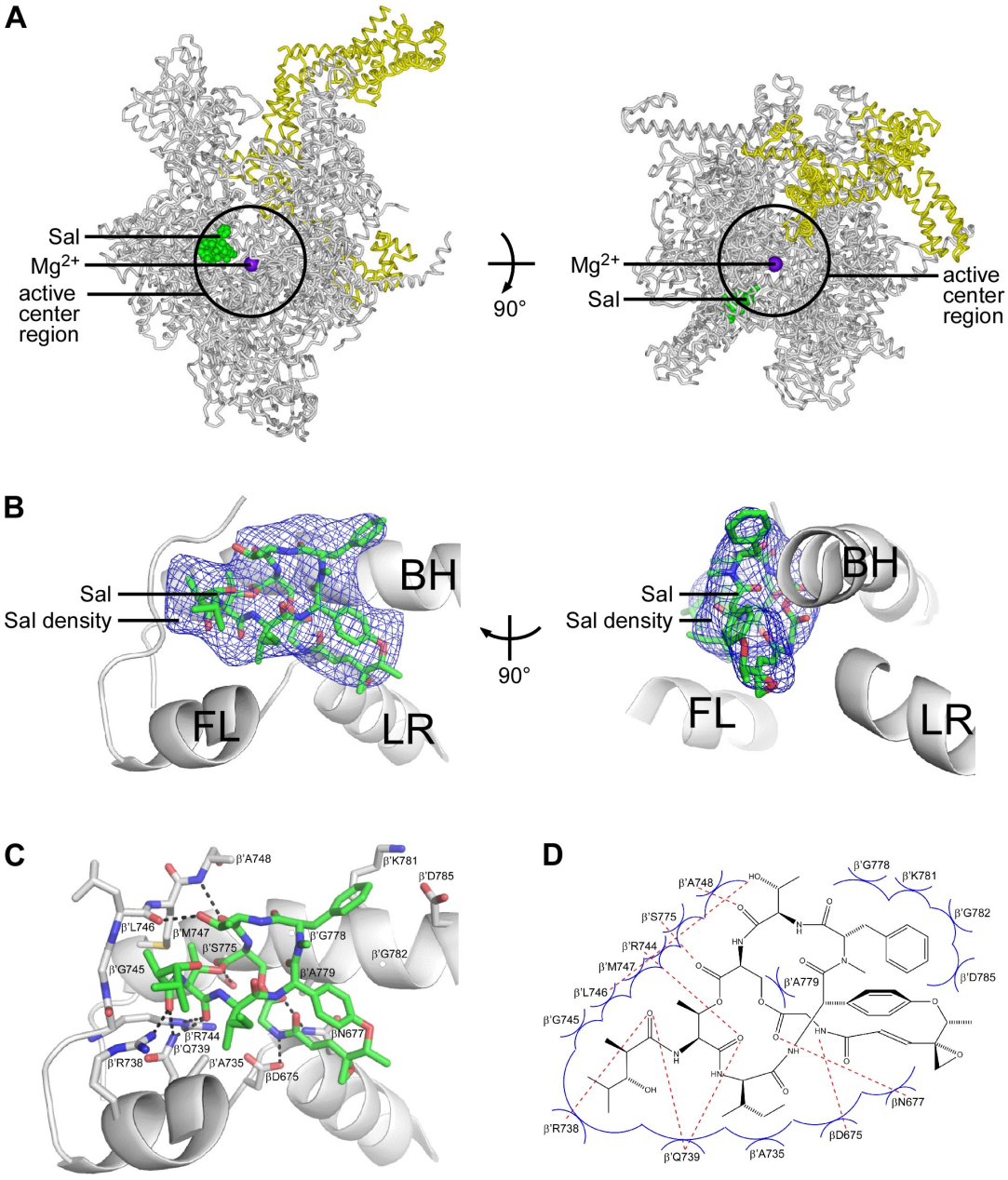

Figure 17. Crystal structure of the RNAP-Sal complex

(A) Sal binds to the Sal target in RNAP. Two orthogonal views of the crystal structure of Sal bound to the *E. coli* RNAP holoenzyme. Green spheres, SalA; yellow trace, σ subunit; black circle, active center region; violet sphere, active-center Mg^{2+}. PDB accession code 4MEX (not yet released).

(B) View of the Sal target showing an electron density for Sal. Sal can be fit into this density. Sal contacts the active center subregions: the N-terminal hinge of the bridge helix (BH), the F-loop (FL), and the link region (LR). Green sticks, SalA; blue mesh, electron density for Sal.

(C) Contacts between RNAP and Sal. The sidechains of RNAP residues that make contact with Sal are shown as sticks and labeled. Green sticks, SalA; red, oxygen atoms; blue, nitrogen atoms; yellow, sulfur atoms; dashed lines, H-bonds.

(D) A schematic representation of the contacts between RNAP and Sal. Red dashed lines, H-bonds; blue arcs, van der Waals interactions. All of the figures shown here were created by Yu Feng.

crystallization trials [Table SD1].) The crystal structure reveals that Sal does, in fact, bind to the Sal target (Figure 17).

As with GE23077, at this resolution, Sal could be fit in multiple orientations within its electron density in the RNAP-Sal complex. In order to confirm its orientation, a bromine-containing derivative of Sal was synthesized by Yon Ebright. By treating SalA with hydrogen bromide, the epoxide ring of SalA is opened and made into a bromohydrin, creating Sal-Br (Figure SD2; Sal-Br is identical to SalB, except that it contains bromine instead of chlorine). Like SalA and SalB, Sal-Br inhibits bacterial RNAP *in vitro* and does not inhibit human RNAP (Table SD12). Sal-Br also exhibits antibacterial activity similar to that of SalA and SalB (Table SD13).

A crystal structure of Sal-Br in complex with *E. coli* RNAP was obtained at a resolution of 4.7 Å. This structure showed a clear anomalous signal for bromine, and allowed for proper orientation of Sal within its electron density (Figure SD2).

The structure of the RNAP-Sal complex, reveals that Sal makes direct contact with all of the residues at which the highest level Sal-resistant mutants were obtained (i.e. β′ A779, β′ G782, β D675, and β N677) (Figures 17C and 17D). Sal also makes direct contact with or is near to the other residues in the Sal target. Sal is in position to form hydrogen bonds with several of the residues in the Sal target, including β′ R738, β′ A748, β′ S775, β D675, and β N677 (Figures 17C and 17D).

Sal directly interacts with residues in the active-center subregions: the BH-H_N, the F-loop, and the link region ("the bridge-helix cap"). In particular, Sal interacts with the BH-H_N in an open (unbent, helical) state (Figure 18). As discussed earlier, the BH-H_N is believed to open (straighten) and close (kink) during each nucleotide addition cycle (Hein

and Landick, 2010; Weinzierl, 2010, 2012; Kireeva et al., 2012). This structure suggests that Sal may function by trapping the BH-H_N in an open (unbent, helical) state.

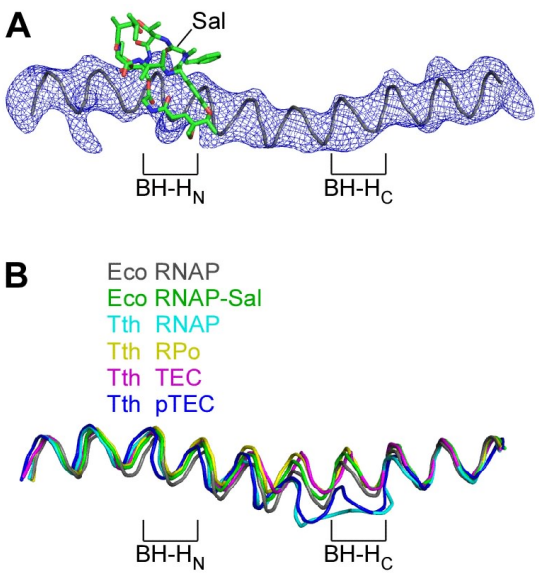

Figure 18. Structural basis of transcription inhibition by Sal

(A) Sal interacts with the N-terminal hinge of the bridge helix (BH-H_N) in a straight (unbent, helical) conformation. Green sticks, SalA; blue mesh, electron density for the bridge helix; gray trace, bridge helix; BH-H_C, C-terminal hinge of the bridge helix.

(B) Structural alignment of the bridge helices from various RNAP crystal structures. The bridge helices from Thermus thermophilus (Tth) RNAP and Tth pTEC RNAP have a kinked BH-H_C. Gray, *E. coli* (Eco) RNAP, PDB 4MEY; green, Eco RNAP in complex with Sal, PDB 4MEX; cyan, Tth RNAP, PDB 2CW0; yellow, Tth RNAP open complex (RPo), PDB 4G7H; pink, Tth RNAP transcription elongation complex (TEC), PDB 2O5J; blue, Tth RNAP paused TEC, PDB 4GZY.

These figures were created by Yu Feng.

Mechanism of transcription inhibition by Sal

Trapping the BH-H_N in an open state would be expected to greatly affect the catalytic activity of RNAP. Sal would be expected to inhibit the nucleotide addition steps of transcription, but would not be expected to interfere with the ability of RNAP to bind DNA or NTPs. In support of these hypotheses, electrophoretic mobility shift assays performed by Yu Feng, show that Sal does not inhibit the interaction of RNAP with DNA (Figure 19A). (All experiments performed here used SalA, as noted in Figure 19.) Experiments performed by Yu Zhang show that Sal inhibits both primer-dependent transcription initiation and transcription elongation (Figures 19C and 19D). (Sal also inhibits *de novo* ribodinucleotide formation [Figure SD3]). I performed kinetic experiments which show that Sal does not interfere with the binding of nucleotides to RNAP, (i.e. Sal does not alter the K_m of RNAP for NTPs) (Figure 19D and supplemental

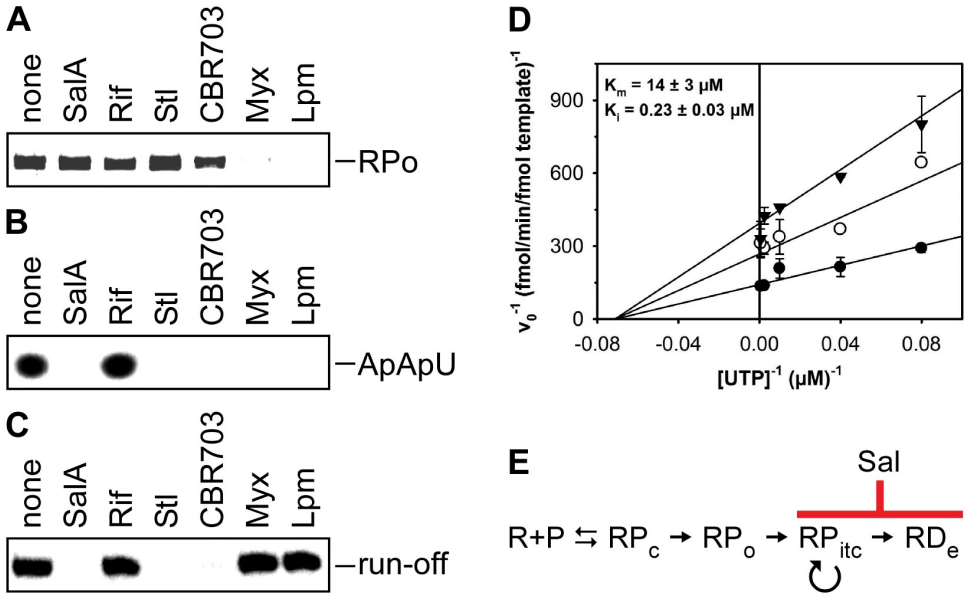

Figure 19. Mechanistic basis of transcription inhibition by Sal

(A) Results from an electrophoretic mobility shift assay. Sal does not inhibit the RNAP-DNA interaction. RPo, heparin-resistant RNAP-promoter open complex. Result from Yu Feng.

(B) Results from a primer-dependent transcription initiation assay. Sal inhibits transcription initiation. Sal inhibits the formation of 3 nucleotide (ApApU) RNA products. Result from Yu Zhang using the *lacUV5(ICAP)* (-42; +426) promoter. Sal also inhibits the formation of dinucleotide RNA products as shown in Figure SD3.

(C) Results from a transcription elongation complex assay. Sal inhibits transcription elongation. Sal inhibits the run-off product from the extension of a pre-formed transcription elongation complex. Result from Yu Zhang with experiments performed essentially as in Revyakin et al., 2006.

(D) Double-reciprocal plot showing results from transcription kinetics experiments assessing the effects of Sal on the "i+1 site" nucleotide (UTP). Sal is noncompetitive with respect to NTPs. Filled circles, no Sal; open circles, 0.2 μM Sal; closed triangles, 0.4 μM Sal. Kinetics values are provided in Table SD14. The statistical parameters used to justify this model fitting are provided in Table SD15. Results from experiments on the "i site" nucleotide (ATP) are shown in Figure SD4.

(E) Simplified schematic showing the steps of transcription inhibited by Sal.

Figure SD4). These results indicate that Sal is a noncompetitive inhibitor of transcription with respect to NTPs, (kinetic parameters and model statistics in Tables SD14 and SD15; Copeland, 2000; Strelow et al., 2012).

When these transcription results are directly compared to those of other bacterial RNAP inhibitors, it becomes clear that Sal is not functioning by a mechanism like those of Rif, Myx, or Lpm (Figure 19). The behavior of Sal is more similar to that of Stl and CBR703, both of which are thought to function by interfering with RNAP active-center

function (Artsimovitch et al., 2003; Tuske et al., 2005, Temiakov et al., 2005; Vassylyev et al., 2007b; Ho et al., 2009). As discussed earlier, however, the Sal target is unique from the targets of, and shows some hypersensitivity to Stl and CBR703. This suggests that Sal's exact mechanism of inhibition is distinct from those of Stl and CBR703.

All of these results are consistent with the hypothesis that Sal functions by trapping the BH-H_N in an open (unbent, helical) conformation. A second possible mechanism is also suggested by the crystal structure of the RNAP-Sal complex. In the crystal structure, the trigger loop is in an open (unfolded) state. Sal is positioned to clash with the trigger loop in a closed (folded) state, and, thereby, potentially interfere with active-center function (Figure SD5). However, when the trigger loop is deleted, Yu Zhang found that Sal is still able to inhibit bacterial RNAP (Figure SD5). This indicates that interference with the trigger loop is not an obligatory component of how Sal inhibits the enzyme.

DISCUSSION

Semi-synthetic Sal derivatives

The crystal structure of the RNAP-Sal complex shows that one sidechain of Sal does not make contact with residues of bacterial RNAP. The epoxide sidechain of SalA protrudes freely out into the active-center cleft (visible in Figures 17B, 17C, 17D and highlighted in Figure SD6). Modifications of this sidechain, (i.e. the chlorohydrin sidechain of SalB or the bromohydrin sidechain of Sal-Br), are tolerated since it does not appear to make interactions that are critical for binding or function (compare results for SalA to results for SalB and Sal-Br in Tables SD12 and SD13). In addition, the presence

of the epoxide moiety makes this one of the most easily modifiable sidechains of Sal. This allows for the creation of semi-synthetic derivatives of Sal.

Through this position, Sal could be modified with sidechains meant to improve its stability, or cell permeability. Sal could also be extended to make interactions with additional nearby residues, possibly improving the potency with which it binds to and inhibits bacterial RNAP. In particular, Sal could be extended through a short carbon sidechain at the epoxide moiety to make additional interactions with residues in the RNAP secondary channel or in the RNAP active-center "i+1 site" (Sosunov et al., 2003; Ebright et al., 2012a, 2012b). Attachment of a sidechain with negatively-charged functionality could make additional favorable interactions with positively-charged residues in the RNAP secondary channel (Ebright et al., 2012a). Attachment of a sidechain carrying a nucleoside analog could make very favorable, additional interactions with the RNAP active-center "i+1 site" (Ebright et al., 2012b).

Conclusions

The data presented here show that Sal is an antibiotic that functions specifically by inhibiting bacterial RNAP. Macromolecular synthesis experiments show that Sal inhibits RNA synthesis in bacterial cells. Spontaneous resistance experiments in *E. coli* D21f2tolC reveal that all mutants that are resistant to Sal have a mutation in the genes encoding the β′ or β subunits of bacterial RNAP. Further, Sal is not cytotoxic to mammalian Vero cells, and Sal does not inhibit human RNAPs *in vitro*.

Sal targets a site on bacterial RNAP that includes residues in the active-center subregions: the BH-H_N, the F-loop, and the link region ("the bridge-helix cap"). This site

is distinct from, and does not overlap the targets of other bacterial RNAP inhibitors. As such, Sal-resistant mutants have minimal to no cross-resistance with Rif, Stl, CBR703, Myx, and Lpm. Conversely, select mutants that are resistant to Rif, Stl, CBR703, Myx, and Lpm, are not cross-resistant to Sal.

Mechanistic studies reveal that Sal does not inhibit the RNAP-DNA interaction, but does inhibit transcription initiation and transcription elongation. Sal is also noncompetitive with respect to NTPs. Consistent with this profile, the crystal structure of the RNAP-Sal complex suggests that Sal functions by trapping the BH-H_N in an open (unbent, helical) conformation.

It is worth mentioning here that α-amanitin, a potent inhibitor of eukaryotic RNAP II (which does not inhibit bacterial RNAP), binds to a structural site that is very similar to the Sal target in bacterial RNAP (Weinmann et al., 1974; Wieland and Faulstich, 1991; Bushnell, et al. 2002; Brueckner and Cramer, 2008; Kaplan, et al. 2008; Bensaude, 2011). The crystal structure of yeast RNAP II in complex with α-amanitin shows that it makes contact with the eukaryotic equivalents of the BH-H_N, the F-loop, the link region, and the trigger loop (Bushnell, et al. 2002; Brueckner and Cramer, 2008; Kaplan, et al. 2008). This suggests that the functional role of this region is very important to both bacterial and eukaryotic RNAP. Important enough, in fact, for inhibitors to have evolved against it in both bacterial and eukaryotes, despite the poor sequence conservation of these regions between bacteria and eukaryotes. The exact mechanisms by which Sal and α-amanitin inhibit transcription are likely different, however, given the proposed binding of α-amanitin to the trigger loop in eukaryotic RNAP (Brueckner and

Cramer, 2008; Kaplan et al., 2008). The trigger loop, as discussed above, is not necessary for Sal to inhibit bacterial RNAP.

Sal and its target represent interesting candidates for the development of new antibacterial drugs. As mentioned earlier, Sal itself has the potential to be modified in order to improve its properties as an antibacterial agent. Like Sal, compounds that function through the Sal target would be expected to have minimal to no cross-resistance with other bacterial RNAP inhibitors. As such, when co-administered with another bacterial RNAP inhibitor, Sal, or a compound that functions through the Sal target, could greatly reduce the occurrence of spontaneous resistance mutants. This effect can be seen with *E. coli* D21f2tolC cells *in vitro*. When Sal is co-administered with Rif, there is a >1000-fold reduction in the spontaneous resistance rate (Table SD3). In the clinic, this has the potential to increase the likelihood of successfully clearing an infection, and extend the useful lifetime of the antibacterial agents being used.

Chapter 6:
Discussion

Summary

This work identifies and characterizes the targets of three bacterial RNAP inhibitors, Lpm, GE, and Sal. Each of these inhibitors binds to a unique target on bacterial RNAP that does not substantially overlap the targets of other known bacterial RNAP inhibitors, including Rif. As such, each of these inhibitors exhibits minimal, to no cross-resistance with Rif and other bacterial RNAP inhibitors.

Experiments performed with Lpm show that Lpm targets a site involving residues in the switch region subregions, switch 2 and switch 3, as well as one wall of the RNA exit channel of bacterial RNAP. Lpm appears to function by a mechanism similar to that of other switch region inhibitors (Myx, Cor, and Rip), i.e. Lpm inhibits the formation of a stable, heparin-resistant RNAP-promoter open complex by locking the β′ clamp in a partly-to-fully closed state.

Experiments performed with GE show that GE targets a site involving residues in the active-center subregions, the β D2-loop and the β link region of bacterial RNAP. GE inhibits transcription initiation. The crystal structure of the RNAP-GE complex suggests that GE may functions by precluding the binding of NTPs to the active-center "i site" and "i+1" site.

Finally, experiments performed with Sal show that Sal targets a site involving residues in active-center subregions: the BH-H_N, the F-loop, and the link region ("the bridge-helix cap") of bacterial RNAP. Sal inhibits both transcription initiation and

transcription elongation. The crystal structure of the RNAP-Sal complex suggests that Sal may function by trapping the BH-H_N in an open (unbent, helical) conformation.

The targets of Lpm, GE, and Sal each represent an attractive candidate for antibacterial drug development. Drugs functioning through these targets would be expected to have minimal cross-resistance with other bacterial RNAP inhibitors. The high sequence conservation of these targets among bacteria would provide these drugs with the potential for broad-spectrum antibacterial activity. The lesser degree of sequence conservation within these targets between bacterial and eukaryotic RNAPs, would provide these drugs with the potential for high therapeutic specificity, (i.e. specific inhibition of bacterial RNAP, while not inhibiting eukaryotic/human RNAP.)

Semisynthetic, synthetic, and biosynthetic derivatives

The simplest method to develop compounds that function through these targets would be to modify the existing inhibitors that target them. A traditional medicinal (and/or combinatorial) chemistry approach could be used to create semi-synthetic versions of Lpm, GE, or Sal; altering the existing natural product scaffolds by adding or modifying functional groups in an attempt to improve the potency and the pharmacological properties of the inhibitors. This approach has been widely used for the development of antibiotic drugs from natural products (Butler and Buss, 1996; Fischbach and Walsh, 2009; reviewed in Donadio et al., 2010). Reiterative cycles of synthesis and testing allow for continual optimization of these compounds through a better understanding of the structure-activity relationships that are involved.

As mentioned in the introduction, the semi-synthetic approach was employed in the development of Rif, (and other Rif derivatives), from the rifamycins. Many of naturally occurring rifamycins have only modest antibacterial activity, moderate stability, and poor oral bioavailability; while some of the semisynthetic derivatives greatly improve upon these properties (Wehrli and Staehelin, 1971; Lester, 1972; Sensi, 1983; Aristoff et al., 2010). Limited attempts have already been made to create semi-synthetic derivatives of GE. Researchers at Vicuron Pharmaceuticals attempted to modify GE in order to increase its lipophilicity, in hopes of improving its ability to pass through the cell membrane (Mariani et al., 2005). Different functional groups were added to three of GE's sidechains, but none of the semisynthetic derivatives had better antibacterial activity (or RNAP inhibitory activity) than the natural scaffold (Mariani et al., 2005).

The process of natural product modification can made easier and even more powerful if a total chemical synthesis has been worked out for a given natural product. Total syntheses have been reported for a number of natural-product bacterial RNAP inhibitors, including rifamycins, Myx, SalA, Stl, Rip, and Cor (Kishi, 1981; Hu, et al., 1998; Tan and Ma, 2008; Pronin and Kozmin, 2010; Winter et al., 2012; Rentsch and Kalesse, 2012). (CBR703 is already completely synthetic compound [Artsimovitch, 2003].) As discussed earlier, a total synthesis of GE is currently being pursued by the Ebright lab. A total synthesis scheme can enable the modification of chemical groups that would be difficult, if not impossible, to selectively target and modify by a semi-synthetic approach.

A total synthesis scheme is not currently available for Lpm. Some simple Lpm derivatives have been isolated by modifying the fermentation conditions in which the

host strain is grown (Hochlowski et al., 1997). More recently, the biosynthetic gene cluster of Lpm has been identified (Xiao, et al. 2011). Knowledge of this gene cluster has enabled isolation of new lipiarmycin analogs (Xiao et al., 2011; Niu et al., 2011); and, in the future, may allow researchers to create, optimize, and increase yields of Lpm analogs through synthetic biology techniques. Synthetic biology offers an exciting new approach to modifying, or possibly even creating new antibacterial agents (Gerth, 2003; Li and Vederas, 2009). The field has a great deal of potential, but is still at the very early stages of development.

Structure-based design

The crystal structures of GE and Sal in complex with RNAP provide a great deal of information to help guide the chemical modifications of these compounds. The crystal structures show what parts of these compounds make important contacts with bacterial RNAP, and what sites are accessible for modification. In the case of Sal, as discussed earlier, the epoxide side chain of Sal does not appear to make any contacts with RNAP, and, therefore, is a good candidate for modification (Ebright et al., 2012a). This strategy of using crystal structure information to guide compound development is now being widely used by both drug companies and academics (Öberg, 2006; Agarwal and Fishwick, 2010; Simmons et al., 2010). The Ebright lab is currently using, and has had success with, this strategy in the development of Myx derivatives with improved potency and pharmacological properties (Ho et al., 2009; Srivastava et al., 2011).

The availability of crystal structure information could also enable the use of *in silico* approaches to identify and design new antibacterial agents that bind to the GE or

Sal targets. Using virtual screening, libraries of existing small molecules can be tested against an enzymatic target to see if they would be predicted to bind to the target (Agarwal and Fishwick, 2010; Simmons et al., 2010; Chopra, 2013). These libraries can be filtered in advance for only those compounds that are predicted to have favorable pharmacological profiles, i.e. compounds that obey Lipinski's 'rule of five', or other, likely better, parameters (Simmons et al., 2010; Lewis, 2013).

Table 8. Bacterial RNAP inhibitors: comparison of physiochemical parameters[a,b,c]

	MW	logP[d]	Number of H-bond donors	Number of H-bond acceptors
Lipinski's rule parameters	≤500	≤5.0	≤5	≤10
natural products				
corallopyronin A	528	4.4	3	8
GE23077 A	804	-8.0	16	25
lipiarmycin A3	1058	8.6	7	18
microcin J25	2107	-4.2	25	50
myxopyronin B	432	6.1	2	6
ripostatin A	495	5.0	2	6
rifamycin SV	698	4.4	6	13
salinamide A	1020	1.7	8	22
sorangicin A	807	7.4	4	11
streptolydigin	601	1.0	3	11
semi-synthetic compounds				
rifampin	823	2.1	6	16
synthetic compounds				
CBR703	280	3.6	2	3

[a] All values reported here were calculated using the default settings of ACD/Labs Percepta software.

[b] The chemical structures used for these calculations are available at the NCBI PubChem website under the following chemical IDs:
corallopyronin A (CID 54737730); GE23077 A (CID 10259764);
lipiarmycin A3 (CID 10034073); microcin J25 (CID 57397977);
myxopyronin B (CID 54707876); ripostatin A (CID 10345643);
rifamycin SV (CID 6324616); salinamide A (CID 44566663);
sorangicin A (CID 657059); streptolydigin (CID 54708748);
rifampin (CID 5381226); CBR703 (SID 5391136)

[c] Values highlighted in red violate Lipinski's 'rule of five'.

[d] Calculated octanol-water partitioning coefficient. The consensus value is reported here which uses a combination of "classical" and "Global, Adjusted Locally According to Similarity" algorithms. More information on this calculation can be found online at: http://www.acdlabs.com/products/percepta/predictors/logp/

Lipinski's rules were developed to favor drug candidates with good oral bioavailability. The basic framework of these rules looks for compounds with a molecular weight below 500, a clog(P) (calculated soluble partition coefficient) less than five, no more than five hydrogen bond donors, and no more than ten hydrogen bond acceptors (Lipinski, 2001). These rules, however, do not take into account the properties of a compound that allow it to enter into bacterial cells (O'Shea and Moser, 2010; Lewis, 2013). This is a critical feature of an effective antibacterial agent, and is still poorly understood. Natural products and many antibacterial agents, (including bacterial RNAP inhibitors), often violate Lipinski's rules (Payne et al., 2007; O'Shea and Moser, 2010;

Lewis, 2013). In fact, of the bacterial RNAP inhibitors discussed in this work, only ripostatin A and CBR703 do not violate Lipinski's 'rule of five;' (with ripostatin A being the only natural product) (Table 8). Even rifampin, which has long been in clinical use and has good oral bioavailability, violates Lipinski's rules (Table 8; Lester, 1972; Wehrli and Staehelin, 1972; Sensi, 1983). This suggests that Lipinski's rules may be poor parameters to use in screening or designing novel bacterial RNAP inhibitors.

Virtual screening has been used extensively by the Ebright lab in the search for new antibacterial agents, (in particular against *M. tuberculosis*), that bind to the Myx target on bacterial RNAP (Ho et al., 2009; Srivastava et al., 2011). Recently, Sahner et al. (2013) also used virtual screening to identify a class of compounds that may bind to the Myx target in *E. coli*. These compounds had some antibacterial activity and poor RNAP inhibitory activity, but Sahner et al. (2013) do not provide direct evidence that the compounds even function through the Myx target of bacterial RNAP.

Programs are also available to perform *de novo* design of compounds that would be predicted to bind to a given target and could be easily synthesized (Agarwal and Fishwick, 2010; Simmons et al., 2010; Chopra, 2013). Using a fragment-based design, Agarwal et al. (2008) designed novel bacterial RNAP inhibitors against the Rif target; but the compounds had very poor inhibitory activity *in vitro*. More recently, McPhillie et al. (2011) designed novel bacterial RNAP inhibitors against the Myx target. They identified six compounds with structures radically different from Myx, which they claim inhibit bacterial RNAP better than Myx. None of these compounds, however, had antibacterial activity, demonstrating one of the primary limitations of a strictly *in silico* approach to compound design and selection. Further caution should be used in interpreting these

studies since, in neither case, were the designed compounds shown to actually function through the intended target.

Bipartite inhibitors

The construction of bipartite inhibitors is another strategy in the development of new antibacterial agents that inhibit bacterial RNAP through the Lpm, GE, or Sal targets. In this strategy, Lpm, GE, or Sal would be linked to another bacterial RNAP inhibitor to create a two-component, "bipartite", bacterial RNAP inhibitor. This strategy is possible since the Lpm, GE, and Sal targets are unique and do not significantly overlap those of other bacterial RNAP inhibitors. In this way, a bipartite inhibitor could inhibit the enzyme through two different targets simultaneously.

Inhibitors constructed in this way would be expected to inhibit the enzyme much more potently than either of their individual components due to increased binding to the enzyme (Brotz-Oesterhelt and Brunner, 2008). Furthermore, these bipartite inhibitors would be expected to have a greatly reduced the occurrence of spontaneous resistance (Brotz-Oesterhelt and Brunner, 2008; Simmons et al., 2009). In order to become resistant to a bipartite inhibitor, an RNAP enzyme would need to have resistance substitutions in the targets of both components of the bipartite inhibitor. Multiple-substitution resistance mutations generally occur at a much lower frequency than single-substitution resistance mutations. This can be seen in the results of the spontaneous resistance experiments presented in this work, where very few, if any, multiple-substitution resistance mutations were isolated (none in Tables 3 and SB9; one in Table SD5). There is also a dramatic reduction in the spontaneous resistance rate when two bacterial RNAP inhibitors are used

in combination (Table SD3). Lastly, RNAP-inhibitor-resistance-mutations are often associated with fitness costs (Billington et al., 1999; Wichelhaus et al., 2002; Gagneux, et al., 2006; O'Neill et al., 2006; Comas et al., 2011; Srivastava et al., 2012), and the fitness cost of resistance substitutions in multiple targets may be so great that they would be very unlikely to occur in a clinical setting (Andersson, 2006).

This bipartite inhibitor strategy has previously been employed by the Ebright lab to create the rifamicrocins, in which derivatives of Rif were connected by a short carbon linker to a derivative of microcinJ25 (Ebright and Wang, 2007). These bipartite compounds were better inhibitors of bacterial RNAP and better inhibitors of bacterial growth than their parent Rif compounds (Ebright and Wang, 2007). They are even able to inhibit Rif-resistant RNAP enzymes better than Rif, since they can still bind to the Rif-resistant enzymes through the microcinJ25 target rather than the Rif target (Ebright and Wang, 2007).

In the case of GE, as was discussed earlier, the crystal structure of GE in complex with RNAP shows that GE is positioned such that a short linker could be used to connect derivatives of Rif with GE, (or derivatives to GE), to create rifaGE compounds (Ebright et al., 2011). RifaGE compounds would be expected to potently inhibit bacterial RNAP, and preliminary antibacterial data indicates that rifaGE compounds are able to inhibit cell growth much better than GE alone (Table SC7; Ebright et al., 2011). This suggests that the cell-permeable rifamycin component of these compounds is able to help overcome the poor cellular permeability of the GE component.

There are many other possibilities for bipartite inhibitors of bacterial RNAP, including, as discussed earlier, sorangicin linked to GE (soraGE) and Sal linked to a

nucleoside analog (Ebright et al., 2011, 2012b). At present, it would be very difficult to rationally link Lpm to another bacterial RNAP inhibitor since the crystal structure of an RNAP-Lpm complex has yet to be solved.

A final bipartite approach is to combine a bacterial RNAP inhibitor with an antibacterial agent that targets a different enzyme entirely. (This strategy is also being pursued by various research groups trying to combine pairs of pharmacores within many different drug classes, including anticancer, antimalarial, and antibacterial agents [Tietze et al., 2003; Brotz-Oesterhelt and Brunner, 2008; Tsogoeva, 2010].) Researchers at Cumbre Pharmaceuticals developed a compound, CBR-2092, that links a Rif derivative to a quinolone derivative (Robertson et al., 2008a, 2008b). Quinolone antibiotics kill bacteria by inhibiting DNA gyrase and DNA topoisomerase IV, preventing proper maintenance of the bacterial chromosome (Emmerson and Jones, 2003). (Ciprofloxacin is a quinolone antibiotic.) CBR-2092 is able to inhibit bacterial RNAP *in vitro* (Robertson et al., 2008a). It is has potent activity against Gram-positive bacteria, and is able to inhibit both Rif-resistant and quinolone-resistant *S. aureus* strains (Robertson et al., 2008a, 2008b). The spontaneous resistance frequency of *S. aureus* against CBR-2092 is also undetectably low ($<1x10^{-12}$); over 1000-fold lower than the spontaneous resistance frequency of Rif alone or ciprofloxacin alone (Robertson et al., 2008b). This compound nicely demonstrates the potential advantages of a bipartite inhibitor in overcoming bacterial resistance. A similar approach could be applied to make any number of bipartite inhibitors containing Lpm, GE, or Sal and an antibacterial agent that functions through a target other than bacterial RNAP.

Screening bacterial extracts

The fact that each of the bacterial RNAP inhibitors presented here has a unique target suggests that there may be additional, as yet unidentified, inhibitory targets within bacterial RNAP enzyme. Lpm, GE, and Sal were all isolated from different species of actinomycete bacteria. Actinomycetes, (and myxobacteria, the source of sorangicin, Myx, Cor, and Rip), may still be an under-exploited source of new compounds that inhibit bacterial RNAP. High throughput screening techniques could be utilized to analyze bacterial extracts (or extracts from other sources) for their ability to inhibit bacterial RNAP in hopes of identifying new inhibitors and potentially new targets. This method is still viewed as having great potential for the discovery of new antibacterial agents, and is also currently being pursued by the Ebright lab (Donadio et al., 2005; Fischbach and Walsh, 2009; Li and Vederas, 2009; Donadio et al., 2010; Lewis, 2013).

In summary, the work presented here not only identifies and characterizes the enzymatic targets of Lpm, GE, and Sal, but provides insights into the functioning of these inhibitors as well as the functioning of the bacterial RNAP enzyme. New antibacterial drugs are urgently needed to help combat the ever increasing rise of pathogen resistance to current antibiotics (Fischbach and Walsh, 2009; Livermore, 2009; Rice, 2009). With some luck, the targets of Lpm, GE, and Sal will prove useful for the discovery and development of such drugs.

References

Agarwal, A.K., Johnson, A.P., and Fishwick, C.W.G. (2008). Synthesis of de novo designed small-molecule inhibitors of bacterial RNA polymerase. Tetrahedron *64*, 10049-10054.

Agarwal, A.K., and Fishwick, C.W.G. (2010). Structure-based design of anti-infectives. Ann. N.Y. Acad. Sci. *1213*, 20-45.

Andersson, D.I. (2006). The biological cost of mutational antibiotic resistance: any practical conclusions?. Curr. Opin. Microbiol. *9*, 461-465.

Aristoff, P.A., Garcia, G.A., Kirchhoff, P.D., and Hollis Showalter, H.D. (2010). Rifamycins – obstacles and opportunities. Tuberculosis (Edinb). *90*, 94-118.

Arnone, A., Nasini, G., and Cavalleri, B. (1987). Structure elucidation of the macrocyclic antibiotic lipiarmycin. J. Chem. Soc. Perkin Trans., 1353-1359.

Artsimovitch, I., Chu, C., Lynch, A.S., and Landick, R. (2003). A new class of bacterial RNA polymerase inhibitor affects nucleotide addition. Science *302*, 650-654.

Artsimovitch, I., Seddon, J., and Sears, P. (2012) Fidaxomicin is an inhibitor of the initiation of bacterial RNA synthesis. Clin. Infect. Dis. *55* Suppl 2, S127-S131.

Babakhani, F., Gomez, A., Robert, N., and Sears, P. (2011). Killing kinetics of fidaxomicin and its major metabolite, OP-1118, against *Clostridium difficile*. J. Med. Microbiol. 60, 1213-1217.

Bar-Nahum, G., Epshtein, V., Ruckenstein, A.E., Rafikov, R., Mustaev, A., and Nudler, E. (2005). A ratchet mechanism of transcription elongation and its control. Cell *120*, 183-193.

Barry, C.E., 3rd, Boshoff, H.I., Dartois, V., Dick, T., Ehrt, S., Flynn, J., Schnappinger, D., Wilkinson, R.J., and Young, D. (2009). The spectrum of latent tuberculosis: rethinking the biology and intervention strategies. Nat. Rev. Microbiol. *7*, 845-855.

Bayer, A.S., Schneider, T., and Sahl, H.G. (2013). Mechanisms of daptomycin resistance in *Staphylococcus aureus*: role of the cell membrane and cell wall. Ann. N.Y. Acad. Sci. *1277*, 139-158.

Bayro, M.J., Mukhopadhyay, J., Swapna, G.V.T., Huang, J.Y., Ma, L.C., Sineva, E., Dawson, P.E., Montelione, G.T., and Ebright, R.H. (2003). Structure of antibacterial peptide microcin J25:□ a 21-residue lariat protoknot. J. Am. Chem. Soc. *125*, 12382-12383.

Belogurov, G.A., Vassylyeva, M.N., Sevostyanova, A., Appleman, J.R., Xiang, A.X., Lira, R., Webber, S.E., Klyuyev, S., Nudler, E., Artsimovitch, I., and Vassylyev, D.G. (2009). Transcription inactivation through local refolding of the RNA polymerase structure. Nature *457*, 332-335.

Bensaude, O. (2011). Inhibiting eukaryotic transcription: Which compound to choose? How to evaluate its activity?. Transcription. *2*, 103-108.

Billington, O.J., McHugh, T.D., and Gillespie, S.H. (1999). Physiological cost of rifampin resistance induced in vitro in *Mycobacterium tuberculosis*. Antimicrob. Agents Chemother. *43*, 1866-1869.

Blair, J.M., Piddock, L.J. (2009). Structure, function and inhibition of RND efflux pumps in Gram-negative bacteria: an update. Curr. Opin. Microbiol. *12*, 512-519.

Brodolin, K. (2011). Antibiotics trapping transcription initiation intermediates: To melt or to bend, what's first?. Transcription *2*, 60-65.

Brötz-Oesterhelt, H., and Brunner, N.A. (2008). How many modes of action should an antibiotic have?. Curr. Opin. Pharmacol. *8*, 564-573.

Brueckner, F., and Cramer, P. (2008). Structural basis of transcription inhibition by α-amanitin and implications for RNA polymerase II translocation. Nat. Stuct. Mol. Biol. *15*, 811-818.

Bullock, W.E. (1983). Rifampin in the treatment of leprosy. Rev. Infect. Dis. *5* Suppl 3, S606-S613.

Bushnell, D.A., Cramer, P., and Kornberg, R.D. (2002). Structural basis of transcription: α-amanitin-RNA polymerase II cocrystal at 2.8 Å resolution. Proc. Natl. Acad. Sci. USA *99*, 1218-1222.

Butler, M.S., and Buss, A.D. (2006). Natural products--the future scaffolds for novel antibiotics?. Biochem. Pharmacol. *71*, 919-929.

Campbell, E.A., Korzheva, N., Mustaev, A., Murakami, K., Nair, S., Goldfarb, A., and Darst, S.A. (2001). Structural mechanism for rifampicin inhibition of bacterial RNA polymerase. Cell *104*, 901-912.

Campbell, E.A., Muzzin, O., Chlenov, M., Sun, J.L., Anders Olson, C., Weinman, O., Trester-Zedlitz, M.L., Darst, S.A. (2002). Structure of the bacterial RNA polymerase promoter specificity σ subunit. Mol. Cell *9*, 527-539.

Campbell, E.A., Pavlova, O., Zenkin, N., Leon, F., Irschik, H., Jansen, R., Severinov, K., and Darst, S.A. (2005). Structural, functional, and genetic analysis of sorangicin inhibition of bacterial RNA polymerase. EMBO J. *24*, 674-682.

Cassani, G., Burgess, R.R., Goodman, H.M., and Gold, L. (1971). Inhibition of RNA polymerase by streptolydigin. Nat. New Biol. *230*, 197-200.

Cattoir V., and Leclercq, R. (2013). Twenty-five years of shared life with vancomycin-resistant enterococci: is it time to divorce?. J. Antimicrob. Chemother. *68*, 731-742.

Cavalleri, B., Arnone, A., Di Modugno, E., Nasini, G., and Goldsein, B.P. (1988). Structure and biological activity of lipiarmycin B. J. Antibot. (Tokyo) *46*, 308-315.

Cech, C.L., and McClure, W.R. (1980). Characterization of ribonucleic acid polymerase-T7 promoter binary complexes. Biochemistry *19*, 2440-2447.

Chakraborty, A., Wang, D., Ebright, Y.W., Korlann, Y., Kortkhonjia, E., Kim, T., Chowdhury, S., Wigneshweraraj, S., Irschik, H., Jansen, R., Nixon, B.T., Knight, J., Weiss, S., and Ebright, R.H. (2012). Opening and closing of the bacterial RNA polymerase clamp. Science *337*, 591-595.

Chopra, I. (2007). Bacterial RNA polymerase: a promising target for the discovery of new antimicrobial agents. Curr. Opin. Investig. Drug *8*, 600-607.

Chopra, I. (2013). The 2012 Garrod lecture: discovery of antibacterial drugs in the 21st century. J. Antimicrob. Chemother. *68*, 496-505.

Christie, G.E., Cale, S.B., Isaksson, L.A., Jin, D.J., Xu, M., Sauer, B., and Calendar, R. (1996). *Escherichia coli* rpoC397 encodes a temperature-sensitive C-terminal frameshift in the β′ subunit of RNA polymerase that blocks growth of bacteriophage P2. J. Bacteriol. *178*, 6991-6993.

Ciciliato, I., Corti, E., Sarubbi, E.G., Stefanelli, S., Montanini, N., Marinelli, F., Kurz, M., and Selva, E. (2003). Antibiotics GE23077, pharmaceutically acceptable salts and compositions, and use thereof. US patent 6586393.

Ciciliato, I., Corti, E., Sarubbi, E., Stefanelli, S., Gastaldo, L., Montanini, N., Kurz, M., Losi, D., Marinelli, F., and Selva, E. (2004). Antibiotics GE23077, novel inhibitors of bacterial RNA polymerase I. Taxonomy, isolation, and characterization. J. Antibiot. (Tokyo) *57*, 210-217.

Clinical and Laboratory Standards Institute (CLSI). (2009a). Methods for Dilution Antimicrobial Susceptibility Tests for Bacteria that Grow Aerobically; Approved Standard-Eighth Edition. (Wayne, PA: CLSI). CLSI Document M07-A8.

Clinical and Laboratory Standards Institute (CLSI). (2009b). Methods for Antimicrobial Susceptibility Testing of Anaerobic Bacteria; Approved Standard-Seventh Edition. (Wayne, PA: CLSI). CLSI Document M11-A7.

Comas, I., Borrell, S., Roetzer, A., Rose, G., Malla, B., Kato-Maeda, M., Galagan, J., Niemann, S., and Gagneux, S. (2011). Whole-genome sequencing of rifampicin-resistant *Mycobacterium tuberculosis* strains identifies compensatory mutations in RNA polymerase genes. Nat. Genet. *44*, 106-110.

Copeland, R.A. (2000). Enzymes: A Practical Introduction to Structure, Mechanism, and Data Analysis. (New York, NY: Wiley-VCH, Inc.).

Coronelli, C., White, R.J., Lancini, G.C., and Parenti, F. (1975). Lipiarmycin, a new antibiotic from *Actinoplanes*. II. Isolation, chemical, biological, and biochemical characterization. J. Antbiot. *28*, 253-259.

Cramer, P., Bushnell, D.A., and Kornberg, R.D. (2001). Structural basis of transcription: RNA polymerase II at 2.8 Ångstrom resolution. Science *292*, 1863-1876.

Credito, K.L., and Appelbaum, P.C. (2004). Activity of OPT-80, a novel macrocycle, compared with those of eight other agents against selected anaerobic species. Antimicrob. Agents Chemother. *48*, 4430-4434.

Crum, G.F., Devries, W.H., Eble, T.E., Large, C.M., and Shell, J.W. (1956). Streptolydigin, a new antimicrobial antibiotic. II. Isolation and characterization. Antibiot. Annu. *3*, 893-896.

Datsenko, K.A., and Wanner, B.L. (2000). One-step inactivation of chromosomal genes in *Escherichia coli* K-12 using PCR products. Proc. Natl. Acad. Sci. USA *97*, 6640-6645.

deHaseth, P., Zupancic, M., and Record, M.T. Jr. (1998). RNA polymerase-promoter interactions: the comings and goings of RNA polymerase. J. Bacteriol. *180*, 3019-3025.

deHaseth, P.L., Zupancic, M.L., and Record, M.T. Jr. (1998). RNA polymerase-promoter interactions: the comings and goings of RNA polymerase. J. Bacteriol. *18*0, 3019-3025.

Delgado, M.A., Rintoul, M.R., Farías, R.N., and Salomón, R.A. (2001). *Escherichia coli* RNA polymerase is the target of the cyclopeptide antibiotic microcin J25. J. Bacteriol. *183*, 4543-4550.

Dignam, J.D., Lebovitz, R.M., and Roeder, R.G. (1983). Accurate transcription initiation by RNA polymerase II in a soluble extract from isolated mammalian nuclei. Nucleic Acid Res. *11*, 1475-1489.

Donadio, S., Brandi, L., Serina, S., Sosio, S., and Stinchi, S. (2005). Discovering novel antibacterial agents by high throughput screening. Front. Drug Des. Discovery *1*, 3-16.

Donadio, S., Maffioli, S., Monciardini, P., Sosio, M., and Jabes, D. (2010). Antibiotic discovery in the twenty-first century: current trends and future perspectives. J. Antibiot. (Tokyo) *63*, 423-430.

Ebright, R.H. (2000). RNA polymerase: structural similarities between bacterial RNA polymerase and eukaryotic RNA polymerase. J. Mol. Biol. *304*, 687-698.

Ebright, R.H. (2005). RNA-exit-channel: target and method for inhibition of bacterial RNA polymerase. WO2005/001034.

Ebright, R.H. and Wang, D. (2007). Bipartite inhibitors of bacterial RNA polymerase. WO2007/089310.

Ebright, R.H., Zhang, Y., Degen, D., and Ebright, Y. (2011). Bipartite inhibitors of bacterial RNA polymerase: Rif-target/GE23077-target. US provisional patent application 61/498,970. (currently unpublished)

Ebright, R.H., Ebright, Y.W., Feng, Y., and Degen, D. (2012a). Antibacterial agents: salinamide derivatives. US provisional patent application 61/736,476. (currently unpublished)

Ebright, R.H., Feng, Y., Zhang, Y., and Ebright, Y. (2012b). Bipartite inhibitors of bacterial RNA polymerase: Sal-target-inhibitor/nucleoside-analog-inhibitor conjugates. US provisional patent application. (currently unpublished)

Ebright, R.H., Degen, D., and Ebright, K.Y. (2012c). Bridge-helix cap: target and method for inhibition of bacterial RNA polymerase. WO2012/129173.

Emmerson A.M., Jones, A.M. (2003). The quinolones: decades of development and use. J. Antimicrob. Chemother. 51 Suppl 1, 13-20.

Enright, M.C., and McKenzie, H. (1997). *Moraxella* (*Branhamella*) *catarrhalis* – clinical and molecular aspects of a rediscovered pathogen. J. Med. Microbiol. *46*, 360-371.

Erb, W., and Zhu, J. (2013). From natural product to marketed drug: the tiacumicin odyssey. Nat. Prod. Rep. *30*, 161-174.

Feklistov, A., Mekler, V., Jiang, Q., Westblade, L.F., Irschik, H., Jansen, R., Mustaev, A., Darst, S.A., and Ebright, R.H. (2008). Rifamycins do not function by allosteric modulation of binding of Mg^{2+} to the RNA polymerase active center. Proc. Natl. Acad. Sci. USA *105*, 14820-14825.

Fishbach, M.A., and Walsh, C.T. (2009). Antibiotics for emerging pathogens. Science *325*, 1089-1093.

Foster, P.L. (2006). Methods for determining spontaneous mutation rates. Methods Enzymol. *409*, 195-213.

Fralick, J.A., and Burns-Keliher, L.L. (1994). Additive effect of *tolC* and *rfa* mutations on the hydrophobic barrier of the outer membrane of *Escherichia coli* K-12. J. Bacteriol. *176*, 6404-6406.

Gagneux, S., Long, C.D., Small, P.M., Van, T., Schoolnik, G.K., and Bohannan, B.J. The competitive cost of antibiotic resistance in *Mycobacterium tuberculosis*. Science *312*, 1944-1946.

Garibyan, L., Huang, T., Kim, M., Wolff, E., Nguyen, A., Nguyen, T., Diep, A., Hu, K., Iverson, A., Yang, H., and Miller, J.H. (2003). Use of the *rpoB* gene to determine the specificity of base substitution mutations on the *Escherichia coli* chromosome. DNA Repair (Amst.) *2*, 593-608.

Gnatt, A.L., Cramer, P., Fu, J., Bushnell, D.A., and Kornberg, R.D. (2001). Structural basis of transcription: an RNA polymerase II elongation complex at 3.3 Å resolution. Science *292*, 1876-1882.

Goldstein, E.J., Babakhani, F., and Citron, D.M. (2012). Antimicrobial activities of fidaxomicin. Clin. Infect. Dis. *55* Suppl 2, S143-S148.

Gualtieri, M., Villain-Guillot, P., Latouche, J., Leonetti, J.P., and Bastide, L. (2006). Mutation in the *Bacillus subtilis* RNA polymerase β′ subunit confers resistance to lipiarmycin. Antimicrob. Agents Chemother. *50*, 401-402.

Gualtieri, M., Tupin, A., Brodolin, K., and Leonetti, J.P. (2009). Frequency and characterization of spontaneous lipiarmycin-resistant *Enterococcus faecalis* mutants selected in vitro. Int. J. Antimicrob. Agents *34*, 605-606.

Hall, B.M., Ma, C.X., Liang, P., and Singh, K.K. (2009). Fluctuation Analysis CalculatOR: a web tool for the determination of mutation rate using Luria-Delbrück fluctuation analysis. Bioinformatics. *25*, 1564-1565.

Hartmann, G., Honikel, K.O., Knüsel, F., and Nüesch, J. (1967). The specific inhibition of the DNA-directed RNA synthesis by rifamycin. Biochim. Biophys. Acta. *145*, 843-844.

Hein, P.P., and Landick, R. (2010). The bridge helix coordinates movements of modules in RNA polymerase. BMC Biol. *8*, 141.

Heisler, L.M., Suzuki, H., Landick, R., and Gross, C.A. (1993). Four contiguous amino acids define the target for streptolydigin resistance in the β subunit of *Escherichia coli* RNA polymerase. J. Biol. Chem. *268*, 25369-25375.

Hermes, J.D., Parekh, S.M., Blacklow, S.C., Koster, H., and Knowles, J.R. (1989). A reliable method for random mutagenesis: the generation of mutant libraries using spiked oligodeoxyribonucleotide primers. Gene *84*, 143-151.

Hermes, J.D., Blacklow, S.C., and Knowles J.R. (1990). Searching sequence space by definably random mutagenesis: improving the catalytic potency of an enzyme. Proc. Natl. Acad. Sci. USA *87*, 696-700.

Ho, M.X., Hudson, B.P., Das, K., Arnold, E., and Ebright, R.H. (2009). Structures of RNA polymerase-antibiotic complexes. Curr. Opin. Struct. Biol. *19*, 715-723.

Hochlowski, J.E., Swanson, S.J., Ranfranz, L.M., Whittern, D.N., Buko, A.M., and McAlpine, J.B. (1987). Tiacumicins, a novel complex of 18-membered macrolides. II. Isolation and structure determination. J. Antibiot. (Tokyo) *40*, 575-588.

Hochlowski, J.E., Jackson, M., Rasmussen, R.R., Buko, A.M., Clement, J.J., Whittern, D.N., and McAlpine, J.B. (1997). Production of brominated tiacumicin derivatives. J. Antibiot. (Tokyo) *50*, 201-205.

Hu, T., Schaus, J.V., Lam, K., Palfreyman, M.G., Wuonola, M., Gustafson, G., and Panek, J.S. (1998). Total synthesis and preliminary antibacterial evaluation of the RNA Polymerase inhibitors (±)-myxopyronin A and B. J. Org. Chem. *63*, 2401-2406.

Hudson, B.P., Quispe, J., Lara-González, S., Kim, Y., Berman, H.M., Arnold, E., Ebright, R.H., and Lawson, C.L. (2009). Three-dimensional EM structure of an intact activator-dependent transcription initiation complex. Proc. Natl. Acad. Sci. USA *106*, 19830-19835.

Irschik, H., Gerth, K., Höfle, G., Kohl, W., and Reichenbach, H. (1983). The myxopyronins, new inhibitors of bacterial RNA synthesis from *Myxococcus fulvus* (Myxobacterales). J. Antibiot. (Tokyo) *36*, 1651-1658.

Irschik, H., Jansen, R., Höfle, G., Gerth, K., and Reichenbach, H. (1985). The corallopyronins, new inhibitors of bacterial RNA synthesis from *Myxobacteria*. J. Antibiot. (Tokyo) *38*, 145-152.

Irschik, H., Augustiniak, H., Gerth, K., Höfle, G., and Reichenbach, H. (1995). The ripostatins, novel inhibitors of eubacterial RNA polymerase isolated from myxobacteria. J. Antibiot. (Tokyo) *48*, 787-792.

Jin, D.J., and Gross, C.A. (1988). Mapping and sequencing of mutations in the *Escherichia coli rpoB* gene that lead to rifampicin resistance. J. Mol. Biol. *202*, 45-58.

Kapanidis, A.N., Margeat, E., Ho, S.O., Kortkhonjia, E., Weiss, S., and Ebright, R.H. (2006). Initial transcription by RNA polymerase proceeds through a DNA-scrunching mechanism. Science *314*, 1144-1147.

Kaplan, C.D., Larsson, K.M., and Kornberg, R.D. (2008). The RNA polymerase II trigger loop functions in substrate selection and is directly targeted by α-amanitin. Mol. Cell 30, 547-556.

Kashlev, M., Lee, J., Zalenskaya, K., Nikiforov, V., and Goldfarb, A. (1990). Blocking of the initiation-to-elongation transition by a transdominant RNA polymerase mutation. Science. *248*, 1006-1009.

King, A.C., and Wu, L. (2009). Macromolecular synthesis and membrane perturbation assays for mechanisms of action studies of antimicrobial agents. In Current Protocols in Pharmacology. S.J. Enna, et al., eds. (New York, NY: John Wiley and Sons, Inc.). 13A.7.1-13A.7.23.

Kireeva, M.L., Opron, K., Seibold, S.A., Domecq, C., Cukier, R.I., Coulombe, B., Kashlev, M., and Burton, Z.F. (2012). Molecular dynamics and mutational analysis of the catalytic and translocation cycle of RNA polymerase. BMC Biophys. *5*, 11.

Kishi, Y. (1981). Total synthesis of rifamycin S. Pure Appl. Chem. *53*, 1163-1180.

Knight, J.L., Mekler, V., Mukhopadhyay, J., Ebright, R.H., and Levy, R.M. (2005). Distance-restrained docking of rifampicin and rifamycin SV to RNA polymerase using systematic FRET measurements: developing benchmarks of model quality and reliability. Biophys J. *88*, 925-938.

Korzheva, N., Mustaev, A., Kozlov, M., Malhotra, A., Nikiforov, V., Goldfarb, A., and Darst, S.A. (2000). A structural model of transcription elongation. Science *289*, 619-625.

Kurabachew, M., Lu, S.H.J., Krastel, P., Schmitt, E.K., Suresh, B.L., Goh, A., Knox, J.E., Ma, N.L., Jiricek, J., Beer, D., Cynamon, M., Peterson, F., Dartois, V., Keller, T., Dick, T., and Sambandamurthy, V.K. (2008). Lipiarmycin-targets RNA polymerase and has good activity against multidrug-resistant strains of *Mycobacterium tuberculosis*. J. Antimicrob. Chemother. *62*, 713-719.

Lancini, G.C., and Sartori, G. (1968). Rifamycins LXI: In vivo inhibition of RNA synthesis of rifamycins. Experientia. *24*, 1105-1106.

Landick, R., Stewart, J., and Lee, D.N. (1990). Amino acid changes in conserved regions of the β-subunit of *Escherichia coli* RNA polymerase alter transcription termination and pausing. Genes Dev. *4*, 1623-1636.

Lea, D., and Coulson, C. (1949). The distribution of the numbers of mutants in bacterial populations. J. Genet. *49*, 264-285.

Leeds, J.A., Sachdeva, M., Mullin, S., Barnes, S.W., and Ruzin, A. (2013). *In vitro* selection, via serial passage, of *Clostridium difficile* mutants with reduced susceptibility to fidaxomicin or vancomycin. J. Antimicrob. Chemother. (in press)

Lenski, R.E. (1988). Experimental studies of pleiotropy and epistasis in Escherichia coli. I. Variation in competitive fitness among mutants resistant to virus T4. Evolution *42*, 425-432.

Lester, W. (1972). Rifampin: a semisynthetic derivative of rifamycin – a prototype for the future. Annu. Rev. Microbiol. *26*, 85-102.

Lewis, K. (2013). Platforms for antibiotic discovery. Nat. Rev. Drug Discov. *12*, 371-387.

Li, J.W., and Vederas, J.C. (2009). Drug discovery and natural products: end of an era or an endless frontier?. Science *325*, 161-165.

Lipinski, C.A., Lombardo, F., Dominy, B.W., and Feeney, P.J. (2001). Experimental and computational approaches to estimate solubility and permeability in drug discovery and development settings. Adv. Drug Deliv. Rev. *46*, 3-26.

Lisitsyn, N.A., Gur'ev, S.O., Sverdlov, E.D., Moiseeva, E.P., and Nikiforov, V.G. (1984). Nucleotide substitutions in the *rpoB* gene leading to rifampicin resistance of *E. coli* RNA polymerase. Bioorg. Khim. *10*, 127-128.

Lisitsyn, N.A., Sverdlov, E.D., Moiseeva, E.P., and Nikiforov, V.G. (1985). Localization of mutation leading to resistance of *E. coli* RNA polymerase to the antibiotic streptolydigin in the gene *rpoB* coding for the β subunit of the enzyme. Bioorg. Khim. *11*, 132-134.

Livermore, D.M. (2009). Has the era of untreatable infections arrived?. J. Antimicrob. Chemother. *64* Suppl 1, i29-i36.

Louie, T., Miller, M., Donskey, C., Mullane, K., and Goldstein, E.J. (2009a). Clinical outcomes, safety, and pharmacokinetics of OPT-80 in a phase 2 trial with patients with *Clostridium difficile* infection. Antimicrob. Agents Chemother. *53*, 223-228.

Louie, T.J., Emery, J., Krulicki, W., Byrne, B., and Mah, M. (2009b). OPT-80 eliminates *Clostridium difficile* and is sparing of *Bacteroides* species during treatment of *C. difficile* infection. Antimicrob. Agents Chemother. *53*, 261-263.

Louie, T.J., Miller, M.A., Mullane, K.M., Weiss, K., Lentnek, A., Golan, Y., Gorbach, S., Sears, P., and Shue, Y.K.; OPT-80-003 Clinical Study Group. (2011). Fidaxomicin versus vancomycin for *Clostridium difficile* infection. N. Engl. J. Med. *364*, 422-431.

Luria, S.E., and Delbrück, M. (1943). Mutations of bacteria from virus sensitivity to virus resistance. Genetics *28*, 491-511.

Ma, W.T., Sandri, G.V., and Sarkar, S. (1992). Analysis of the Luria-Delbrück distribution using discrete convolution powers. J. Appl. Probab. *29*, 255-267.

Maggi, N., Arioli, V., and Sensi, P. (1965). Rifamycins. XLI. A new class of active semisynthetic rifamycins. N-substituted aminomethyl derivatives of rifamycin SV. J. Med. Chem. *8*, 790-793.

Marazzi, A., Kurz, M., Stefnaelli, S. and Colombo, L. (2005). Antibiotics GE23077, novel inhibitors of bacterial RNA polymerase. II. Structure elucidation. J. Antibiot. (Tokyo) *58*, 260-267.

Mariani, R., Granata, G., Maffioli, S., Serina, S., Brunati, C., Sosio, M., Marazzi, A., Vannini, A., Patel, D., White, R., and Ciabatti, R. (2005). Antibiotics GE23077, novel inhibitors of bacterial RNA polymerase. Part 3: Chemical derivatization. Bioorg. Med. Chem. Lett. *15*, 3748-3752.

Martinelli, E., Faniulo, L., Tuan, G., Gallo, G.G., and Cavalleri, B. (1983). Structural studies on lipiarmycin. I. Characterization by ^{1}H and ^{13}C NMR spectroscopy and isolation of methyl 2-*O*-methyl-4-*O*-homodichloroorsellinate-β-rhamnoside. J. Antibiot. (Tokyo) *36*, 1312-1322.

McClure, W.R. and Cech, C.L. (1978). On the mechanism of rifampicin inhibition of RNA synthesis. J. Biol. Chem. *253*, 8949-8956.

McPhillie, M.J., Trowbridge, R., Mariner, K.R., O'Neill, A.J., Johnson, A.P., Chopra, I., and Fishwick, C.W.G. (2011). Structure-based ligand design of novel bacterial RNA polymerase inhibitors. ACS Med. Chem. Lett. 2, 729-734.

Mekler, V., Kortkhonjia, E., Mukhopadhyay, J., Kapanidis, A.N., Niu, W., Ebright, Y.W., Levy, R., and Ebright, R.H. (2002). Structural organization of bacterial RNA polymerase holoenzyme and the RNA polymerase-promoter open complex. Cell *108*, 599-614.

Miao, S., Antsee, M.R., LaMarco, K., Matthew, J., Huang, L.H.T., and Brasseur, M.M. (1997). Inhibition of bacterial RNA polymerases. Peptide metabolites from the cultures of *Streptomyces* sp.. J. Nat. Prod. *60*, 858-861.

Miller, M. (2010). Fidaxomicin (OPT-80) for the treatment of *Clostridium difficile* infection. Expert Opin. Pharmacother. *11*, 1569-1578.

Minakhin, L., Bhagat, S., Brunning, A., Campbell, E.A., Darst, S.A., Ebright, R.H., and Severinov, K. (2001). Bacterial RNA polymerase subunit ω and eukaryotic RNA polymerase subunit RPB6 are sequence, structural, and functional homologs and promoter RNA polymerase assembly. Proc. Natl. Acad. Sci. USA *98*, 892-897.

Mitchison, D.A. (2000). Role of individual drugs in the chemotherapy of tuberculosis. Int. J. Tuberc. Lung Dis. *4*, 796-806.

Mooney, R.A., Darst, S.A., and Landick, R. (2005). Sigma and RNA polymerase: an on-again, off-again relationship?. Mol. Cell *20*, 335-345.

Moore, B.S., and Seng, D. (1998). Biosynthesis of the bicyclic depsipeptide salinamide A in *Streptomyces* sp. CNB-091: origin of the carbons. Tetrahedron Lett. *39*, 3915-3918.

Moore, B.S., Trischman, J.A., Seng, D., Kho, D., Jensen, P.R., and Fenical, W. (1999). Salinamides, antiinflammatory depsipeptides from a marine streptomycete. J. Org. Chem. *64*, 1145-1150.

Mosberg, J.A., Lajoie, M.J., and Church, G.M. (2010). Lambda red recombineering in *Escherichia coli* occurs through a fully single-stranded intermediate. Genetics. *186*, 791-799.

Mukhopadhyay, J., Kapanidis, A.N., Mekler, V., Kortkhonjia, E., Ebright, Y.W., and Ebright, R.H. (2001). Translocation of σ^{70} with RNA polymerase during transcription: fluorescence resonance energy transfer assay for movement relative to DNA. Cell *106*, 453-463.

Mukhopadhyay, J., Sineva, E., Knight, J., Levy, R.M., and Ebright, R.H. (2004). Antibacterial peptide microcin J25 inhibits transcription by binding within and obstructing the RNA polymerase secondary channel. Mol. Cell *14*, 739-751.

Mukhopadhyay, J., Da, K., Ismail, S., Koppstein, D., Jang, M., Hudson, B., Sarafianos, S., Tuske, S., Patel, J., Jansen, R., Irschik, H., Arnold, E., and Ebright, R.H. (2008). The RNA polymerase "switch region" is a target for inhibitors. Cell *135*, 295-307.

Murakami, K.S., Masuda, S., and Darst, S.A. (2002a). Structural basis of transcription initiation: RNA polymerase holoenzyme at 4 Å resolution. Science *296*, 1280-1284.

Murakami, K.S, Masuda, S., Campbell, E.A., Muzzin, O., and Darst, S.A. (2002b). Structural basis of transcription initiation: an RNA polymerase holoenzyme-DNA complex. Science *296*, 1285-1290.

Murakami, K.S., and Darst, S.A. (2003). Bacterial RNA polymerases: the wholo story. Curr. Opin. Struct. Biol. *13*, 31-39.

Mustaev, A., Kashlev, M., Lee, J.Y., Polyakov, A., Lebedev, A., Zalenskaya, K., Grachev, M., Goldfarb, A., and Nikiforov, V. (1991). Mapping of the priming substrate contacts in the active center of *Escherichia coli* RNA polymerase. J. Biol. Chem. *266*, 23927-23931.

Naryshkin, N., Revyakin, A., Kim, Y., Mekler, V., Ebright, R.H. (2000). Structural organization of the RNA polymerase-promoter open complex. Cell *101*, 601-611.

Naryshkin, N., Kim, Y., Dong, Q., and Ebright, R.H. (2001). Site-specific protein-DNA photocrosslinking. Analysis of bacterial transcription initiation complexes. Methods Mol. Biol. *148*, 337-361.

Nedialkov, Y.A., Opron, K., Assaf, F., Artsimovitch, I., Kireeva, M.L., Kashlev, M., Cukier, R.I., Nudler, E., and Burton, Z.F. (2013). The RNA polymerase bridge helix YFI motif in catalysis, fidelity and translocation. Biochim. Biophys. Acta. *1829*, 187-198.

Nikaido, H. (1994). Prevention of drug access to bacterial targets: permeability barriers and active efflux. Science *264*, 382-388.

Niu, S., Hu, T., Li, S., Xiao, Y., Ma, L., Zhang, G., Zhang, H., Yang, X., Ju, J., and Zhang, C. (2011). Characterization of a sugar-O-methyltransferase TiaS5 affords new tiacumicin analogues with improved antibacterial properties and reveals substrate promiscuity. Chembiochem. *12*, 1740-1748.

Niu, W., Kim, Y., Tau, G., Heyduk, T., and Ebright, R.H. (1996). Transcription activation at class II CAP-dependent promoters: two interactions between CAP and RNA polymerase. Cell *87*, 1123-1134.

Nudler, E. (1999). Transcription elongation: structural basis and mechanisms. J. Mol. Biol. *288*, 1-12.

Nudler, E. (2009). RNA polymerase active center: the molecular engine of transcription. Annu. Rev. Biochem. *78*, 335-361.

Öberg, B. (2006). Rational design of polymerase inhibitors as antiviral drugs. Antiviral Res. *71*, 90-95.

Omura, S., Nobutaka, I., Oiwa, R., Kuga, H., Iwata, R., Masuma, R., and Iwai, Y. (1986). Clostomicins, new antibiotics produced by *Micromonospora echinospora* subsp. *armeniaca* subsp. nov. I. Production, isolation, and physico-chemical and biological properties. J. Antibiot. (Tokyo) *39*, 1407-1412.

O'Neill, A.J., Huovinen, T., Fishwick, C.W., and Chopra, I. (2006). Molecular genetic and structural modeling studies of *Staphylococcus aureus* RNA polymerase and the fitness of rifampin resistance genotypes in relation to clinical prevalence. Antimicrob. Agents Chemother. 50, 298-309.

O'Shea, R., and Moser, H.E. (2008). Physicochemical properties of antibacterial compounds: implications for drug discovery. J. Med. Chem. *51*, 2871-2878.

Ovchinnikov, Y.A., Monastyrskaya, G.S., Guriev, S.O., Kalinina, N.F., Sverdlov, E.D., Gragerov, A.I., Bass, I.A., Kiver, I.F., Moiseyeva, E.P., Igumnov, V.N., Mindlin, S.Z., Nikiforov, V.G., and Khesin, R.B. (1983). RNA polymerase rifampicin resistance mutations in *Escherichia coli*: sequence changes and dominance. Mol. Gen. Genet. *190*, 344-348.

Parenti, F., Pagani, H., and Beretta, G. (1975). Lipiarmycin, a new antibiotic from *Actinoplanes*. I. Description of the producer strain and fermentation studies. J. Antbiot. *28*, 247-252.

Paton, J. H., Holt, H.A., and Bywater, M.J. (1990). Measurement of MICs of antibacterial agents by spiral gradient endpoint compared with conventional dilution method. Int. J. Exp. Clin. Chemother. *3*, 31-38.

Payne, D.J., Gwynn, M.N., Holmes, D.J., and Pompliano, D.L. (2007). Drugs for bad bugs: confronting the challenges of antibacterial discovery. Nat. Rev. Drug Discov. *6*, 29-40.

Poxton, I.R. (2010). Fidaxomicin: a new macrocyclic, RNA polymerase-inhibiting antibiotic for the treatment of *Clostridium difficile* infections. Future Microbiol. *5*, 539-548.

Pronin, S.V., and Kozmin, S.A. (2010). Synthesis of streptolydigin, a potent bacterial RNA polymerase inhibitor. J. Am. Chem. Soc. *132*, 14394-14396.

Ramaswamy, S., and Musser, J.M. (1998). Molecular genetic basis of antimicrobial agent resistance in *Mycobacterium tuberculosis*: 1998 update. Tuber. Lung Dis. *79*, 3-29.

Record, M.T. Jr., Reznikoff, W., Craig, M., McQuade, K., and Schlax, P. (1996). *Escherichia coli* RNA polymerase ($E\sigma^{70}$), promoters, and the kinetics of the steps of transcription initiation. In *Escherichia coli* and *Salmonella*. F. Neidhardt, ed. (Washington, D.C.: ASM Press). Chapter 54.

Rentsch, A., and Kalesse, M. (2012). The total synthesis of corallopyronin A and myxopyronin B. Angew. Chem. Int. Ed. Engl. *51*, 11381-11384.

Revyakin, A., Liu, C., Ebright, R.H., and Strick, T.R. (2006). Abortive initiation and productive initiation by RNA polymerase involve DNA scrunching. Science *314*, 1139-1143.

Reynolds, M.G. (2000). Compensatory evolution in rifampin-resistant *Escherichia coli*. Genetics *156*, 1471-1481.

Rice, L.B. (2009). The clinical consequences of antimicrobial resistance. Curr. Opin. Microbiol. *12*, 476-481.

Richardson, J.P., and Greenblatt, J. (1996). Control of RNA chain elongation and termination. In *Escherichia coli* and *Salmonella*. F. Neidhardt, ed. (Washington, D.C.: ASM Press). Chapter 55.

Robertson, G.T., Bonventre, E.J., Doyle, T.B., Du, Q., Duncan, L., Morris, T.W., Roche, E.D., Yan, D., and Lynch, A.S. (2008a). In vitro evaluation of CBR-2092, a novel rifamycin-quinolone hybrid antibiotic: studies of the mode of action in *Staphylococcus aureus*. Antimicrob Agents Chemother. *52*, 2313-2323.

Robertson, G.T., Bonventre, E.J., Doyle, T.B., Du, Q., Duncan, L., Morris, T.W., Roche, E.D., Yan, D., and Lynch, A.S. (2008b). In vitro evaluation of CBR-2092, a novel rifamycin-quinolone hybrid antibiotic: microbiology profiling studies with staphylococci and streptococci. Antimicrob Agents Chemother. *52*, 2324-2334.

Saecker, R.M., Record, M.T. Jr., and deHaseth, P.L. (2011). Mechanism of bacterial transcription initiation: RNA polymerase - promoter binding, isomerization to initiation-competent open complexes, and initiation of RNA synthesis. J. Mol. Biol. *412*, 754-771.

Sagitov, V., Nikiforov, V., and Goldfarb, A. (1993). Dominant lethal mutations near the 5' substrate binding site affect RNA polymerase propagation. J. Biol. Chem. *268*, 2195-2202.

Sahner, J.H., Groh, M., Negri, M., Haupenthal, J., and Hartmann, R.W. (2013). Novel small molecule inhibitors targeting the "switch region" of bacterial RNAP: structure-based optimization of a virtual screening hit. Eur. J. Med. Chem. *65*, 223-231.

Salomón, R.A., Farías, R.N. (1992). Microcin 25, a novel antimicrobial peptide produced by *Escherichia coli*. J. Bacteriol. *174*, 7428-7435.

Sambrook, J., and Russell, D. (2001). Molecular Cloning: A Laboratory Manual. Third Edition. (Cold Spring Harbor, NY: Cold Spring Harbor Laboratory Press).

Sander, P., Springer, B., Prammananan, T., Sturmfels, A., Kappler, M., Pletschette, M., and Böttger, E.C. (2002). Fitness cost of chromosomal drug resistance-conferring mutations. Antimicrob. Agents Chemother. *46*, 1204-1211.

Sarkar, S., Ma, W.T., Sandri, G.H. (1992). On fluctuation analysis: a new, simple and efficient method for computing the expected number of mutants. Genetica. *85*, 173-179.

Sarubbi, E., Monti, F., Corti, E., Miele, A., and Selva, E. (2004). Mode of action of the microbial metabolite GE23077, a novel potent and selective inhibitor of bacterial RNA polymerase. Eur. J. Biochem. *271*, 3146-3152.

Sawadogo, M., Roeder, R.G. (1985). Factors involved in specific transcription by human RNA polymerase II: analysis by a rapid and quantitative *in vitro* assay. Proc. Natl. Acad. Sci. USA 82, 4394-4398.

Sawitzke, J.A., Thomason, L.C., Costantino, N., Bubunenko, M., Datta, S., and Court, D.L. (2007). Recombineering: *in vivo* genetic engineering in *E. coli*, *S. enterica*, and beyond. Methods Enzymol. *421*, 171-199.

Schalkowsky, S. (1994). Measures of susceptibility from a spiral gradient of drug concentrations. Adv. Exp. Med. Biol. *349*, 107-120.

Sensi, P., Margalith, P., and Timbal, M.T. (1959). Rifomycin, a new antibiotic; preliminary report. Farmaco. Sci. *14*, 146-147.

Sensi, P., Maggi, N., Ballotta, R., Fürész, S., Pallanza, R., and Arioli, V. (1964). Rifamycins. XXXV. Amides and Hydrazides of Rifamycin B. J. Med. Chem. *7*, 596-602.

Sensi, P. (1983). History of the development of rifampin. Rev. Infect. Dis. *5* Suppl 3, S402-S406.

Sergio, S., Pirali, G., White, R., and Parenti, F. (1975). Lipiarmycin, a new antibiotic from *Actinoplanes*. III. Mechanism of action. J. Antbiot. (Tokyo) *28*, 543-549.

Severinov, K., Soushko, M., Goldfarb, A., and Nikiforov, V. (1993). Rifampicin region revisited. New rifampicin-resistant and streptolydigin-resistant mutants in the β subunit of *Escherichia coli* RNA polymerase. J. Biol. Chem. *268*, 14820-14825.

Severinov, K., Soushko, M., Goldfarb, A., and Nikiforov, V. (1994). Rif^R mutations in the beginning of the *Escherichia coli rpoB* gene. Mol. Gen. Genet. *244*, 120-126.

Severinov, K., Markov, D., Severinova, E., Nikiforov, V., Landick, R., Darst, S.A., and Goldfarb, A. (1995). Streptolydigin-resistant mutants in an evolutionarily conserved region of the β' subunit of *Escherichia coli* RNA polymerase. J. Biol. Chem. *270*, 23926-23929.

Severinov, K., Mooney, R., Darst, S.A., and Landick, R. (1997). Tethering of the large subunits of *Escherichia coli* RNA polymerase. J. Biol. Chem. *272*, 24137-24140.

Siddhikol, C., Erbstoeszer, J.W., and Weisblum, B. (1969). Mode of action of streptolydigin. J. Bacteriol. *99*, 151-155.

Simmons, K.J., Chopra, I., and Fishwick, C.W. (2010). Structure-based discovery of antibacterial drugs. Nat. Rev. Microbiol. *8*, 501-510.

Sonenshein, A.L., Alexander, H.B., Rothstein, D.M., and Fisher, S.H. (1977). Lipiarmycin-resistant ribonucleic acid polymerase mutants of *Bacillus subtilis*. J. Bacteriol. *132*, 73-79.

Sonenshein, A.L., and Alexander, H.B. (1979). Initiation of transcription *in vitro* is inhibited by lipiarmycin. J. Mol. Biol. *127*, 55-72.

Sosunov, V., Sosunova, E., Mustaev, A., Bass, I., Nikiforov, V., and Goldfarb, A. (2003). Unified two-metal mechanism of RNA synthesis and degradation by RNA polymerase. EMBO J. *22*, 2234-2244.

Sosunov, V., Zorov, S., Sosunova, E., Nikolaev, A., Zakeyeva, I., Bass, I., Goldfarb, A., Nikiforov, V., Severinov, K., and Mustaev, A. (2005). The involvement of the aspartate triad of the active center in all catalytic activities of multisubunit RNA polymerase. Nucleic Acids Res. *33*, 4202-4211.

Sousa, R. (2008). Tie me up, tie me down: inhibiting RNA polymerase. Cell *135*, 205-207.

Srivastava, A., Talaue, M., Liu, S., Degen, D., Ebright, R.Y., Sineva, E., Chakraborty, A., Druzhinin, S.Y., Chatterjee, S., Mukhopadhyay, J., Ebright, Y.W., Zozula, A., Shen, J., Sengupta, S., Niedfeldt, R.R., Xin, C., Kaneko, T., Irschik, H., Jansen, R., Donadio, S., Connell, N., and Ebright, R.H. (2011). New target for inhibition of bacterial RNA polymerase: 'switch region'. Curr. Opin. Microbiol. *14*, 532-543.

Srivastava, A., Degen, D., Ebright, Y.W., and Ebright, R.H. (2012). Frequency, spectrum, and nonzero fitness costs of resistance to myxopyronin in *Staphylococcus aureus*. Antimicrob. Agents Chemother. *56*, 6250-6255.

Stackhouse, T.M., Telesnitsky, A.P., and Meares, C.F. (1989). Release of the σ subunit from *Escherichia coli* RNA polymerase transcription complexes is dependent on the promoter sequence. Biochemistry. *28*, 7781-7788.

Stewart, F.M. (1994). Fluctuation tests: how reliable are the estimates of mutation rates?. Genetics. 137, 1139-1146.

Strelow, J., Dewe, W., Iversen, P.W., Brooks, H.B., Radding, J.A., McGee, J., and Weidner, J. (2012). Mechanism of action assays for enzymes. In Assay Guidance Manual. G.S. Sittampalam, et al., eds. (Bethesda, MD: Eli Lilly Co. and the National Center for Advancing Translational Sciences). Online. NCBI Book: NBK53196.

Swanson, R.N., Hardy, D.J., Shipkowitz, N.L., Hanson, C.W., Ramer, N.C., Fernandes, P.B., and Clement, J.J. (1991). *In vitro* and *in vivo* evaluation of tiacumicins B and C against *Clostridium difficile*. Antimicrob. Agents Chemother. *35*, 1108-1111.

Talpaert, M., Campagnari, F., and Clerici, L. (1975). Lipiarmycin: an antibiotic inhibiting nucleic acid polymerases. Biochem. Biophy. Res. Comm. *63*, 328-334.

Tan L., and Ma D. (2008). Total synthesis of salinamide A: a potent anti-inflammatory bicyclic depsipeptide. Angew Chem. Int. Ed. Engl. *47*, 3614-3617.

Tang, H., Severinov, K., Goldfarb, A., Fenyo, D., Chait, B., and Ebright, R.H. (1994). Location, structure, and function of the target of a transcriptional activator protein. Genes Dev. *8*, 3058-3067.

Tavormina, P.L., Landick, R., and Gross, C.A. (1996). Isolation, purification, and in vitro characterization of recessive-lethal-mutant RNA polymerases from *Escherichia coli*. J. Bacteriol. *178*, 5263-5271.

Temiakov, D., Zenkin, N., Vassylyeva, M.N., Perederina, A., Tahirov, T.H., Kashkina, E., Savkina, M., Zorov, S., Nikiforov, V., Igarashi, N., Matsugaki, N., Wakatsuki, S., Severinov, K., and Vassylyev, D.G. (2005). Structural basis of transcription inhibition by antibiotic streptolydigin. Mol. Cell *19*, 655-666.

Theriault, R.J., Karwowski, J.P., Jackson, M., Girolami, R.L., Sunga, G.N., Vojtko, C.M., and Coes, L.J. (1987). Tiacumicins, a novel complex of 18-membered macrolides. I. Taxonomy, fermentation, and antibacterial activity. J. Antibiot. (Tokyo) *40*, 567-574.

Tietze, L.F., Bell, H.P., and Chandrasekhar, S. (2003). Natural product hybrids as new leads for drug discovery. Angew. Chem. Int. Ed. Engl. *42*, 3996-4028.

Traynor, K. (2011). Fidaxomicin approved for *C. difficile* infections. Am. J. Health Syst. Pharm. *68*, 1276.

Trischman, J.A., Tapiolas, D.M., Jensen, P.R., Dwight, R., and Fenical, W. (1994). Salinamides A and B: anti-inflammatory depsipeptides from a marine streptomycete. J. Am. Chem. Soc. *116*, 757-758.

Tsogoeva, S.B. (2010). Recent progress in the development of synthetic hybrids of natural or unnatural bioactive compounds for medicinal chemistry. Mini Rev. Med. Chem. *10*, 773-793.

Tupin, A., Gualtieri, M., Roquet-Banères, F., Morichaud, Z., Brodolin, K., and Leonetti, J.P. (2010a). Resistance to rifampicin: at the crossroads between ecological, genomic and medical concerns. Int. J. Antimicrob. Agents *35*, 519-523.

Tupin, A., Gualtieri, M., Leonetti, J.P., and Brodolin, K. (2010b). The transcription inhibitor lipiarmycin blocks DNA fitting into the RNA polymerase catalytic site. EMBO J. *29*, 2527-2537.

Tuske, S., Sarafianos, S.G., Wang, X., Hudson, B., Sineva, E., Mukhopadhyay, J., Birktoft, J.J., Leroy, O., Ismail, S., Clark, A.D. Jr., Dharia, C., Napoli, A., Laptenko, O., Lee, J., Borukhov, S., Ebright, R.H., and Arnold, E. (2005). Inhibition of bacterial RNA polymerase by streptolydigin: stabilization of a straight-bridge-helix active-center conformation. Cell *122*, 541-552.

Vassylyev, D.G., Sekine, S., Laptenko, O., Lee, J., Vassylyeva, M.N., Borukhov, S., and Yokoyama, S. (2002). Crystal structure of a bacterial RNA polymerase holoenzyme at 2.6Å resolution. Nature *417*, 712-719.

Vassylyev, D.G., Vassylyeva, M.N., Perederina, A., Tahirov, T.H., and Artsimovitch, I. (2007a). Structural basis for transcription elongation by bacterial RNA polymerase. Nature *448*, 157-162.

Vassylyev, D.G., Vassylyeva, M.N., Zhang, J., Palangat, M., Artsimovitch, I., and Landick, R. (2007b). Structural basis for substrate loading in bacterial RNA polymerase. Nature *448*, 163-168.

Vesely, J.J., Pien, F.D., and Pien, B.C. (1998). Rifampin, a useful drug for nonmycobacterial infections. Pharmacotherapy. *18*, 345-357.

Villain-Guillot, P., Bastide, L., Gualtieri, M., and Leonetti, J.P. (2007). Progress in targeting bacterial transcription. Drug Discov. Today *12*, 200-208.

von Hippel, P.H. (1998). An integrated model of the transcription complex in elongation, termination, and editing. Science *281*, 660-665.

Wallace, A.S., and Corkill, J.E. (1989). Application of the spiral plating method to study antimicrobial action. J. Microbiol. Methods *10*, 303-310.

Walter, G., Zillig, W., Palm, P., and Fuchs, E. (1967). Initiation of DNA-dependent RNA synthesis and the effect of heparin on RNA polymerase. Eur. J. Biochem. *3*, 194-201.

Wang, D., Meier, T.I., Chan, C.L., Feng, G., Lee, D.N., and Landick, R. (1995). Discontinuous movements of DNA and RNA in RNA polymerase accompany formation of a paused transcription complex. Cell *81*, 341-150.

Wang, Y., Severinov, K., Loizos, N., Fenyö, D., Heyduk, E., Heyduk, T., Chait, B.T., and Darst, S.A. (1997). Determinants for *Escherichia coli* RNA polymerase assembly within the β subunit. J. Mol. Biol. 270, 648-662.

Wehrli, W., and Staehelin, M. (1971). Actions of the rifamycins. Bacteriol. Rev. *35*, 290-309.

Weinmann, R., Raskas, H.J., and Roeder, R.G. (1974). Role of DNA-dependent RNA polymerases II and III in transcription of the adenovirus genome late in productive infection. Proc. Natl. Acad. Sci. USA *71*, 3426-3439.

Weinzierl, R.O. (2010). The nucleotide addition cycle of RNA polymerase is controlled by two molecular hinges in the bridge helix domain. BMC Biol. *8*, 134.

Weinzierl, O.J. (2012) High-throughput simulations of protein dynamics in molecular machines: the 'link' domain of RNA polymerase. In Molecular Dynamics - Studies of Synthetic and Biological Macromolecules. L. Wang, ed. (Open Access: InTech).

Wichelhaus, T.A., Boddinghaus, B., Besier, S., Schafer, V., Brade, V., and Ludwig, A. (2002). Biological cost of rifampin resistance from the perspective of *Staphylococcus aureus*. Antimicrob. Agents Chemother. *46*, 3381-3385.

Wieland, T., and Faulstich, H. (1991). Fifty years of amanitin. Experientia *47*, 1186-1193.

Williams, D.L., Waguespack, C., Eisenbach, K., Crawford, J.T., Portaels, F., Salfinger, M., Nolan, C.M., Abe, C., Sticht-Groh, V., and Gillis, T.P. (1994). Characterization of rifampin resistance in pathogenic mycobacteria. Antimicrob. Agents Chemother. *38*, 2380-2386.

Winter, P., Hiller, W., and Christmann, M. (2012). Access to skipped polyene macrolides through ring-closing metathesis: total synthesis of the RNA polymerase inhibitor ripostatin B. Angew. Chem. Int. Ed. Engl. *51*, 3396-3400.

World Health Organization (WHO). (2012). Global tuberculosis report 2012. (Geneva, Switzerland: WHO Press).

Xiao, Y., Li, S., Niu, S., Ma, L., Zhang, G., Zhang, H., Zhang, G., Ju, J., and Zhang, C. (2011). Characterization of tiacumicin B biosynthetic gene cluster affording diversified tiacumicin analogues and revealing a tailoring dihalogenase. J. Am. Chem. Soc. *133*, 1092-1105.

Young, K. (2006). In Vitro Antibacterial Resistance Selection and Quantitation. In Current Protocols in Pharmacology. S.J. Enna, et al., eds. (New York, NY: John Wiley and Sons, Inc.). 13A.6.1-13A.6.22.

Yuzenkova, J., Delgado, M., Nechaev, S., Savalia, D., Epshtein, V., Artsimovitch, I., Mooney, R.A., Landick, R., Farias, R.N., Salomon, R., and Severinov, K. (2002). Mutations of bacterial RNA polymerase leading to resistance to microcin J25. J. Biol. Chem. *277*, 50867-50875.

Zhang, G., Campbell, E.A., Minakhin, L., Richter, C., Severinov, K., and Darst, S.A. (1999). Crystal structure of *Thermus aquaticus* core RNA polymerase at 3.3 Å resolution. Cell *98*, 811-824.

Zhang, Y., Feng, Y., Chatterjee, S., Tuske, S., Ho, M.X., Arnold, E., and Ebright, R.H. (2012). Science *338*, 1076-1080.

Appendix SA:
Methods (Chapter 2) Supplements

Supplemental Experimental Procedures

Random mutagenesis libraries

Random mutagenesis of pRL706 (*rpoB*) and pRL663 (*rpoC)* was performed by use of PCR amplification, exploiting the baseline error rate of PCR amplification (essentially as in Mukhopadhyay et al., 2008). Mutagenesis reactions were performed using the QuikChange Site-Directed Mutagenesis Kit (PfuTurbo enzyme; Agilent/Stratagene) with pRL706 as the template and oligodeoxyribonucleotide forward and reverse primers corresponding to nucleotides 427-446 of *lacI* (5'-GTTCCGGCGTTATTTCTTGA-3' and 5'-TCAAGAAATAACGCCGGAAC-3'); or pRL663 as the template and oligodeoxyribonucleotide forward and reverse primers corresponding to nucleotides 217-246 of *lacI* (5'-CTGCACGCGCCGTCGAAAATTGTCGCGGCG-3' and 5'-CGCCGCGACAATTTTCGACGGCGCGTGCAG-3') (primers at 160 nM; all other components at concentrations as specified by the manufacturer). Mutagenized plasmid DNA was introduced by transformation into *E. coli* XL1-Blue (Agilent/Stratagene). Transformants (~$5x10^3$ cells) were applied to LB-agar plates containing 200 μg/ml ampicillin and plates were incubated 16 h at 37°C. The resulting colonies were then pooled together and their plasmid DNA purified using a plasmid DNA purification kit (Qiagen or Sigma).

Transcription assays: ribogreen fluorescence-detected transcription

Fluorescence-detected transcription assays were performed essentially as in Srivastava et al., 2011. Reaction mixtures contained (20 μl): 0-100 μM test compound, bacterial RNAP holoenzyme [75 nM *E. coli* RNAP holoenzyme or 75 nM *E. coli* [Asp565]β-RNAP holoenzyme], 20 nM DNA fragment containing the bacteriophage T4 N25 promoter [positions -72 to +367 PCR amplified from pARTaqN25-340-tR2; Liu, 2007], 100 μM ATP, 100 μM GTP, 100 μM UTP, and 100 μM CTP, in TB (50 mM Tris-HCl, pH 8.0, 100 mM KCl, 10 mM $MgCl_2$, 1 mM DTT, 10 μg/ml bovine serum albumin, and 5.5% glycerol). Reaction components other than DNA and NTPs were pre-incubated for 10 min at 37°C. Reactions were carried out by the addition of DNA and incubation for 15 min at 37°C, followed by the addition of NTPs and incubation for 60 min at 37°C. DNA was then removed by the addition of 1 μl 5 mM $CaCl_2$ and 2 U DNaseI (Ambion), followed by incubation for 90 min at 37°C. RNA was quantified by the addition of 100 μl Quant-iT RiboGreen RNA Reagent (Life Technologies; 1:500 dilution in 10 mM Tris-HCl, pH 8.0, 1 mM EDTA), followed by incubation for 10 min at 22°C, followed by measurement of fluorescence intensity [excitation wavelength = 485 nm and emission wavelength = 535 nm; GENios Pro microplate reader (Tecan)]. Half-maximal inhibitory concentrations (IC50s) were calculated by non-linear regression in SigmaPlot (SPSS).

Supplemental References for Appendix SA

Liu, C. (2007). The use of single-molecule DNA nanomanipulation to study transcription kinetics. Ph.D. Dissertation. (Rutgers University, NJ: UMI Dissertations Publishing).

Mukhopadhyay, J., Da, K., Ismail, S., Koppstein, D., Jang, M., Hudson, B., Sarafianos, S., Tuske, S., Patel, J., Jansen, R., Irschik, H., Arnold, E., and Ebright, R.H. (2008). The RNA polymerase "switch region" is a target for inhibitors. Cell *135*, 295-307.

Srivastava, A., Talaue, M., Liu, S., Degen, D., Ebright, R.Y., Sineva, E., Chakraborty, A., Druzhinin, S.Y., Chatterjee, S., Mukhopadhyay, J., Ebright, Y.W., Zozula, A., Shen, J., Sengupta, S., Niedfeldt, R.R., Xin, C., Kaneko, T., Irschik, H., Jansen, R., Donadio, S., Connell, N., and Ebright, R.H. (2011). New target for inhibition of bacterial RNA polymerase: 'switch region'. Curr. Opin. Microbiol. 14, 532-543.

Table SA1. PCR primer pairs used to amplify chromosomal *rpoB* and *rpoC* genes

organism	gene	primer sequence
E. coli	*rpoC*	5'- AGGTCACTGCTGTCGGGTTAAAACC -3'
		5'- TGACAAATGCTCTTTCCCTAAACTCC -3'
	rpoB	5'- GTTGCACAAACTGTCCGCTCAATGG -3'
		5'- TCGGAGTTAGCACAATCCGCTGC -3'
S. aureus	*rpoC*	5'- GCCATTTTAAATAAATGCAAATCAATCAAATAGC -3'
		5'- CCTTTAATATATTAACATTGAACAAGAGAATTCG -3'
	rpoB	5'- CGTTAAATAGATAAGTTAATTAAGAATAAATATAGAATCG -3'
		5'- TGGCTTAAAGTACTAAACTGAATCATC -3'
S. pyogenes	*rpoC*	5'- AGGTCACTGCTGTCGGGTTAAAACC -3'
		5'- TGACAAATGCTCTTTCCCTAAACTCC -3'
	rpoB	5'- GTTGCACAAACTGTCCGCTCAATGG -3'
		5'- TCGGAGTTAGCACAATCCGCTGC -3'

Table SA2. "Doped" oligonucleotide primers for *rpoC* used in saturation mutagenesis against Lpm

codons	sequence
rpoC	
1-10[b]	5'- GGGAGCAAATCCATGAAAGATTTATTAAAGTTTCTGAAAGCGCAGACTAAAA CCG -3'
11-20[b]	5'- GTTTCTGAAAGCGCAGACTAAAACCGAAGAGTTTGATGCGATCAAAATTGCTC TGG -3'
67-68[a]	5'- GGGCCGGTAAAAGATTACGAGTGCCTGTGCGG -3'
77-81[a]	5'- CGGTAAGTACAAGCGCCTGAAACACCGTGGCGTCATCTG -3'
93-100[b]	5'- GGCGTTGAAGTGACCCAGACTAAAGTACGCCGTGAGCGTATGGGCC -3'
245-256[b]	5'- CCGTTCTGCCGGTACTGCCGCCAGATCTGCGTCCGCTGGTTCCGCTGGATGGTGG TCGTTTCGCG -3'
259-265[b]	5'- CCGCTGGATGGTGGTCGTTTCGCGACTTCTGACCTGAACGATCTGTATCGTC -3'
325-335[b]	5'- GCGTCCTCTGAAATCTTTGGCCGACATGATCAAAGGTAAACAGGGTCGTTTCCG -3'
336-346[b]	5'- GGTAAACAGGGTCGTTTCCGTCAGAACCTGCTCGGTAAGCGTGTTGACTACTCC -3'
347-355[b]	5'- CGGTAAGCGTGTTGACTACTCCGGTCGTTCTGTAATCACCGTAGGTCC -3'
378-382[a]	5'- GGAGCTGTTCAAACCGTTCATCTACGGCAAGCTGGAAC -3'
393-403[b]	5'- GTGGTCTTGCTACCACCATTAAAGCTGCGAAGAAAATGGTTGAGCGCGAAGAAGCT GTC -3'
425-429[a]	5'- GGTACTGCTGAACCGTGCACCGACTCTGCACCGTCTGG -3'
429-433[a]	5'- CCGTGCACCGACTCTGCACCGTCTGGGTATCCAGGCATTTG -3'
466-481[b]	5'- GGTGACCAGATGGCTGTTCACGTACCGCTGACGCTGGAAGCCCAGCTGGAAGCGC GTGCGCTGATG -3'
1319-1327[b]	5'- GGCAACCGAGTCCTTCATCTCCGCGGCATCGTTCCAGGAGACCACTCGC -3'
1347-1360[b]	5'- CTGCGCGGCCTGAAAGAGAACGTTATCGTGGGTCGTCTGATCCCGGCAGGTACCG GTTACGC -3'

[a] The underlined regions were synthesized using a mixture of 92% of the correct phophoramidite and 8% of a 1:1:1:1 mixture of dA, dC, dG, and dT phosphoramidities at each position.

[b] The underlined regions were synthesized using a mixture of 98% of the correct phophoramidite and 2% of a 1:1:1:1 mixture of dA, dC, dG, and dT phosphoramidities at each position.

Table SA3. "Doped" oligonucleotide primers for *rpoB* used in saturation mutagenesis against Lpm

codons	sequence
rpoB	
854-857[a]	5'- CACCGCTGACATCCCGAACGTGGGTGAAGCTGCGC -3'
890-899[b]	5'- GGTAACGCCGAAAGGTGAAACTCAGCTGACCCCAGAAGAAAAACTGCTGCG -3'
914-922[a]	5'- GCCTCTGACGTTAAAGACTCTTCTCTGCGCGTACCAAACGGTGTATCCGG -3'
1246-1256[b]	5'- GATGCACGCGCGTTCCACCGGTTCTTACAGCCTGGTTACTCAGCAGCCGCT GGG -3'
1248-1256[b]	5'- GCACGCGCGTTCCACCGGTTCTTACAGCCTGGTTACTCAGCAGCCGCTGGG -3'
1257-1262[a]	5'- CCTGGTTACTCAGCAGCCGCTGGGTGGTAAGGCACAGTTCGG -3'
1262-1264[a]	5'- GCCGCTGGGTGGTAAGGCACAGTTCGGTGGTCAG -3'
1265-1274[b]	5'- GTAAGGCACAGTTCGGTGGTCAGCGTTTCGGGGAGATGGAAGTGTGGGC -3'
1269-1276[b]	5'- GTTCGGTGGTCAGCGTTTCGGGGAGATGGAAGTGTGGGCGCTGGAAGC -3'
1277-1287[b]	5'- GGAAGTGTGGGCGCTGGAAGCATACGGCGCAGCATACACCCTGCAGGAAATGC -3'
1288-1297[b]	5'- GCATACACCCTGCAGGAAATGCTCACCGTTAAGTCTGATGACGTGAACGGTCG -3'
1298-1310[b]	5'- GTCTGATGACGTGAACGGTCGTACCAAGATGTATAAAAACATCGTGGACGGCAACC ATCAG -3'
1311-1321[b]	5'- CATCGTGGACGGCAACCATCAGATGGAGCCGGGCATGCCAGAATCCTTCAACGTA TTG -3'
1322-1329[b]	5'- GGGCATGCCAGAATCCTTCAACGTATTGTTGAAAGAGATTCGTTCGCTGG -3'
1330-1342[b]	5'- GTTGAAAGAGATTCGTTCGCTGGGTATCAACATCGAACTGGAAGACGAACTCGAGG TGC -3'

[a] The underlined regions were synthesized using a mixture of 92% of the correct phophoramidite and 8% of a 1:1:1:1 mixture of dA, dC, dG, and dT phosphoramidities at each position.

[b] The underlined regions were synthesized using a mixture of 98% of the correct phophoramidite and 2% of a 1:1:1:1 mixture of dA, dC, dG, and dT phosphoramidities at each position.

Table SA4. "Doped" oligonucleotide primers used in saturation mutagenesis against GE

codons	sequence
rpoC	
347-355[b]	5'- CGGTAAGCGTGTTGACTACTCCGGTCGTTCTGTAATCACCGTAGGTCC -3'
425-429[a]	5'- GGTACTGCTGAACCGTGCACCGACTCTGCACCGTCTGG -3'
456-465[b]	5'- GTTTGTGCGGCATATAACGCCGACTTCGATGGTGACCAGATGGCTGTTC -3'
779-792[b]	5'- CCACCCACGGTGCTCGTAAAGGTCTGGCGGATACCGCACTGAAAACTGCGAACTCCG GTTACC -3'
934-943[b]	5'- GCTGACCATGCGTACGTTCCACATCGGTGGTGCGGCATCTCGTGCGGCTGCTG -3'
rpoB	
136-143[b]	5'- CAGACAACGGTACCTTTGTTATCAACGGTACTGAGCGTGTTATCGTTTCCC -3'
504-511[b]	5'- CCGCAGCAGTGAAAGAGTTCTTCGGTTCCAGCCAGCTGTCTCAGTTTATGGACC -3'
512-522[b]	5'- CAGCCAGCTGTCTCAGTTTATGGACCAGAACAACCCGCTGTCTGAGATTACG -3'
523-534[b]	5'- CCCGCTGTCTGAGATTACGCACAAACGTCGTATCTCCGCACTCGGCCCAGGCG GTC-3'
535-541[b]	5'- CCGCACTCGGCCCAGGCGGTCTGACCCGTGAACGTGCAGGCTTC -3'
542-549[b]	5'- CTGACCCGTGAACGTGCAGGCTTCGAAGTTCGAGACGTACACCCG -3'
563-573[b]	5'- CCAATCGAAACCCCTGAAGGTCCGAACATCGGTCTGATCAACTCTCTGTCCG -3'
677-690[b]	5'- GATGACGCCAACCGTGCATTGATGGGTGCGAACATGCAACGTCAGGCCGTTCCGACT CTG -3'
758-763[a]	5'- GACCAAATACACCCGTTCTAACCAGAACACCTGTATCAACCAG -3'
813-814[a]	5'- GGTTACAACTTCGAAGACTCCATCCTCG -3'
829-835[b]	5'- CAGGAAGACCGTTTCACCACCATCCACATTCAGGAACTGGCGTGTGTG -3'
1054-1060[b]	5'- GTTAAGGTATATCTGGCGGTTAAACGCCGTATCCAGCCTGGTGAC -3'
1064-1074[b]	5'- CCAGCCTGGTGACAAGATGGCAGGTCGTCACGGTAACAAGGGTGTAATTTCTAAG -3'
1102-1108[b]	5'- GAACCCGCTGGGCGTACCGTCTCGTATGAACATCGGTCAG -3'
1233-1242[b]	5'- CATGTACATGCTGAAACTGAACCACCTGGTCGACGACAAGATGCACGCGC -3'

[a] The underlined regions were synthesized using a mixture of 92% of the correct phophoramidite and 8% of a 1:1:1:1 mixture of dA, dC, dG, and dT phosphoramidities at each position.

[b] The underlined regions were synthesized using a mixture of 98% of the correct phophoramidite and 2% of a 1:1:1:1 mixture of dA, dC, dG, and dT phosphoramidities at each position.

Appendix SB:
Lipiarmycin (Chapter 3) Supplements

Supplemental references for Appendix SB

Ebright, R.H. (2005). RNA-exit-channel: target and method for inhibition of bacterial RNA polymerase. WO2005/001034.

Mukhopadhyay, J., Da, K., Ismail, S., Koppstein, D., Jang, M., Hudson, B., Sarafianos, S., Tuske, S., Patel, J., Jansen, R., Irschik, H., Arnold, E., and Ebright, R.H. (2008). The RNA polymerase "switch region" is a target for inhibitors. Cell *135*, 295-307.

Tuske, S., Sarafianos, S.G., Wang, X., Hudson, B., Sineva, E., Mukhopadhyay, J., Birktoft, J.J., Leroy, O., Ismail, S., Clark, A.D. Jr., Dharia, C., Napoli, A., Laptenko, O., Lee, J., Borukhov, S., Ebright, R.H., and Arnold, E. (2005). Inhibition of bacterial RNA polymerase by streptolydigin: stabilization of a straight-bridge-helix active-center conformation. Cell *122*, 541-552.

Table SB1. Lpm-resistant mutants from saturation mutagenesis of *rpoC*: sequences and properties

amino acid substitution	number of independent isolates	resistance level (MIC/MIC$_{wild\text{-}type}$)[a]		ability to complement *rpoC*^{ts} or *rpoB*^{ts}
		broth microdilution	spiral gradient endpoint (SGE)	
***rpoC* (RNAP β′ subunit)**				
single-substitution mutants				
96 Lys→Asn	1	1	2	+
96 Lys→Ileb	9	2	2	+
248 Asp→Tyr[b]	2	1	2	+
249 Leu→Arg[b, c]	6	4	4	+
263 Ser→Thr	1	2	2	+
330 Met→Arg[b]	1	1	2	+
334 Lys→Asn	2	1	2	+
334 Lys→Ile	2	2	1	+
337 Arg→Cys[b, c]	2	2	2	+
337 Arg→His[b]	22	4	4	+
337 Arg→Ser[b]	13	2	4	+
341 Asn→Ser	1	2	2	+
348 Asp→His	1	1	2	+
348 Asp→Tyr	4	4	2	-
349 Tyr→Ser	1	1	2	+
428 Thr→Ala	2	1	2	+
1323 Ala→Pro	1	1	2	-
1325 Phe→Val	1	1	2	-
1326 Gln→Glu	1	1	2	+
1327 Glu→Ala	1	1	2	+
1327 Glu→Gly	1	1	2	+
1354 Gly→Ala	2	1	2	+
multiple-substitution mutants				
84 Ile→Phe; 89 Gly→Asp; 330 Met→Lys	1			
245 Met→Leu; 349 Tyr→Ser	1			
337 Arg→His; 709 Arg→Ser	1			
338 Phe→Ser; 341 Asn→His; 342 Leu→Pro[b]	1			
348 Asp→His; 355 Ile→Gly	1			
348 Asp→Tyr; 1296 Gly→Asp	1			
1319 Phe→Leu; 1322 Ala→Pro; 1325 Phe→Ile	1			
1319 Phe→Cys; 1323 Ala→Ser; 1326 Gln→Glu	3			
1320 Ile→Thr; 1323 Ala→Pro	1			
1320 Ile→Met; 1327 Glu→Gly	1			
1323 Ala→Glu; 1326 Gln→Arg	1			
1326 Gln→Glu; 1327 Glu→Asp	2			

[a] The MIC value with wild-type *rpoC* is 3.13 μg/ml in broth microdilution assays, and is 6.25 μg/ml in SGE assays. [b] This Lpm-resistance mutation was initially identified by Elena Sineva and Sajida Ismail (Ebright, 2005). [c] This mutation was also identified by Elena when sequencing the Lpm-resistant *B. subtilis* isolates from the Sonenshein lab (Ebright, 2005).

Table SB2. Lpm-resistant mutants from saturation mutagenesis of *rpoB*: sequences and properties

amino acid substitution	number of independent isolates	resistance level (MIC/MIC$_{wild\text{-}type}$)[a]		ability to complement *rpoC*^{ts} or *rpoB*^{ts}
		broth microdilution	spiral gradient endpoint (SGE)	
***rpoB* (RNAP β subunit)**				
single-substitution mutants				
892 Glu→Ala	1	8	2	+
1251 Tyr→Phe[b]	12	16	8	+
1252 Ser→Gly	1	2	2	+
1256 Gln→Glu[b, c]	7	8	4	+
1256 Gln→Leu[b, c]	1	2	2	+
1263 Ala→Leu[b]	3	1	2	+
1288 Gly→Leu	1	2	2	+
1297 Asp→Ala	5	16	8	+
1297 Asp→Tyr	3	16	4	+
1302 Thr→Pro[b]	1	16	2	+
1308 Ile→Asn	1	1	2	+
1318 Gly→Ser	1	2	2	+
1319 Met→Arg[b]	10	16	8	+
1319 Met→Ile	7	2	2	+
1319 Met→Lys[b]	6	16	8	+
1321 Glu→Val[b]	5	16	4	+
1323 Phe→Leu	1	2	2	+
1324 Asn→Lys	1	2	2	+
1325 Val→Ala[b]	6	16	8	+
1325 Val→Glu	2	8	8	+
1325 Val→Gly[b]	4	8	8	+
1325 Val→Leu[b]	4	8	4	+
multiple-substitution mutants				
294 Gly→Asp; 1319 Met→Arg	1			
667 Leu→Met; 1297 Asp→Ala	1			
802 Val→Ile; 1319 Met→Arg	1			
863 Ser→Tyr; 1324 Asn→Lys	1			
1253 Leu→Arg; 1256 Gln→Leu[b]	1			
1253 Leu→Arg; 1256 Gln→Pro[b]	1			
1272 Glu→Asp; 1276 Trp→Leu	1			
1288 Gln→His; 1297 Asp→Tyr	1			
1288 Gln→Glu; 1297 Asp→Gly	1			
1302 Thr→Pro; 1304 Met→Ile[b]	1			
1302 Thr→Pro; 1310 Asp→Tyr[b]	4			
1311 Gly→Ala; 1319 Met→Arg	1			
1312 Asn→His; 1321 Glu→Val	1			
1318 Gly→Ser; 1319 Met→Arg[b]	1			
1318 Gly→Ser; 1319 Met→Lys[b]	1			
1318 Gly→Ser; 1319 Met→Thr[b]	2			
1318 Gly→Ser; 1323 Phe→Ser[b]	1			
1324 Asn→Ser; 1325 Val→Leu	1			
1324 Asn→Lys; 1326 Leu→Val; 1329 Glu→Lys	2			
1325 Val→Gly; 1326 Leu→Met; 1327 Leu→Met	2			

[a] The MIC value with wild-type *rpoB* is 3.13 µg/ml in broth microdilution and SGE assays.
[b] This Lpm-resistance mutation was initially identified by Elena Sineva and Sajida Ismail (Ebright, 2005).
[c] A mutation at this residue was also identified by Elena when sequencing the Lpm-resistant *B. subtilis* isolates from the Sonenshein lab (Ebright, 2005).

Table SB3. Plasmid-based Rif-resistant mutants[a]: absence of significant cross-resistance to Lpm

amino acid substitution	MIC ratio ($MIC/MIC_{wild\text{-}type}$)[b]	
	Rif	Lpm
***rpoB* (RNAP β subunit)**		
516 Asp→Val	2	1
526 His→Asp	4	2
526 His→Tyr	2	1
531 Ser→Leu	16	2

[a] These mutants are from Sajida Ismail, D.D., and R.H.E., unpublished.

[a] The MIC value with wild-type *rpoB* is 3.13 μg/ml for Lpm, and is 0.39 μg/ml for Rif.

Table SB4. Plasmid-based Stl-resistant mutants[a]: absence of cross-resistance to Lpm

amino acid substitution	MIC ratio (MIC/MIC$_{wild-type}$)[b]	
	Stl	**Lpm**
***rpoC* (RNAP β′ subunit)**		
788 Leu→Met	32	1
1139 Pro→Leu	8	1
***rpoB* (RNAP β subunit)**		
543 Ala→Val	64	1
545 Phe→Cys	>64	1

[a] These mutants are from Tuske et al., 2005.

[b] The MIC value with wild-type *rpoC* is 3.13 µg/ml for Stl, and is 1.56 µg/ml for Lpm. The MIC value with wild-type *rpoB* is 3.13 µg/ml for Stl, and is 0.78 µg/ml for Lpm.

Table SB5. Plasmid-based CBR703-resistant mutants[a]: absence of cross-resistance to Lpm

amino acid substitution	MIC ratio ($MIC/MIC_{wild\text{-}type}$)[b]	
	CBR703	Lpm
***rpoB* (RNAP β subunit)**		
552 Pro→Arg	4	1
618 Gln→Leu	4	1
642 Ser→Ala	4	1
642 Ser→Phe	4	1
654 Asp→His	4	1
657 Thr→Ile	4	1

[a] These mutants are from Xinyue Wang and R.H.E., unpublished.

[b] The MIC value with wild-type *rpoB* is 6.25 μg/ml for CBR703, and is 1.56 μg/ml for Lpm.

Table SB6. Plasmid-based Myx/Cor/Rip-resistant mutants[a]: minimal cross-resistance to Lpm

amino acid substitution	Lpm cross-resistance level ($MIC/MIC_{wild\text{-}type}$)[b]
***rpoC* (RNAP β′ subunit)**	
345 Lys→Arg	1
345 Lys→Asn	0.5
345 Lys→Gln	0.5
345 Lys→Glu	1
345 Lys→Thr	0.25
1346 Gly→Asp	2
1351 Val→Phe	1
1352 Ile→Asn	1
1352 Ile→Ser	1
1354 Gly→Cys	4
***rpoB* (RNAP β subunit)**	
1232 Met→Ile	1
1255 Thr→Ile	0.5
1275 Val→Phe	1
1275 Val→Met	0.5
1278 Leu→Val	1
1279 Glu→Gly	1
1279 Glu→Lys	1
1283 Ala→Val	1
1285 Tyr→Asp	1
1291 Leu→Phe	2
1298 Val→Leu	1
1315 Met→Leu	1
1317 Pro→Leu	1
1320 Pro→Ala	2
1322 Ser→Pro	0.5
1322 Ser→Thr	1
1322 Ser→Tyr	1
1322 Ser→Val	1
1325 Val→Leu	4
1326 Leu→Trp	0.5

[a] These mutants are from Mukhopadhyay et al., 2008.

[b] The MIC value with wild-type *rpoC* is 6.25 μg/ml, and the MIC value with wild-type *rpoB* is 3.13 μg/ml.

Table SB7. Chromosomal Myx-resistant mutants in *E. coli* D21f2tolC: minimal cross-resistance to Lpm

amino acid substitution	MIC ratio (MIC/MIC$_{wild-type}$)	
	Myx	**Lpm**
***rpoC* (RNAP β′ subunit)**		
345 Lys→Asn	256	0.125
345 Lys→Arg	128	1
***rpoB* (RNAP β subunit)**		
1275 Val→Met	128	0.25
1291 Leu→Phe	128	8

[a] The wild-type MIC value for Myx is 0.20 μg/ml, and the wild-type MIC value for Lpm is 1.56 μg/ml.

Table SB8. Chromosomal Rif-resistant mutants in *E. coli* D21f2tolC: minimal cross-resistance to Lpm

amino acid substitution	MIC ratio ($MIC/MIC_{wild\text{-}type}$)	
	Rif	**Lpm**
***rpoB* (RNAP β subunit)**		
516 Asp→Val	512	1
526 His→Asp	>1024	4
526 His→Tyr	>1024	0.25
531 Ser→Leu	1024	2

[a] The wild-type MIC value for Rif is 0.20 µg/ml, and the wild-type MIC value for Lpm is 1.56 µg/ml.

Table SB9. Spontaneous Lpm derivative-resistant mutants in *S. aureus*: sequences

amino acid substitution[a]	number of independent isolates[b]
***rpoC* (RNAP β′ subunit)**	
98 [88] Arg→His	2[c]
99 [89] Arg→Cys	1[d]
99 [89] Arg→His	4
246 [235] Pro→Arg	1[d]
248 [237] Glu→Lys	1[d]
337 [326] Arg→Ser	6
1332 [1150] Leu→Phe	2
***rpoB* (RNAP β subunit)**	
1256 [1061] Gln→Lys	2[c]

[a] Residues are numbered as in *E. coli* RNAP and, in brackets, as in *S. aureus* RNAP.

[b] Mutants were isolated against both deschloro-Lpm and dideschloro-Lpm unless otherwise indicated.

[c] Mutant was only isolated against dechloro-Lpm.

[d] Mutant was only isolated against dideschloro-Lpm.

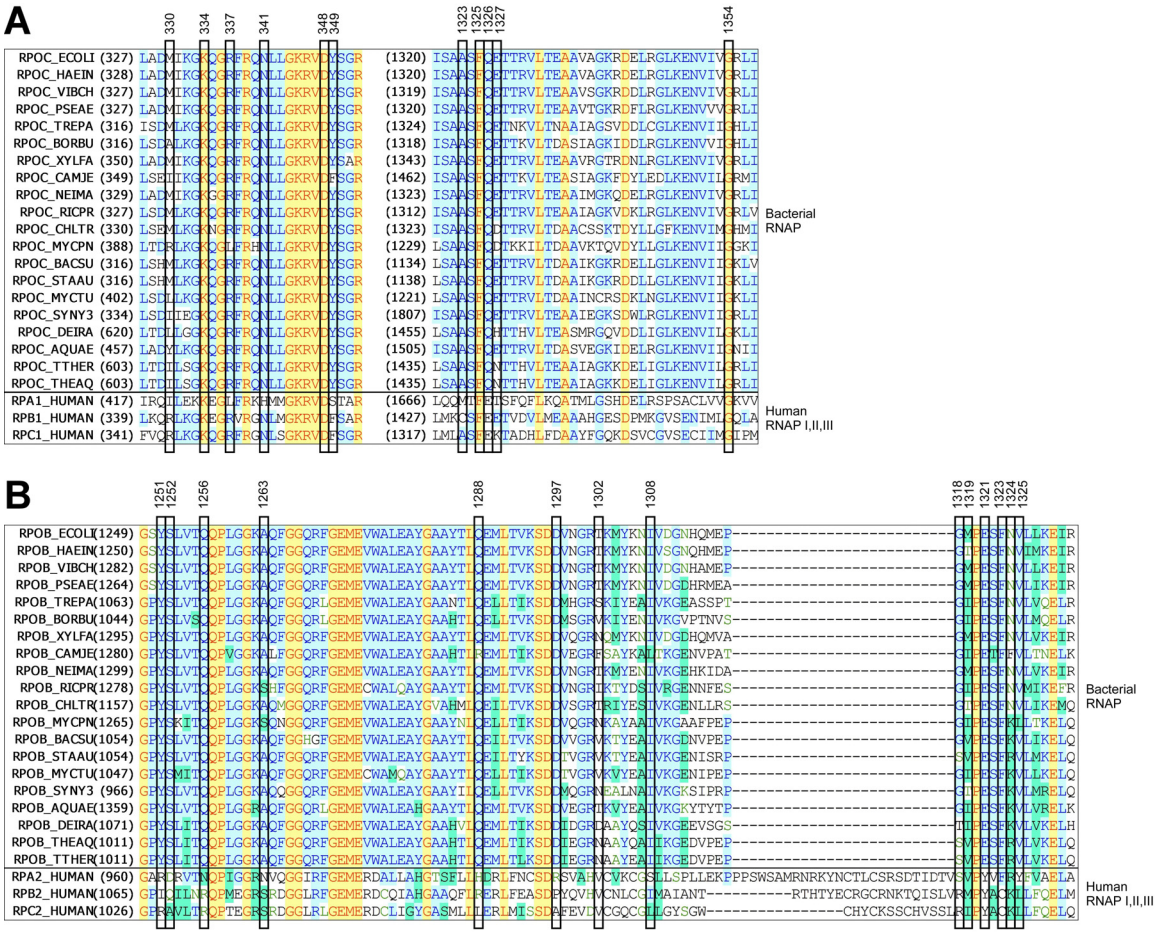

Figure SB1. Conservation of the Lpm target: highly conserved among bacteria, less well conserved with human RNAP

(A) Amino acid sequence alignments for regions of the RNAP β subunit.

(B) Amino acid sequence alignments for regions of the RNAP β′ subunit.

Residues at which single-substitution Lpm-resistant mutants were obtained are boxed, and labeled with the *E. coli* residue number. Species names and SwissProt locus identifiers for the sequences are, in order: *E. coli* (RPOB_ECOLI, RPOC_ECOLI), *Haemophilus influenzae* (RPOB_HAEIN, RPOC_HAEIN), *Vibrio cholerae* (RPOB_VIBCH, RPOC_VIBCH), *Pseudomonas aeruginosa* (RPOB_PSEAE, RPOC_PSEAE), *Treponema pallidum* (RPOB_TREPA, RPOC_TREPA), *Bordetella pertussis* (RPOB_BORPE, RPOC_BORPE), *Xylella fastidiosa* (RPOB_XYLFA, RPOC_XYLFA), *Campylobacter jejuni* (RPOB_CAMJE, RPOC_CAMJE), *Neisseria meningitidis* (RPOB_NEIME, RPOC_NEIMA), *Rickettsia prowazekii* (RPOB_RICPR, RPOC_RICPR), *Chlamydia trachomatis* (RPOB_CHLTR, RPOC_CHLTR), *Mycoplasma pneumoniae* (RPOB_MYCPN, RPOC_MYCPN), *Bacillus subtilis* (RPOB_BACSU, RPOC_BACSU), *Staphylococcus aureus* (RPOB_STAAU, BACSU, RPOC_STAAU), *Mycobacterium tuberculosis* (RPOB_MYCTU, RPOC_MYCTU), *Synechocystis sp.* PCC 6803 (RPOB_SYNY3, RPOC2_SYNY3), *Aquifex aeolicus* (RPOB_AQUAE, RPOC_AQUAE), *Deinococcus radiodurans* (RPOB_DEIRA, RPOC_DEIRA), *Thermus aquaticus* (RPOB_THEAQ, RPOC_THEAQ), *Thermus thermophilus* (RPOB_THETH, RPOC_THETH), *Homo sapiens* RNAPI (RPA2_HUMAN, RPA1_HUMAN), *Homo sapiens* RNAPII (RPB2_HUMAN, RPB1_HUMAN), and *Homo sapiens* RNAPIII (RPC2_HUMAN, RPC1_HUMAN).

Appendix SC:
GE23077 (Chapter 4) Supplements

Supplemental References for Appendix SC

Ebright, R.H., Zhang, Y., Degen, D., and Ebright, Y. (2011). Bipartite Inhibitors of Bacterial RNA Polymerase: Rif-Target/GE23077-Target. US provisional patent application 61/498,970. (currently unpublished)

Feklistov, A., Mekler, V., Jiang, Q., Westblade, L.F., Irschik, H., Jansen, R., Mustaev, A., Darst, S.A., and Ebright, R.H. (2008). Rifamycins do not function by allosteric modulation of binding of Mg^{2+} to the RNA polymerase active center. Proc. Natl. Acad. Sci. USA *105*, 14820-14825.

Table SC1. GE partially competes with Rif for binding to RNAP

	k_{on}, $M^{-1} \cdot s^{-1}$	k_{off}, s^{-1}	K_d (nM)
in absence of GE			
Rif-RNAP interaction	4×10^5	2×10^{-4}	0.5
in presence of GE[a]			
Rif-RNAP interaction	10×10^5	6×10^{-4}	60

[a] GE23077 at a saturating concentration of 1 μM (110 x K_i) or 5 μM (500 x K_i).

Table SC2. GE-resistant mutants from saturation mutagenesis: sequences and properties

amino acid substitution	number of independent isolates	resistance level ($MIC/MIC_{wild\text{-}type}$)[a]	ability to complement *rpoC*^{ts} or *rpoB*^{ts}
***rpoB* (RNAP β subunit)**			
single-substitution mutants			
563 Thr→Pro	1	2	+
564 Pro→Arg	1	2	+
565 Glu→Asp[b]	18	>16	+
566 Gly→Arg	1	8	+
566 Gly→Cys	1	16	+
566 Gly→Ser	2	4	+
684 Asn→Lys[b]	10	>16	+
684 Asn→Thr	1	4	+
multiple-substitution mutants			
546 Glu→Ala; 566 Gly→Cys	1		
565 Glu→Gly; 570 Gly→Ala	1		
565 Glu→Val; 566 Gly→Ser; 568 Asn→Ser[b]	2		
565 Glu→Asp; 572 Ile→Ser[b]	1		
566 Gly→Arg; 1097 Val→Ile	1		
680 Leu→Ser; 684 Asn→Lys; 1040 Asp→Tyr	1		
683 Ala→Thr; 684 Asn→Ile	1		

[a] The MIC value with wild-type *rpoB* is 500 μg/ml.

[b] This GE-resistance mutation was initially identified by Elena Sineva and Sajida Ismail.

Table SC3. Plasmid-based Rif-resistant mutants[a]: minimal cross-resistance to GE

amino acid substitution	MIC ratio ($MIC/MIC_{wild\text{-}type}$)[b]	
	Rif	GE
***rpoB* (RNAP β subunit)**		
516 Asp→Val	2	2
526 His→Asp	4	1
526 His→Tyr	2	1
531 Ser→Leu	16	1

[a] These mutants are from Sajida Ismail, D.D., and R.H.E., unpublished.

[b] The MIC value with wild-type *rpoB* is 0.39 μg/ml for Rif, and is 500 μg/ml for GE.

Table SC4. GE: *E. coli* RNAP inhibitory activity

enzyme	IC50[a] (μM)
wild-type RNAP	0.03
[Asp565]β-RNAP	>100

[a] These relative values were determined using a ribogreen fluorescence–detected transcription assay (see the supplemental method at the beginning of Appendix SA).

Table SC5. Chromosomal Rif-resistant mutants in *E. coli* D21f2tolC: absence of cross-resistance to GE

amino acid substitution	MIC ratio (MIC/MIC$_{wild\text{-}type}$)[a]	
	Rif	**GE**
***rpoB* (RNAP β subunit)**		
516 Asp→Val	512	0.5
526 His→Asp	>1024	0.5
526 His→Tyr	>1024	2
531 Ser→Leu	1024	1

[a] The wild-type MIC value is 0.20 µg/ml for Rif, and is 1000 µg/ml for GE.

Table SC6. Chromosomal GE-resistant mutants in *E. coli* D21f2tolC: fitness costs

amino acid substitution	resistance level ($MIC/MIC_{wild\text{-}type}$)[a]	fitness cost[b] (% per generation) (± SEM)
***rpoB* (RNAP β subunit)**		
565 Glu→Asp	>16	4
684 Asn→Thr	16	0 (-12)

[a] The wild-type MIC value is 500 μg/ml.

[b] The observed fitness cost that is less than zero is shown as zero, with the actual value displayed in parenthesis.

Table SC7. RifaGEs: better growth inhibitory activity than GE alone

organism	MIC (μg/ml)				
	RifSV[a]	GE	RifaGE-4'NCCNr	RifaGE (3-6-1)	RifaGE (3-6-2)
E. coli D21f2tolC	0.39	500	1.56	3.13	1.56

[a] RifSV = rifamycin SV.

Table SC8. RifaGEs: compounds synthesized so far strongly interact with the Rif target, but not the GE target in *E. coli* D21f2tolC cells

***E. coli* D21f2tolC strain**	**MIC ratio (MIC/MIC$_{wild\text{-}type}$)[a]**				
	RifSV	**GE**	**RifaGE-4'NCCNr**	**RifaGE (3-6-1)**	**RifaGE (3-6-2)**
Rif-resistant [β D516V]	>256	0.5	>256	>256	>64
GE-resistant [β E565D]	1	>16	1	1	2

[a] See Table SC7 for wild-type MIC values.

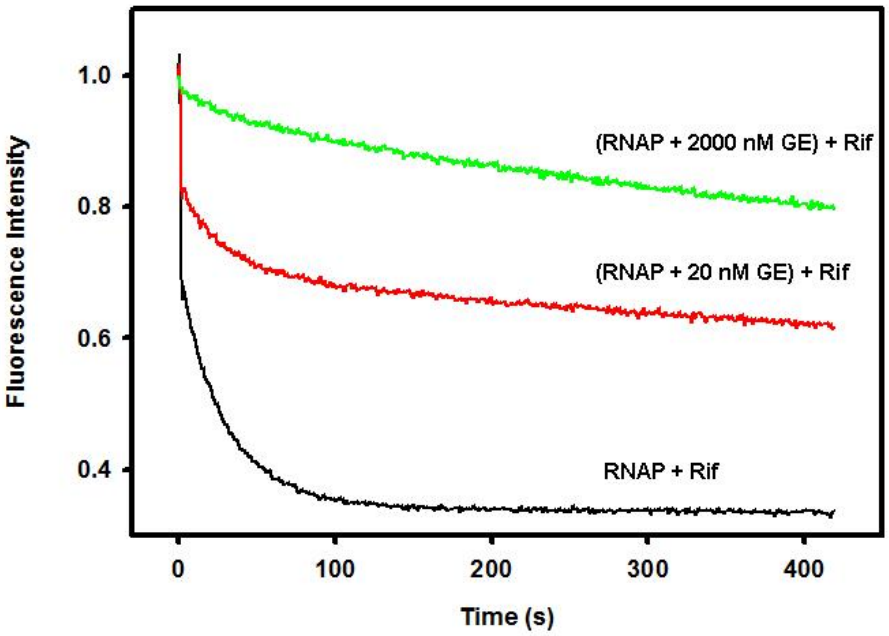

Figure SC1. FRET experiments: GE partially competes with Rif for binding to RNAP

Increasing concentrations of GE decrease, but do not abolish, the fluorescence quenching resulting from Rif binding to a fluorescein-labeled RNAP holoenzyme. This indicates partial competition for binding. Black line, 1 nM RNAP with 50 nM Rif; red line, 1 nM RNAP with 20 nM GE and 50 nM Rif; green line, 1 nM RNAP with 2000 nM GE and 50 nM Rif; method as in Feklistov et al., 2008.

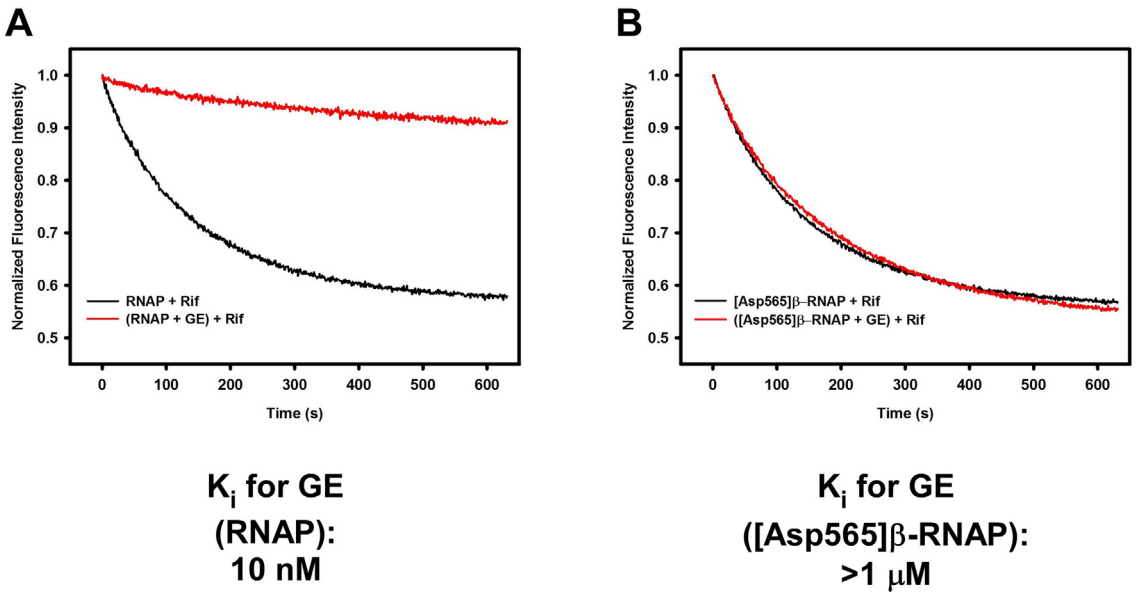

Figure SC2. FRET experiments: [Asp565]β-RNAP is highly resistant to the binding of GE

(A) Wild-type *E. coli* RNAP with Rif in the presence or absence of GE. Black line, wild-type RNAP with Rif; red line, wild-type RNAP with GE and Rif.

(B) [Asp565]β-RNAP with Rif in the presence or absence of GE. Black line, [Asp565]β-RNAP with Rif; red line, [Asp565]β-RNAP with GE and Rif.

The GE-resistant substitution E565D increases the inhibition constant, (K_i), of *E. coli* RNAP for GE by more than 100-fold, indicating that this enzyme is highly resistant to the binding of GE (method as in Feklistov et al., 2008).

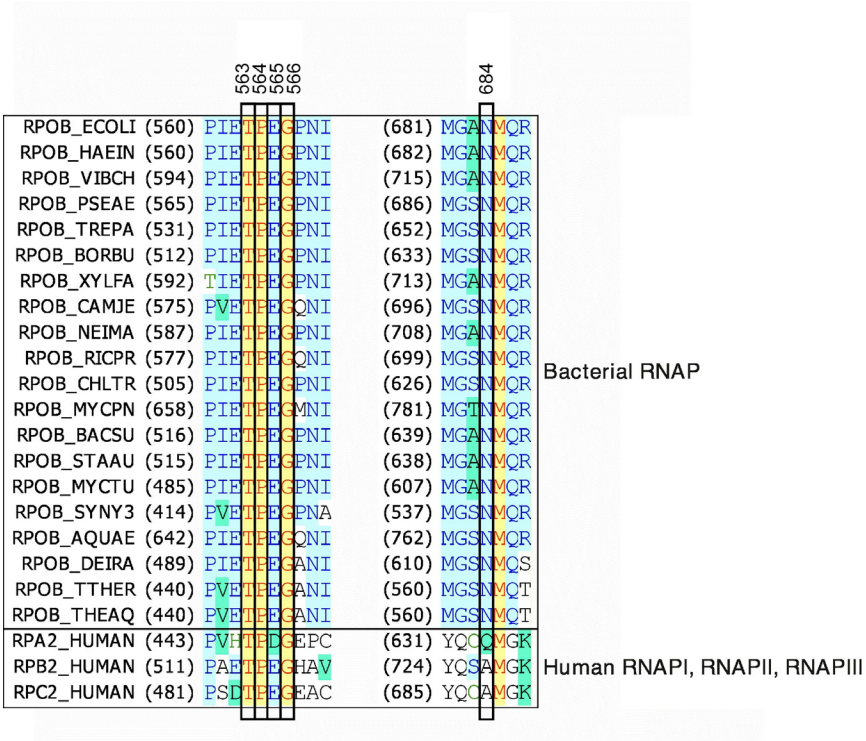

Figure SC3. Conservation of the GE target: highly conserved among bacteria, slightly less well conserved with human RNAP

Amino acid sequence alignments for regions of the RNAP β subunit. Residues at which single-substitution GE-resistant mutants were obtained are boxed, and labeled with the *E. coli* residue number. Species names and SwissProt locus identifiers for the sequences are, in order: *E. coli* (RPOB_ECOLI), *Haemophilus influenzae* (RPOB_HAEIN), *Vibrio cholerae* (RPOB_VIBCH), *Pseudomonas aeruginosa* (RPOB_PSEAE), *Treponema pallidum* (RPOB_TREPA), *Bordetella pertussis* (RPOB_BORPE), *Xylella fastidiosa* (RPOB_XYLFA), *Campylobacter jejuni* (RPOB_CAMJE), *Neisseria meningitidis* (RPOB_NEIME), *Rickettsia prowazekii* (RPOB_RICPR), *Chlamydia trachomatis* (RPOB_CHLTR), *Mycoplasma pneumoniae* (RPOB_MYCPN), *Bacillus subtilis* (RPOB_BACSU), *Staphylococcus aureus* (RPOB_STAAU, BACSU), *Mycobacterium tuberculosis* (RPOB_MYCTU), *Synechocystis sp.* PCC 6803 (RPOB_SYNY3), *Aquifex aeolicus* (RPOB_AQUAE), *Deinococcus radiodurans* (RPOB_DEIRA), *Thermus aquaticus* (RPOB_THEAQ), *Thermus thermophilus* (RPOB_THETH), *Homo sapiens* RNAPI (RPA2_HUMAN), *Homo sapiens* RNAPII (RPB2_HUMAN), and *Homo sapiens* RNAPIII (RPC2_HUMAN).

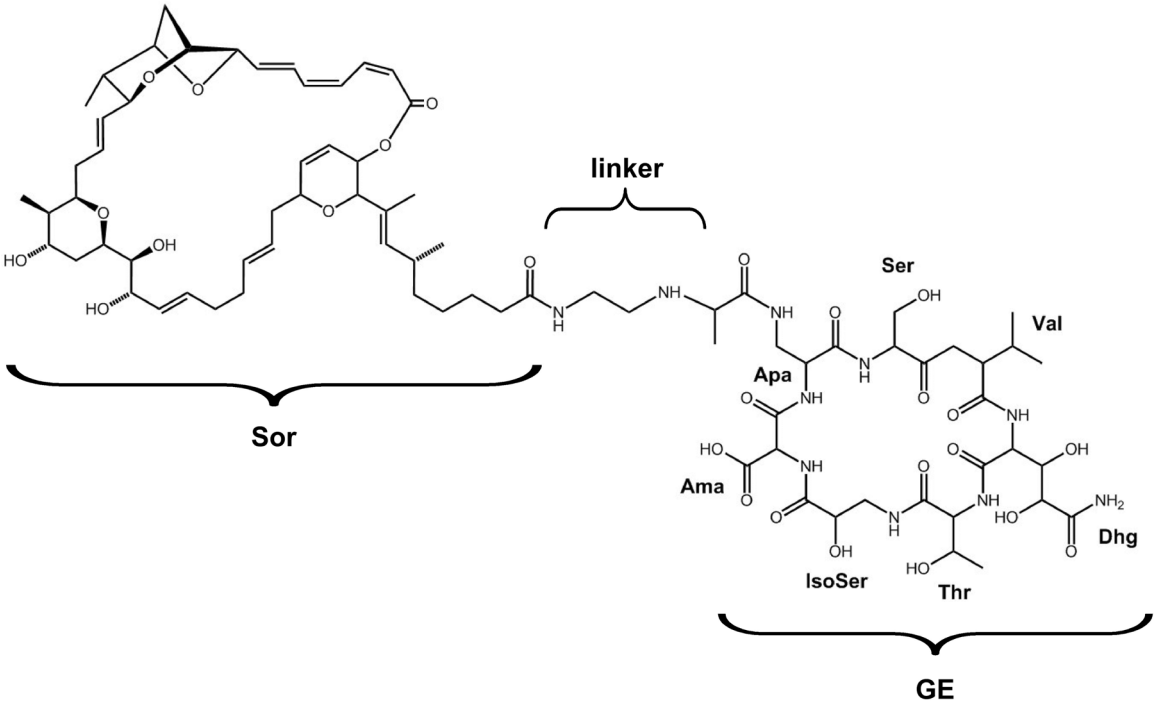

Figure SC4. Structure of a proposed SoraGE compound

Sorangicin (left) is connected to GE (right) through a short carbon linker (middle). The linker would connect the Apa sidechain of GE to the long tail sidechain of sorangicin. Several of the amino acids within GE are labeled for reference. Dhg = β,γ-dihydroxyglutamine; Thr = threonine; IsoSer = isoserine; Ama = α-amino-malonic acid; ApA = α,β-diaminopropanoic acid; Ser = serine; Val = valine. Image modified from Ebright et al., 2011.

Appendix SD:
Salinamide (Chapter 5) Supplements

Supplemental References for Appendix SD

Barry, A.L., Pfaller, M.A., and Fuchs, P.C. (1993). Haemophilus test medium versus Mueller-Hinton broth with lysed horse blood for antimicrobial susceptibility testing of four bacterial species. Eur. J. Clin. Microbiol. Infect. Dis. *12*, 548-553.

Holmes, S.F., Santangelo, T.J., Cunningham, C.K., Roberts, J.W., and Erie, D.A. (2006). Kinetic investigation of *Escherichia coli* RNA polymerase mutants that influence nucleotide discrimination and transcription fidelity. J. Biol. Chem. 281, 18677-18683.

Naryshkin, N., Kim, Y., Dong, Q., and Ebright, R.H. (2001). Site-specific protein-DNA photocrosslinking. Analysis of bacterial transcription initiation complexes. Methods Mol. Biol. *148*, 337-361.

Pupov, D., Miropolskaya, N., Sevostyanova, A., Bass, I., Artsimovitch, I., and Kulbachinskiy, A. (2010). Multiple roles of the RNA polymerase β' SW2 region in transcription initiation, promoter escape, and RNA elongation. Nucleic Acids Res. *38*, 5784-5796.

Toulokhonov, I., Zhang, J., Palangat, M., and Landick, R. (2007). A central role of the RNA polymerase trigger loop in active-site rearrangement during transcriptional pausing. Mol. Cell *27*, 406-419.

Tuske, S., Sarafianos, S.G., Wang, X., Hudson, B., Sineva, E., Mukhopadhyay, J., Birktoft, J.J., Leroy, O., Ismail, S., Clark, A.D. Jr., Dharia, C., Napoli, A., Laptenko, O., Lee, J., Borukhov, S., Ebright, R.H., and Arnold, E. (2005). Inhibition of bacterial RNA polymerase by streptolydigin: stabilization of a straight-bridge-helix active-center conformation. Cell *122*, 541-552.

Table SD1. Sal: RNAP-inhibitory activity

RNAP	IC50 (μM)	
	SalA	**SalB**
Gram-positive bacterial RNAP		
Staphylococcus aureus RNAP[a]	0.2	0.8
Gram-negative bacterial RNAP		
Escherichia coli RNAP[a]	0.2	0.5
Thermus/Deinococcus clade RNAP		
Thermus thermophilus RNAP[a]	>100	>100
Human RNAP I / II / III		
HeLa nuclear extract	>100	>100

[a] The IC50 values presented for these enzymes were determined by Yu Zhang using a modified radiochemical transcription assay whose method was developed by Sukhendu Mandal.

Table SD2. SalI: antibacterial activity

organism	MIC[a] (µg/ml)	
	SalA	**SalB**
Gram-positive bacteria		
Bacillus anthracis Vollum 1B[b,c]	25	>50
Streptococcus pneumoniae ATCC 49619[d]	100	>100
Streptococcus pyogenes ATCC 12344[d]	100	>100
Gram-negative bacteria		
Enterobacter cloacae ATCC 13047[c]	1.56	12.5
Haemophilus influenzae ATCC 49247[d]	6.25	12.5
Neisseria gonorrhoeae ATCC 19424[d]	25	25
Burkholderia mallei CHN7[b,c]	25	50
Pseudomonas aeruginosa ATCC 10145[c]	50	100
Moraxella catarrhalis ATCC 25238[d]	50	100
Yersinia pestis CO92[b,c]	50	>50
Acinetobacter baumannii ATCC 19606[c]	100	>100
Escherichia coli ATCC 25922[c]	100	>100
Escherichia coli D21f2tolC (*rfaH tolC*)[c]	0.049	0.20
Mammalian cells		
Vero E6 ATCC CRL 1586[b]	>50	>50

[a] MIC measurements were determined with a starting cell density of ~2-5 x 10^5 cfu/ml.

[b] These MIC measurements were made by Meliza Talaue at the Center for Biodefense, New Jersey Medical School, Rutgers University, Newark, NJ.

[c] MIC measurements were determined by growing cultures in Mueller-Hinton II cation-adjusted broth (BD Biosciences) under aerobic conditions.

[d] MIC measurements were determined by growing cultures in Haemophilus Test Medium broth (Barry et al., 1993) under a 7% CO_2/6% O_2/4% H_2/83% N_2 atmosphere.

Table SD3. Comparison of Rif and Sal resistance rates at 2x MIC

antibacterial agent[a]	resistance rate (per generation)[b]
Rif[c]	1×10^{-9}
Sal	2×10^{-9}
Rif + Sal[c]	$<2 \times 10^{-12}$

[a] Antibacterial agents were present at 2x MIC: 1 μg/ml for Rif, and 0.6 μg/ml for Sal.

[b] MSS-MLE resistance rates from fluctuation assays with *E. coli* D21f2tolC.

[c] Rates were determined by Matthew Gigliotti.

Table SD4. Spontaneous Sal-resistant mutants in *E. coli* D21f2tolC: summary statistics

frequency of spontaneous mutation to Sal-resistance	~1x10^{-9}
number of Sal-resistant isolates	47
number of Sal-resistant isolates containing single-substitution mutations in *rpoC*	35
number of Sal-resistant isolates containing multiple-substitution mutations in *rpoC*	1
number of Sal-resistant isolates containing single-substitution mutations in *rpoB*	11
number of Sal-resistant isolates containing multiple-substitution mutations in *rpoB*	0
percentage of Sal-resistant isolates containing mutations in RNAP-subunit genes	100

Table SD5. Spontaneous Sal-resistant mutants in *E. coli* D21f2tolC: sequences and properties

amino acid substitution	number of independent isolates	resistance level (MIC/MIC$_{wild-type}$)[a]	
		SalA	SalB
***rpoC* (RNAP β′ subunit)**			
690 Asn→Asp	2	32	32
697 Met→Val[b]	3	64	32
738 Arg→Cys	2	32	16
738 Arg→His	1	32	32
738 Arg→Pro	2	128	64
738 Arg→Ser	1	32	16
748 Ala→Glu	3	32	16
758 Pro→Ser	1	32	16
763 Phe→Cys	4	16	16
775 Ser→Ala	1	16	16
779 Ala→Thr	2	>256	256
779 Ala→Val	6	256	128
780 Arg→Cys	3	64	32
782 Gly→Ala	2	>256	256
782 Gly→Cys	1	>256	128
783 Leu→Arg	1	64	32
***rpoB* (RNAP β subunit)**			
569 Ile→Ser	2	32	32
675 Asp→Ala	2	>256	128
675 Asp→Gly[c]	2	256	128
677 Asn→His	1	128	64
677 Asn→Lys	4	>256	256

[a] The wild-type MIC value is 0.049 μg/ml for SalA, and is 0.20 μg/ml for SalB.

[b] One multiple substitution mutant was also isolated that contained a substitution at this residue 697 Met→Thr; 1054 Thr→Ala.

[c] This mutant was notable for its very low apparent fitness when grown in liquid culture. Experiments by Holmes et al. (2006) have indicated that this residue plays a role in transcription fidelity. As such, substitutions at this residue can result in increased nucleotide misincorporation, which would be expected to have negative effects on cell viability.

Table SD6. Plasmid-based Sal-resistant mutants from induced mutagenesis: sequences and properties

amino acid substitution	number of independent isolates	resistance level (MIC/MIC$_{wild\text{-}type}$)[a]		ability to complement *rpoC*^{ts} or *rpoB*^{ts}
		SalA	SalB	
***rpoC* (RNAP β′ subunit)**				
504 Gln→Pro	1	2	1	+
735 Ala→Thr	1	2	2	+
758[b] Pro→Ser	1	4	2	+
758[b] Pro→Thr	1	4	2	+
780[b] Arg→Cys	1	16	8	+
782[b] Gly→Cys	1	2	2	+
***rpoB* (RNAP β subunit)**				
561 Ile→Ser	2	2	2	+
665 Ala→Glu	1	4	4	+
680 Leu→Met	1	2	2	+

[a] The MIC value with wild-type *rpoC* and wild-type *rpoB* is 0.049 μg/ml for SalA, and is 0.20 μg/ml for SalB.

[b] Sal-resistant mutants were isolated at the same residue during spontaneous resistance screening (see Table SD5).

Table SD7. Chromosomal Rif-resistant mutants in *E. coli* D21f2tolC: absence of cross-resistance to Sal

amino acid substitution	MIC ratio (MIC/MIC$_{wild\text{-}type}$)[a]	
	Rif	**Sal**
***rpoB* (RNAP β subunit)**		
516 Asp→Val	512	1
526 His→Asp	>1024	1
526 His→Tyr	>1024	1
531 Ser→Leu	1024	1

[a] The wild-type MIC value is 0.20 µg/ml for Rif, and is 0.049 µg/ml for Sal (SalA).

Table SD8. Plasmid-based Stl-resistant mutants[a]: absence of cross-resistance to Sal

amino acid substitution	MIC ratio (MIC/MIC$_{wild\text{-}type}$)[b]	
	Stl	**Sal**
***rpoC* (RNAP β′ subunit)**		
788 Leu→Met	32	1
1139 Pro→Arg	8	1
1139 Pro→Leu	8	1
***rpoB* (RNAP β subunit)**		
543 Ala→Val	64	1

[a] These mutants are from Tuske et al., 2005.

[b] The MIC value with wild-type *rpoB* and wild-type *rpoC* is 1.56 μg/ml for Stl, and is 0.049 μg/ml for Sal (SalA).

Table SD9. Plasmid-based CBR703-resistant mutants[a]: absence of cross-resistance to Sal

amino acid substitution	MIC ratio ($MIC/MIC_{wild\text{-}type}$)[b]	
	CBR703	**Sal**
***rpoB* (RNAP β subunit)**		
642 Ser→Ala	4	1
642 Ser→Phe	4	1
654 Asp→His	4	1
657 Thr→Ile	4	1

[a] These mutants are from Xinyue Wang and R.H.E., unpublished.

[b] The MIC value with wild-type *rpoB* is 6.25 μg/ml for CBR703, and is 0.049 μg/ml for Sal (SalA).

Table SD10. Chromosomal Myx-resistant mutants in *E. coli* D21f2tolC: absence of cross-resistance to Sal

amino acid substitution	MIC ratio ($MIC/MIC_{wild\text{-}type}$)[a]	
	Myx	**Sal**
***rpoC* (RNAP β′ subunit)**		
345 Lys→Asn	256	1
345 Lys→Arg	128	1
***rpoB* (RNAP β subunit)**		
1275 Val→Met	128	1
1291 Leu→Phe	128	1

[a] The wild-type MIC value is 0.20 μg/ml for Myx, and is 0.049 μg/ml for Sal (SalA).

Table SD11. Chromosomal Lpm-resistant mutants in *E. coli* D21f2tolC: absence of cross-resistance to Sal

amino acid substitution	MIC ratio (MIC/MIC$_{wild\text{-}type}$)[a]	
	Lpm	Sal
***rpoC* (RNAP β′ subunit)**		
337 Arg→His	8	1
348 Asp→His	8	1
348 Asp→Tyr	8	1
349 Tyr→Ser	8	1
***rpoB* (RNAP β subunit)**		
1251 Tyr→Phe	8	1
1256 Gln→Glu	8	1
1256 Gln→Leu	8	1

[a] The wild-type MIC value is 1.56 μg/ml for Lpm, and is 0.049 μg/ml for Sal (SalA).

Table SD12. Sal-Br: RNAP-inhibitory activity

RNAP	IC50 (μM)		
	SalA	SalB	Sal-Br
Gram-positive bacterial RNAP			
Escherichia coli RNAP[a]	0.2	0.5	0.9
Gram-negative bacterial RNAP			
Staphylococcus aureus RNAP[a]	0.2	0.8	0.7
Human RNAP I / II / III			
HeLa nuclear extract	>100	>100	>100

[a] The IC50 values presented for these enzymes were determined by Yu Zhang using a modified radiochemical transcription assay whose method was developed by Sukhendu Mandal.

Table SD13. Sal-Br: antibacterial activity

organism	MIC[a] (μg/ml)		
	SalA	**SalB**	**Sal-Br**
Gram-positive bacteria			
Streptococcus pneumoniae ATCC 49619[b]	100	>100	100
Streptococcus pyogenes ATCC 12344[b]	100	>100	100
Gram-negative bacteria			
Enterobacter cloacae ATCC 13047[c]	1.56	12.5	3.13
Haemophilus influenzae ATCC 49247[b]	6.25	12.5	6.25
Neisseria gonorrhoeae ATCC 19424[b]	25	25	25
Pseudomonas aeruginosa ATCC 10145[c]	50	100	100
Moraxella catarrhalis ATCC 25238[b]	50	100	100
Acinetobacter baumannii ATCC 19606[c]	100	>100	>100
Escherichia coli ATCC 25922[c]	100	>100	>100
Escherichia coli D21f2tolC (*rfaH tolC*)[c]	0.049	0.20	0.098
Mammalian cells			
Vero E6 ATCC CRL 1586[d]	>50	>50	>50

[a] MIC measurements were determined with a starting cell density of ~2-5 x 10^5 cfu/ml.

[b] MIC measurements were determined by growing cultures in Haemophilus Test Medium broth (Barry et al., 1993) under a 7% CO_2/6% O_2/4% H_2/83% N_2 atmosphere.

[c] MIC measurements were determined by growing cultures in Mueller-Hinton II cation-adjusted broth (BD Biosciences) under aerobic conditions.

[d] These MIC measurements were made by Meliza Talaue at the Center for Biodefense, New Jersey Medical School, Rutgers University, Newark, NJ.

Table SD14. Sal mechanism: Sal[a] is noncompetitive with respect to NTPs

	V_{max} (fmol/min/ nmol template) (± SEM)	K_m (μM) (± SEM)	K_i (μM) (± SEM)
"i site" NTP (ATP)	0.01 ± 0.001	460 ± 200[b]	0.10 ± 0.03[c]
"i+1 site" NTP (UTP)	0.01 ± 0.0003	14 ± 3[b]	0.23 ± 0.03[c]

[a] These experiments were performed using SalA.

[b] These values are in rough agreement with those previously reported in Pupov et al., 2010.

[c] These values are the same, within error, as the IC50 value for SalA against *E. coli* RNAP (see Table SD1 or Table SD12).

Table SD15. Sal mechanism: justification for noncompetitive model fit[a]

	AICc[b]	Sy.x[c]	R^2 [d]	number of parameters[e]
"i site" NTP (ATP)				
full noncompetitive inhibition	-314.1	0.0012	0.81	3
next-best model[f] (full uncompetitive inhibition)	-312.5	0.0013	0.80	3
"i+1 site" NTP (UTP)				
full noncompetitive inhibition	-432.5	0.0007	0.89	3
next-best model[f] (partial noncompetitive inhibition)	-430.7	0.0007	0.89	4

[a] The better value for each comparison is highlighted in red.

[b] Akaike Information Criterion corrected; lowest value best.

[c] standard error of the estimate; lowest value best.

[d] coefficient of multiple determination; highest value best.

[e] lowest value best.

[f] next-best model based on cumulative analysis of the parameters listed here.

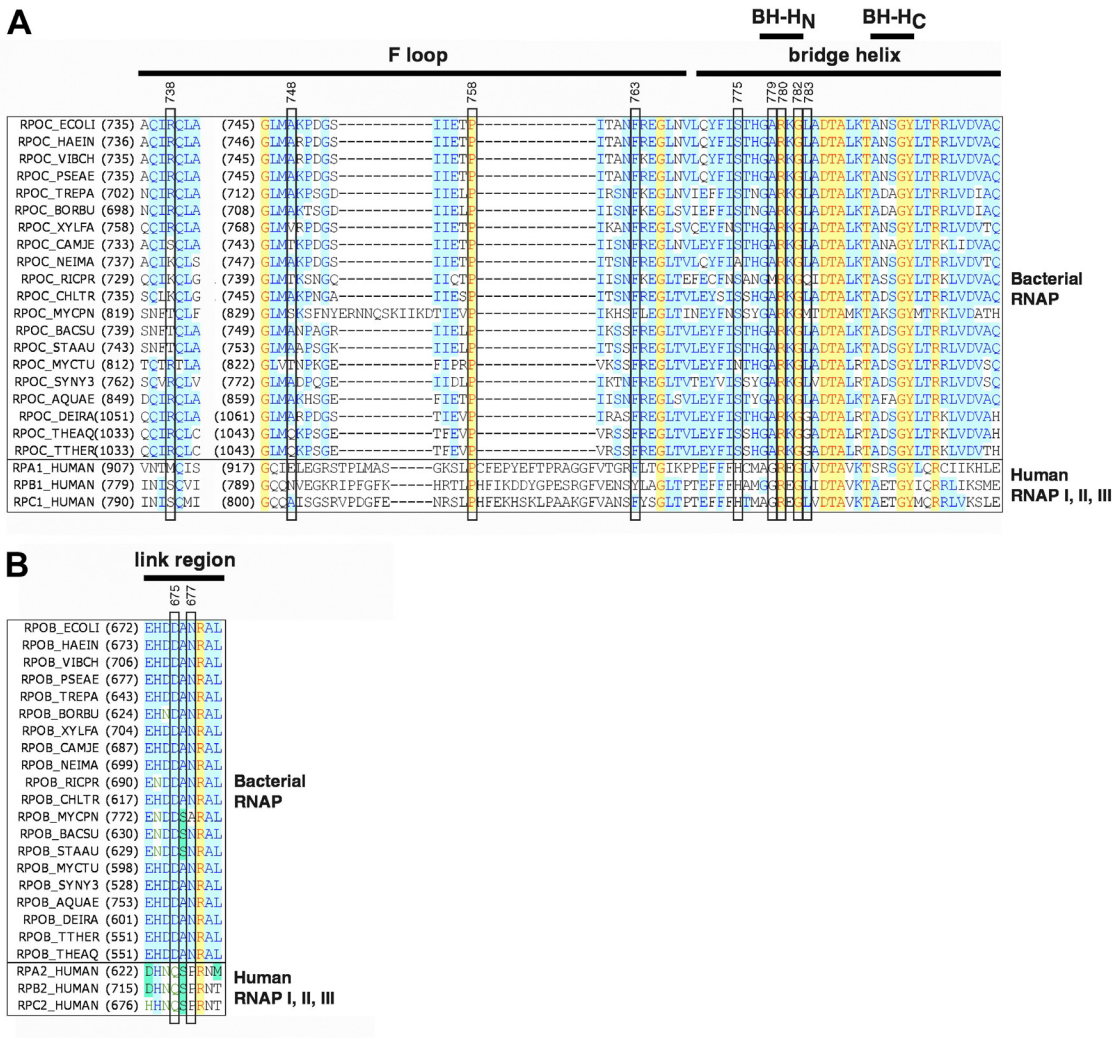

Figure SD1. Conservation of the Sal target: highly conserved among bacteria, less well conserved with human RNAP

(A) Amino acid sequence alignments for regions of the RNAP β′ subunit.

(B) Amino acid sequence alignments for regions of the RNAP β subunit.

Residues at which single-substitution Sal-resistant mutants were obtained are boxed, and labeled with the *E. coli* residue number. Species names and SwissProt locus identifiers for the sequences are, in order: *E. coli* (RPOB_ECOLI, RPOC_ECOLI), *Haemophilus influenzae* (RPOB_HAEIN, RPOC_HAEIN), *Vibrio cholerae* (RPOB_VIBCH, RPOC_VIBCH), *Pseudomonas aeruginosa* (RPOB_PSEAE, RPOC_PSEAE), *Treponema pallidum* (RPOB_TREPA, RPOC_TREPA), *Bordetella pertussis* (RPOB_BORPE, RPOC_BORPE), *Xylella fastidiosa* (RPOB_XYLFA, RPOC_XYLFA), *Campylobacter jejuni* (RPOB_CAMJE, RPOC_CAMJE), *Neisseria meningitidis* (RPOB_NEIME, RPOC_NEIMA), *Rickettsia prowazekii* (RPOB_RICPR, RPOC_RICPR), *Chlamydia trachomatis* (RPOB_CHLTR, RPOC_CHLTR), *Mycoplasma pneumoniae* (RPOB_MYCPN, RPOC_MYCPN), *Bacillus subtilis* (RPOB_BACSU, RPOC_BACSU), *Staphylococcus aureus* (RPOB_STAAU, BACSU, RPOC_STAAU), *Mycobacterium tuberculosis* (RPOB_MYCTU, RPOC_MYCTU), *Synechocystis sp.* PCC 6803 (RPOB_SYNY3, RPOC2_SYNY3), *Aquifex aeolicus* (RPOB_AQUAE, RPOC_AQUAE), *Deinococcus radiodurans* (RPOB_DEIRA, RPOC_DEIRA), *Thermus aquaticus* (RPOB_THEAQ, RPOC_THEAQ), *Thermus thermophilus* (RPOB_THETH, RPOC_THETH), *Homo sapiens* RNAPI (RPA2_HUMAN, RPA1_HUMAN), *Homo sapiens* RNAPII (RPB2_HUMAN, RPB1_HUMAN), and *Homo sapiens* RNAPIII (RPC2_HUMAN, RPC1_HUMAN). This figure was prepared by RHE.

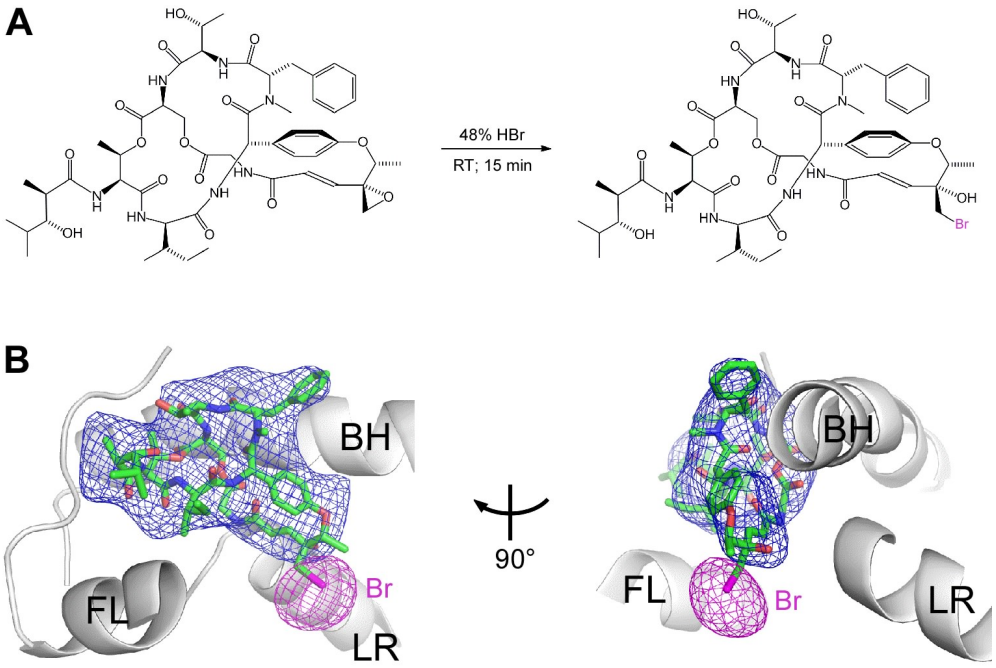

Figure SD2. Use of Sal-Br to confirm the orientation of Sal in the RNAP-Sal complex

(A) Synthesis of Sal-Br. Treatment of SalA (left panel) for 15 min at room temperature with 48% HBr causes the epoxide ring of SalA to open, forming a bromohydrin-derivative of Sal (Sal-Br). The bromine is labeled in pink.

(B) Two orthogonal views of the electron density for Sal-Br in complex with *E. coli* RNAP. A clear anomalous electron density can be seen for the bromine group (pink mesh), confirming the proper orientation for Sal within the electron density. Blue mesh, electron density for Sal; FL, F-loop; BH, bridge helix; LR, link region.

These figures were modified from originals created by RHE and Yu Feng.

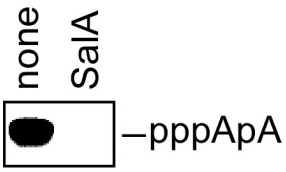

Figure SD3. Mechanistic basis of transcription inhibition by Sal: Sal inhibits *de novo* initiation

Sal inhibits the formation of dinucleotide (pppApA) RNA products in *de novo* initiation experiments. Result from Yu Feng using the *lacUV5(ICAP)* (-42;+426) promoter fragment (Naryshkin et al., 2001).

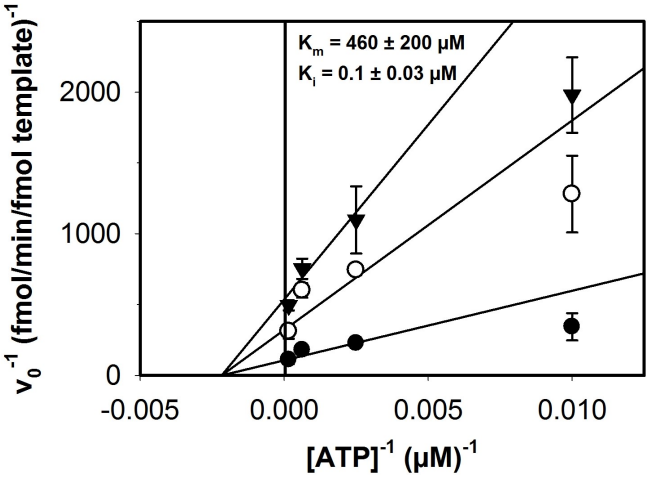

Figure SD4. Mechanistic basis of transcription inhibition by Sal: Sal is noncompetitive with respect to the "i site" nucleotide

Double-reciprocal plot showing results from transcription kinetics experiments assessing the effects of Sal on the "i site" nucleotide (ATP). Sal is noncompetitive with respect to the "i site" nucleotide. Filled circles, no Sal; open circles, 0.2 µM Sal; closed triangles, 0.4 µM Sal. Kinetics values are provided in Table SD14. The statistical parameters used to justify this model fitting are provided in Table SD15.

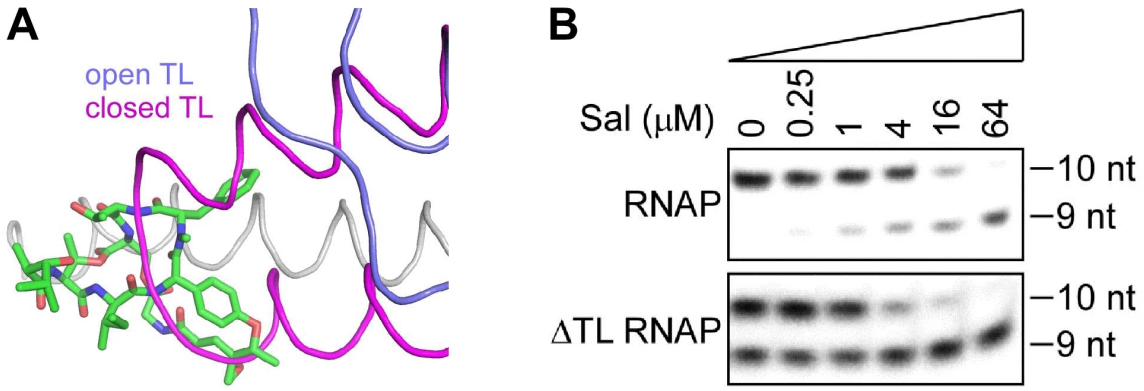

Figure SD5. Structural basis of transcription inhibition by Sal: Sal is positioned to clash with a closed (folded) trigger loop

(A) Model showing that Sal is positioned to clash with a closed (folded) trigger loop. Green sticks, SalA; gray trace, bridge helix; purple trace, open trigger loop; magenta trace, closed trigger loop. This figure was prepared by Yu Feng.

(B) Results from transcription experiments looking at the one nucleotide extension of a 9 nucleotide radiolabeled RNA scaffold. Experiments were performed with an *E. coli* RNAP enzyme (RNAP) or an *E. coli* RNAP enzyme lacking the trigger loop (ΔTL RNAP; purified using pRL4455-β'Δ(931-1137)ΩAla3 from Toulokhonov et al., 2007). Sal is able to inhibit both enzymes; as such, the trigger loop is not required for RNAP to be inhibited by Sal. These results are from Yu Zhang.

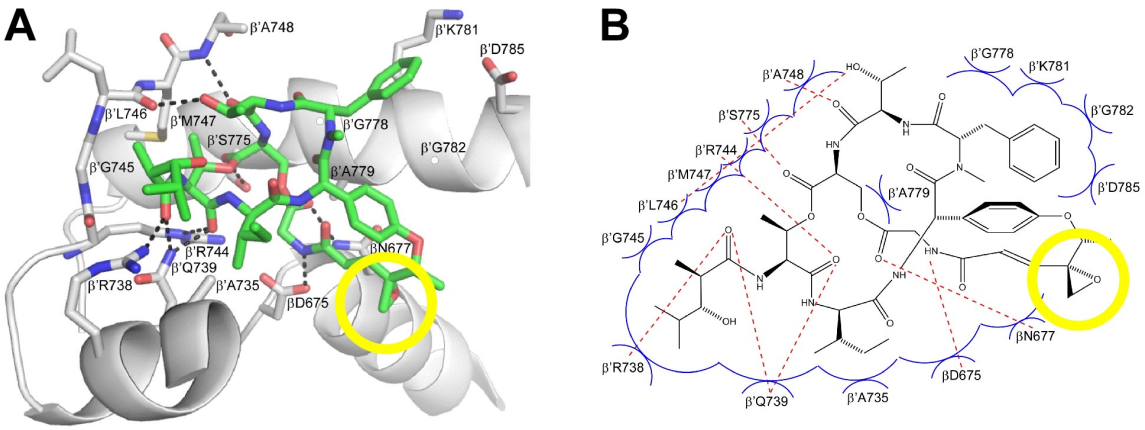

Figure SD6. The epoxide moiety of Sal is accessible for semi-synthetic modifications

(A) The epoxide moiety of Sal (circled in yellow) does not make contact with residues of RNAP. Gray sticks, RNAP sidechains; green sticks, SalA; red, oxygen atoms; blue, nitrogen atoms; yellow, sulfur atoms; dashed lines, H-bonds.

(B) A schematic representation of panel A. Red dashed lines, H-bonds; blue arcs, van der Waals interactions.

These figures are identical to Figure 17C and Figure17D, and were prepared by Yu Feng and R.H.E.